

Aus der Klinik und Poliklinik für Orthopädie, Physikalische Medizin und Rehabilitation  
Klinikum der Ludwig-Maximilians-Universität zu München

Direktor: Prof. Dr. med. Dipl.-Ing. Volkmar Jansson

**Evaluation of Large Acetabular Bone Defects**

-

**Conception and Implementation of Suitable  
Biomechanical Test Methods**

Dissertation  
zum Erwerb des Doktorgrades der Humanbiologie  
an der Medizinischen Fakultät der  
Ludwig-Maximilians-Universität zu München

vorgelegt von  
*Ronja Alissa Schierjott*  
aus  
*Singen a. Hohentwiel*

2021

Mit Genehmigung der Medizinischen Fakultät  
der Universität München

Berichterstatter: Prof. Dr. med. habil. Dr.-Ing. Thomas M. Grupp, FIOR

Mitberichterstatter: Prof. Dr. Christian Zeckey

Priv. Doz. Dr. Carl Neuerburg

Prof. Dr. Matthias Pietschmann

Mitbetreuung durch  
den promovierten

Mitarbeiter: Dr. Christoph Schilling

Dekan: Prof. Dr. med. dent. Reinhard HICKEL

Tag der  
mündlichen Prüfung: 02.03.2021



## Eidesstattliche Versicherung

# Schierjott, Ronja Alissa

Name, Vorname

Ich erkläre hiermit an Eides statt,

dass ich die vorliegende Dissertation mit dem Titel

**Evaluation of Large Acetabular Bone Defects -  
Conception and Implementation of Suitable Biomechanical Test Methods**

selbständig verfasst, mich außer der angegebenen keiner weiteren Hilfsmittel bedient und alle Erkenntnisse, die aus dem Schrifttum ganz oder annähernd übernommen sind, als solche kenntlich gemacht und nach ihrer Herkunft unter Bezeichnung der Fundstelle einzeln nachgewiesen habe.

Ich erkläre des Weiteren, dass die hier vorgelegte Dissertation nicht in gleicher oder in ähnlicher Form bei einer anderen Stelle zur Erlangung eines akademischen Grades eingereicht wurde.

Tuttlingen, 04.03.2021

Ort, Datum

Ronja A. Schierjott

Unterschrift Doktorandin bzw. Doktorand

This page was intentionally left blank.

---

**Table of contents**

List of abbreviations .....	II
List of tables .....	IV
List of figures .....	V
List of publications .....	1
List of congresses .....	2
Confirmation of co-authors .....	4
1 Introduction .....	5
1.1 Overall research questions .....	5
1.2 Total hip arthroplasty and reasons for revision .....	5
1.3 Acetabular bone defects .....	6
1.4 Acetabular revision treatment .....	11
1.5 Conclusions .....	17
1.6 Author contribution .....	18
2 Zusammenfassung (Deutsch) .....	19
3 Abstract (English) .....	22
4 Publications .....	25
4.1 Publication I: Quantitative assessment acetabular bone defects: A study of 50 computed tomography data sets .....	25
4.2 Publication II: A method to assess primary stability of acetabular components in association with bone defects .....	48
4.3 Publication III: Primary stability of a press-fit cup in combination with impaction grafting in an acetabular defect model .....	59
5 Additional content .....	72
5.1 Additional content I: Accuracy assessment of the optical measurement system .....	72
5.2 Additional content II: Simplification of the representative defect and development of a scaling procedure for the implementation in human donor specimens .....	81
References .....	92
Acknowledgements .....	100

**List of abbreviations**

µm	Micrometer
3D	Three-dimensional
AM	Acetabular model / Acetabulummodell
ASIS	Anterior superior iliac spine
AW	Anterior column width
b.a.glass	Bioactive glass granules
BCI	Bone-cement-interface
BGS	Bone graft substitute
BII	Bone-implant-interface
bone chips	Cancellous bone chips
CAD	Computer aided design
CCD	Charge-coupled device
CoR	Center of rotation
CS	Coordinate system
CT	Computed tomography / Computertomographie
DIC	Digital image correlation
HA	Hydroxyapatite
IBG	Impaction bone grafting
KEM	Knochenersatzmaterial
ml	Milliliter
mm	Millimeter
MP	Megapixel
MT	Medial wall thickness
NR	Native acetabular radius
OR	Operating room
PE	Polyethylene
PEG	Polyethylene-glycol-glycerol
PT	Pubic tubercle
PW	Posterior column width
RR	Planned reaming radius
SAP	Standard acetabular plane
SSM	Statistical shape model
TCP	Tricalciumphosphate

TEP	Totalendoprothese
tetrapods+coll	$\beta$ -tricalcium phosphate tetrapods in a collagen matrix
THA	Total hip arthroplasty

**List of tables**

**Table 1.** Calculation of theoretical angles based on thickness of Johansen gauges and the tangent function..... 79

**Table 2.** Overview of developed scaling procedure. For each reaming step (Reamer 1 to Reamer 5\_POST), the position in X, Y, and Z (reaming depth), as well as the reamer size is scaled using the corresponding scaling factor and parameter..... 88

---

**List of figures**

- Figure 1.** Overview of acetabular bone defect types according to Paprosky classification. Adapted and simplified from Wright and Paprosky, 2016 [36]. .....7
- Figure 2.** Abstract of derived bone defect groups based on the distribution of relative bone volume loss in % among the sectors Cranial roof (C), Anterior column (A), Posterior column (P) and Medial wall (M). Four defect groups with one case each are exemplarily shown (Anterior-Medial, Posterior-Medial, Anterior-Posterior-Medial, All sectors). The spider plots depict the definitions of the defect groups based on the thresholds for relative bone volume loss of 25% (C, A, M) and 15% (P) in gray and the distribution of relative bone volume loss of the individual cases (red lines). The 3D-models of the individual cases with color-coded defect sectors (C: purple, A: green, P: blue, M: yellow) are shown to the right. Adapted from Schierjott et al. [41]. ..... 10
- Figure 3.** Overview of a few of the available acetabular revision implants. Images adapted from DePuy Synthes, Zimmer Biomet, implantcast and Kawanabe et al. 2011 [45–50].... 11
- Figure 4.** Impaction bone grafting technique, exemplarily shown with metal mesh and cemented PE-cup. Adapted from van Haaren [72]. ..... 13
- Figure 5.** Overview of bone defect increments derived from the simplified defect (increment 4) by exclusion of specific reaming procedures as indicated in the tables. Adapted from Schierjott et al. [86]. ..... 15
- Figure 6.** Exemplary image noise measurement. Image noise was exemplarily assessed for one specimen at zero load as the relative displacement between cup and acetabular test model, shown as vectors in the 33 tracking points, which were also used in the second and third publication of this dissertation. Values are given in mm. .... 73
- Figure 7.** Setup to assess displacement measurement error with XY-table, tracking points and reference block for rigid body motion compensation. .... 75
- Figure 8.** Field of view and measurement principle for displacement measurement error in X, Y, and Z with starting positions and maximum displacement positions. .... 76
- Figure 9.** Setup to assess angle measurement error. (A) Starting position with definition of components / lines for angle measurement. (B) Maximum angular displacement using a Johansen gauge with 2500  $\mu\text{m}$  thickness. .... 78

- Figure 10.** Bone volume loss in the representative defect (red) derived by subtraction of 3D-model of defect pelvis (gray) from 3D-model of native pelvis (beige). ..... 82
- Figure 11.** Analysis of original bone defect volume after removal of reconstruction inaccuracies and screw holes (red). Total bone volume loss was 18.9 ml, which could be further distinguished in bone volume loss in the defined defect sectors Cranial roof (purple), Anterior column (green), Posterior column (blue) and Medial wall (yellow). Values in % correspond to the bone volume loss in relation to the initial / native bone volume in each defined sector..... 83
- Figure 12.** Coordinate systems for defect simplification and implementation. SAP-CS based on the standard acetabular plane and the line connecting ASIS and PT, as well as Anterior-CS and Posterior-CS which resulted from tilting the SAP-CS / the specimens around the line connecting ASIS and PT..... 84
- Figure 13.** Nine reaming procedures for simplified defect implementation with hemispherical reamers. Shown are the implementation schemes with the corresponding coordinate systems (CS), reamer positions and sizes (radius), as well as the resulting virtual reaming procedures (gray). Positions and reamer radii are given in mm. Adapted from Schierjott et al. [86]..... 85
- Figure 14.** Resulting simplified defect and comparison of its corresponding volume (gray) with original defect volume (red) shows high volume conformity and comparable shape, as well as comparable distribution of relative bone loss (% of native bone volume in each sector) among the four defined defect sectors Cranial roof, Anterior column, Posterior column and Medial wall (spider plot). Adapted from Schierjott et al. [86] ..... 86
- Figure 15.** Implementation using five reaming procedures and resulting bone defect increment 1 with rim damage of approximately one-third of the circumference (marked in red). Adapted from Schierjott et al. [86] ..... 86
- Figure 16.** Measurements for defect scaling, exemplarily shown on virtual 3D-model of native pelvis. .... 87
- Figure 17.** Comparison of representative simplified defect (increment 1), including the virtually implanted press-fit cup in comparison with two specimens in which the scaling procedure was applied to implement defect increment 1 (top). At the bottom, the specimens are depicted with virtually implanted press-fit cups, whereby the red area indicates the approximately 1/3 of circumference without implant-bone contact. .... 89

**Figure 18.** Screenshot of excel-template to calculate the required reamer sizes, positions (X and Y) and reaming depth (Z) (blue-white box) based on the measurement values inserted above (orange box) and the defined scaling factors (bottom). .....90

**Figure 19.** Exemplary application of defect scaling and implementation procedure in human donor hemipelvises, performed within a study of Morosato et al., 2020 with implemented defect (left), which was filled with a synthetic BGS (right). Adapted from Morosato et al. [93]. .....91

This page was intentionally left blank.

## List of publications

**Mozzafari-Jovein H**, Schierjott R, Soares T. Abscheidung von Mikro- und Nanopartikeln auf WC-Basis auf metallischen Oberflächen durch galvanische Prozesse. Forschungsreport für den Maschinenbau WS 2013/14: 22-23. ISSN 2196-8659.

**Schierjott R A**, Giurea A, Neuhaus H-J, Schwiesau J, Pfaff A M, Utzschneider S, Tozzi G, Grupp T M. Analysis of carbon fiber reinforced PEEK hinge mechanism articulation components in a rotating hinge knee design: A comparison of in vitro and retrieval findings. *BioMed Research International* 2016; 2016: 7032830. DOI: 10.1155/2016/7032830.

**Hettich G**, Schierjott R A, Ramm H, Graichen H, Jansson V, Rudert M, Traina F, Grupp T M. Method for quantitative assessment of acetabular bone defects. *Journal of Orthopaedic Research* 2019; 37(1):181-189. DOI: 10.1002/jor.24165.

**Schierjott R A**, Hettich G, Graichen H, Jansson V, Rudert M, Traina F, Weber P, Grupp T M. Quantitative assessment of acetabular bone defects: A study of 50 computed tomography data sets. *PLoS ONE* 2019; 14(10):e0222511. DOI: 10.1371/journal.pone.0222511.

**Hettich G**, Schierjott R A, Epple M, Gbureck U, Heinemann S, Mozaffari-Jovein H, Grupp T M. Calcium phosphate bone graft substitutes with high mechanical load capacity and high degree of interconnecting porosity. *Materials* 2019; 12(21). DOI: 10.3390/ma12213471.

**Schierjott R A**, Hettich G, Ringkamp A, Baxmann M, Morosato F, Damm P, Grupp T M. A method to assess primary stability of acetabular components in association with bone defects. *Journal of Orthopaedic Research* 2020; 38(8):1769–1778. DOI: 10.1002/jor.24591.

**Schierjott R A**, Hettich G, Baxmann M, Morosato F, Cristofolini L, Grupp T M. Primary stability of a press-fit cup in combination with impaction grafting in an acetabular defect model. *Journal of Orthopaedic Research* 2020. DOI: 10.1002/jor.24810.

**Morosato F**, Traina F, Schierjott R A, Hettich G, Grupp T M, Cristofolini L. Primary stability of revision acetabular reconstructions using an innovative bone graft substitute. A comparative biomechanical study on cadaveric pelvises. Manuscript submitted to *HIP International* 2020.

## List of congresses

### I. Podium presentations:

**Grupp T M**, Schierjott R A, Pfaff A, Tozzi G, Schwiesau J, Giurea A, Utzschneider S (2016). Carbon fibre reinforced PEEK as new biomaterial in a rotating hinge knee design – a comparison of biotribology in vitro to retrieval findings. *SICOT Specialized Knee Surgery Meeting, June 30 – July 2, Würzburg, Germany*

**Grupp T M**, Fritz B, Kutzner I, Bergmann G, Schierjott R A, Tozzi G, Kaddick C, Schwiesau J, Giurea A, Utzschneider S (2017). Keynote – Advanced Biomaterials in Total Knee Arthroplasty. *EMN Biomaterials Meeting, August 14-17, Milano, Italy.*

**Schierjott R A**, Parwani P, Barber A, Grupp T M, Tozzi G (2017). Micro-CT analysis of carbon fiber reinforced PEEK components after in vivo service. *23rd Congress of the European Society of Biomechanics, July 2 - 5, Seville, Spain.*

**Hettich G**, Schierjott R A, Schilling C, Maas A, Ramm H, Lamecker H, Grupp T M (2018). Validation of a Statistical Shape Model for Acetabular Bone Defect Analysis. *31st International Society of Technology in Arthroplasty, October 10-13, London, United Kingdom.*

**Grupp T M**, Schilling C, Clarius M, Aldinger P, Chevalier Y, Hirt M, Schierjott R A, Mozaffari-Jovein H, Jaeger S, Kretzer JP (2019). Neue Biomechanische Prüfmethode zur Designoptimierung zementfreier orthopädischer Implantate. Key Note – Session Chair: IX. *Münchener Symposium für Experimentelle Orthopädie, Unfallchirurgie und muskuloskelettale Forschung. Carl Friedrich von Siemens Stiftung, February 28 - March 1, Munich, Germany.*

**Schierjott R A**, Hettich G, Graichen H, Jansson V, Rudert M, Traina F, Weber P, Grupp T M (2019). Quantitative Analyse von 45 acetabulären Knochendefekten, IX. *Münchener Symposium für Experimentelle Orthopädie, Unfallchirurgie und Muskuloskelettale Forschung, Carl Friedrich von Siemens Stiftung, February 28 - March 1, Munich, Germany*

**Schierjott R A**, Hettich G, Graichen H, Jansson V, Rudert M, Traina F, Weber P, Grupp T M (2019). Quantitative Analyse von 50 acetabulären Knochendefekten. *11. Kongress der Deutschen Gesellschaft für Biomechanik (DGfB), April 3 - 5, Berlin, Germany.*

**Schierjott R A**, Ringkamp A, Hettich G, Baxmann M, Grupp T M (2019). Effect of acetabular bone defect and defect filling on primary stability of a hemispherical cup. *25th Congress of the European Society of Biomechanics, July 7 - 10, Vienna, Austria.*

**Schierjott R A**, Hettich G, Ringkamp A, Morosato F, Baxmann M, Grupp T M (2019). An acetabular defect model to assess primary stability of different revision components. *32nd Annual Congress of the International Society for Technology in Arthroplasty, October 2 – 5, Toronto, Canada.*

**Hettich G S**, Schierjott R A, Graichen H, Jansson V, Rudert M, Traina F, Weber P, Grupp T M (2019). Impartial and quantitative assessment of 50 acetabular bone defects. *32nd Annual Congress of the International Society for Technology in Arthroplasty, October 2 – 5, Toronto, Canada.*

## **II. Poster presentations:**

**Grupp T M**, Yue J J, Garcia R, Schierjott R, Fritz B, Schilling C, Schwiesau J (2015). A new method to evaluate impingement in cervical and lumbar spinal disc arthroplasty in vitro. *21st Congress of the European Society of Biomechanics, July 5-9, Prague, Czech Republic.*

**Grupp T M**, Schierjott R A, Pfaff A, Tozzi G, Schwiesau J, Giurea A, Utzschneider S (2016). Carbon fiber reinforced PEEK in a rotating hinge knee design – a comparison of in vitro and retrieval findings. *24th Annual Meeting of the European Orthopaedic Research Society, September 14-16, Bologna, Italy.*

**Schierjott R A**, Hettich G, Schilling C, Maas A, Jansson V, Traina F, Grupp T M (2018). A method for quantitative analysis of large acetabular bone defects. *8th World Congress of Biomechanics, July 8 - 12, Dublin, Ireland.*

**Confirmation of co-authors**

The contributions of all co-authors (M. Baxmann, L. Cristofolini, P. Damm, H. Graichen, T. M. Grupp, G. Hettich, V. Jansson, F. Morosato, A. Ringkamp, M. Rudert, F. Traina, P. Weber) were confirmed and submitted separately. All named co-authors acknowledge the fact that the publications used within the present dissertation must not be part of another doctoral thesis.

## 1 Introduction

### 1.1 Overall research questions

The overall research questions of this dissertation were (1) which kind of acetabular bone defects in association with revision surgery exist clinically, (2) how these defects could be quantified and transferred to pre-clinical testing, and (3) how bone graft substitutes, used to treat these defects, could be tested pre-clinically in terms of primary stability.

The dissertation consists of three publications, whereby the first one is concerned with the quantitative analysis of acetabular bone defects based on clinical computed tomography (CT) data sets. The second and third publication are concerned with the development and application of a novel acetabular defect model to assess the primary stability of a press-fit cup in combination with bone chips and different bone graft substitutes (BGS) in a standardized way.

### 1.2 Total hip arthroplasty and reasons for revision

Total hip arthroplasty (THA) enables pain-relief, restoration of joint function and general improvement of quality of living in patients with end-stage osteoarthritis of the hip joint [1–3]. It represents one of the most frequently performed joint replacement surgeries [4,5] and is among the most cost-effective and successful orthopedic procedures [1,6].

Nevertheless, there is a risk of revision surgery, which correlates with patient age at primary implantation, patient gender and implant choice [7–9]. Numerous revision surgeries are reported by arthroplasty registries worldwide each year [10–13], including the Endoprothesenregister Deutschland (EPRD), which recorded 17 081 hip revision procedures in Germany in 2018 [13].

One of the main reasons for revision in THA is aseptic loosening [10–14], which is more common on the acetabular than on the femoral side [13]. Aseptic loosening can, among others, be caused by wear debris [15–18] or excessive relative motions between the implant and the surrounding bone [19,20].

Osseointegration of the implant, defined as direct formation of bone tissue in contact with the implant [21], is essential for long-term success of the joint replacement [22].

It is recognized that the limit of relative motion at the bone-implant-interface (BII) / bone-cement-interface (BCI) in order to achieve osseointegration is between 20  $\mu\text{m}$  and 150  $\mu\text{m}$  [23,24]. It seems that with 20-30  $\mu\text{m}$  relative motion, direct bone ingrowth can be achieved [23,24], whereas with 40  $\mu\text{m}$  relative motion either direct bone ingrowth [25] or a mixture of

bone ingrowth and fibrocallus may be present [23]. Relative motions of 150  $\mu\text{m}$  or greater have found to be associated with fibrous tissue formation around the implant which prevents osseointegration [23,24].

Fibrous tissue formation is related to the biological processes at the BII / BCI, i.e. proliferation and differentiation of pluripotential tissue after surgery, which can differentiate in bone, cartilage, or fibrous tissue [26]. This process is strongly affected by mechanical influences, i.e. relative motions [22], stresses [27] and strains at the BII / BCI [28].

The implantation surgery leads to bleeding and local tissue trauma which induces an acute inflammatory response in the bone and surrounding tissue [29,30]. Then, proliferation, differentiation, and maturation of osteoblast precursors is initiated by growth factors [22]. Additionally, osteoclastic precursors that resorb dead bony and cellular debris are stimulated by hormonal signals, autocrine and paracrine [22]. When the acute inflammation resolves, an initial trabecular bone layer can be found around the implant [22]. In case of excessive motions at the BII / BCI, the initial inflammation can become chronic and lead to the formation of fibrous tissue [22]. The presence of fibrous tissue leads to a “vicious circle”, in which relative motions at the BII are further increased due to the inferior mechanical properties of the fibrous tissue [31].

When eventually revision of a THA is required, for example due to the mentioned aseptic loosening, it is often associated with acetabular bone defects.

### 1.3 Acetabular bone defects

Numerous classification schemes have been published to characterize and grade acetabular bone defects, such as the American Academy of Orthopaedic Surgeons (AAOS), German society of Orthopedics and Traumatology (DGOT), Paprosky or Saleh classification [32–35]. They were introduced to provide a basis for communication among surgeons, to derive potential treatment options for the different defect types, and to compare treatment outcomes.

One of the most commonly used classification schemes was developed by Paprosky et al. [32,36]. Within this scheme, the acetabular bone defects can be distinguished into six different types, namely type 1, 2A, 2B, 2C, 3A and 3B (Figure 1) [32]. These are based on specific landmarks / parameters (implant position relative to the superior obturator line and Kohler's line, and degree of osteolysis of the teardrop figure and ischium) visible in conventional anterior-posterior radiographs [36,37].

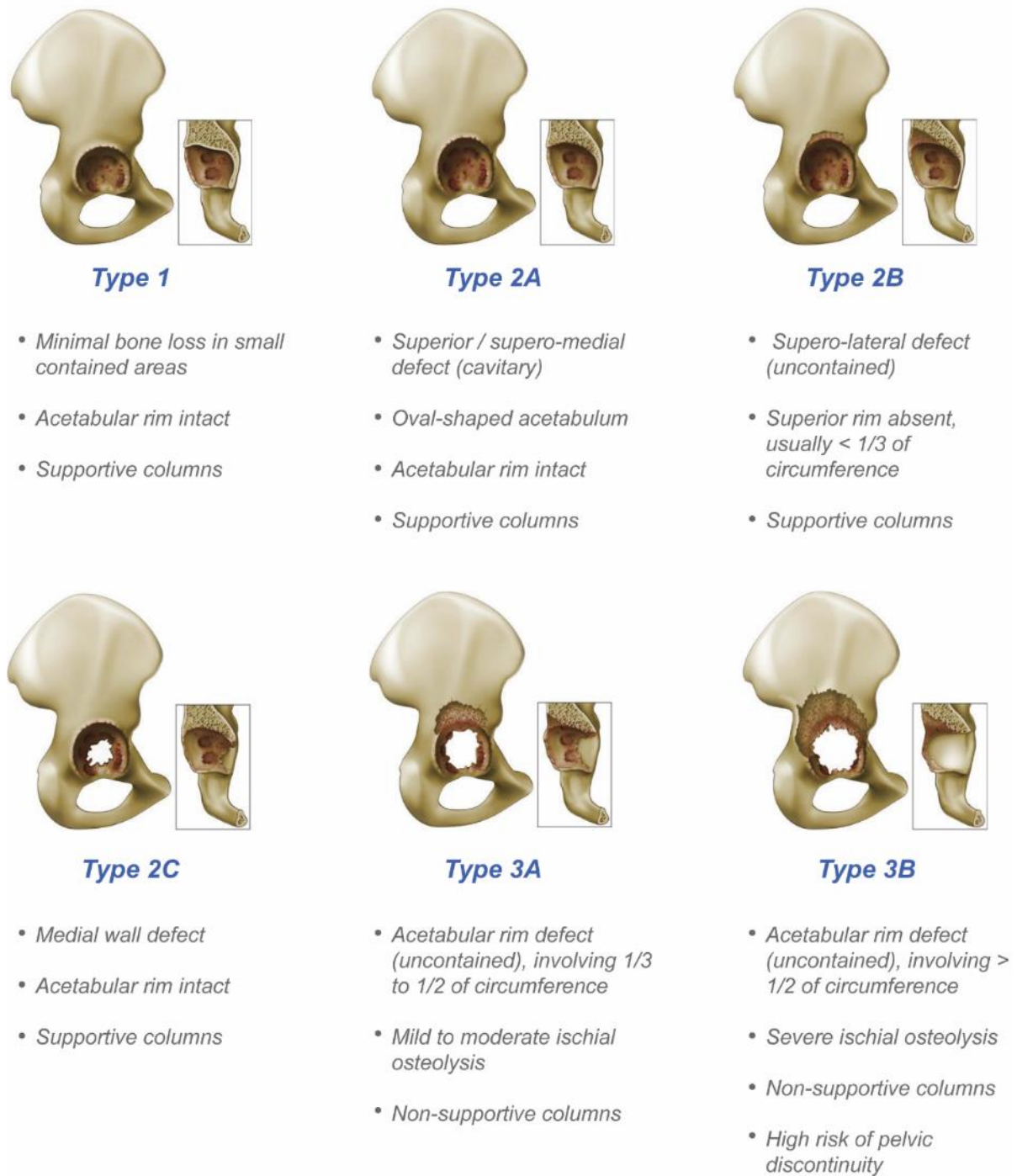


**Figure 1.** Overview of acetabular bone defect types according to Paprosky classification. Adapted and simplified from Wright and Paprosky, 2016 [36].

Although the Paprosky-classification is well-established, poor inter-observer reliability and intra-observer repeatability were found [38]. Paprosky, alongside with the other currently existing classification systems, is mainly descriptive and relies on the interpretation of plain radiographs which could be the reason for the partially reported poor reliability and

repeatability. Furthermore, the descriptive nature of these classification systems makes it difficult to transfer them to implant development and pre-clinical testing.

This resulted in the **first publication** of this dissertation, entitled “*Quantitative assessment of acetabular bone defects: A study of 50 computed tomography data sets*” with the overall aim to provide a basis for a quantitative, reproducible, objective and unambiguous classification scheme for acetabular bone defects.

The specific objectives were: (1) Definition of several parameters for the quantitative analysis of acetabular bone defects based on clinical computed tomography (CT) data, (2) Quantitative analysis of 50 acetabular bone defects using the defined parameters, (3) Assessment of potential correlations between the parameters.

50 clinical CT-data sets of pelvises with acetabular bone defects, provided from four European clinical centers, were segmented resulting in 50 3D-models of *defect pelvises*. Based on a method previously developed and validated within our research group (Hettich et al., 2018) [39], the native situation (*native pelvis*) of each individual defect pelvis was reconstructed using a statistical shape model (SSM), which consisted of 66 healthy pelvises.

In consultation with five senior hip revision surgeons, six analysis parameters with clinical relevance for revision treatment choice were defined for the quantitative assessment of the acetabular bone defects: Bone volume loss, new bone formation, lateral center-edge angle, ovality of the acetabulum, implant migration and wall defects.

Bone volume loss and new bone formation could be obtained by Boolean operations, i.e. subtraction of the *defect pelvis* 3D-model from the *native pelvis* 3D-model (bone volume loss) and vice versa (new bone formation). Four specific defect sectors (Cranial roof, Anterior column, Posterior column, and Medial wall) were defined to assess the distribution of bone volume loss within the acetabulum. Bone volume loss was assessed in terms of total volume in ml and relative bone volume loss in % in relation to the initial / native bone volume in each of the four defined defect sectors.

The 50 defect cases showed a large variation of values in all six analyzed parameters. Correlations between several parameters could be found, for example between bone volume loss in the Cranial roof and implant migration in cranial direction and lateral center-edge angle, respectively.

Based on the relative bone volume loss in each sector, defect groups could be derived. In order to do so, threshold values were defined in consultation with the senior hip revision surgeons to separate actual bone volume loss from reconstruction inaccuracies and to distinguish between minor bone loss and relevant bone loss.

Threshold values of 25% were defined for the Cranial roof, Anterior column, and Medial wall, oriented towards the definition of “moderate bone loss” in a study by Gelaude et al. [40]. Assuming that the Posterior column is critical for implant stability, a more conservative threshold of 15% bone volume loss was defined for this sector. Applying these thresholds to the relative bone volume loss results of the 50 analyzed defects, defect groups could be defined based on the combination of defect sectors concerned with relevant bone volume loss. This scheme mathematically results in a total of 16 defect groups. Within the 50 analyzed CT-data sets, not all of the 16 possible groups have yet been represented. However, an abstract of the represented groups, including an exemplary defect case each, is shown in Figure 2.

The obtained quantitative information, as well as the information about the defect geometry could now be used to transfer clinically existing defects to pre-clinical testing. Moreover, the presented defect categories based on the distribution of relative bone volume loss and specific thresholds could represent an approach towards an unambiguous, objective and reproducible defect classification method, which could ease communication among surgeons, facilitate treatment choice and improve comparability among studies.

Future work should include the analysis of additional defects, alongside with the chosen treatment strategies and the validation of the chosen thresholds for relevant bone volume loss.

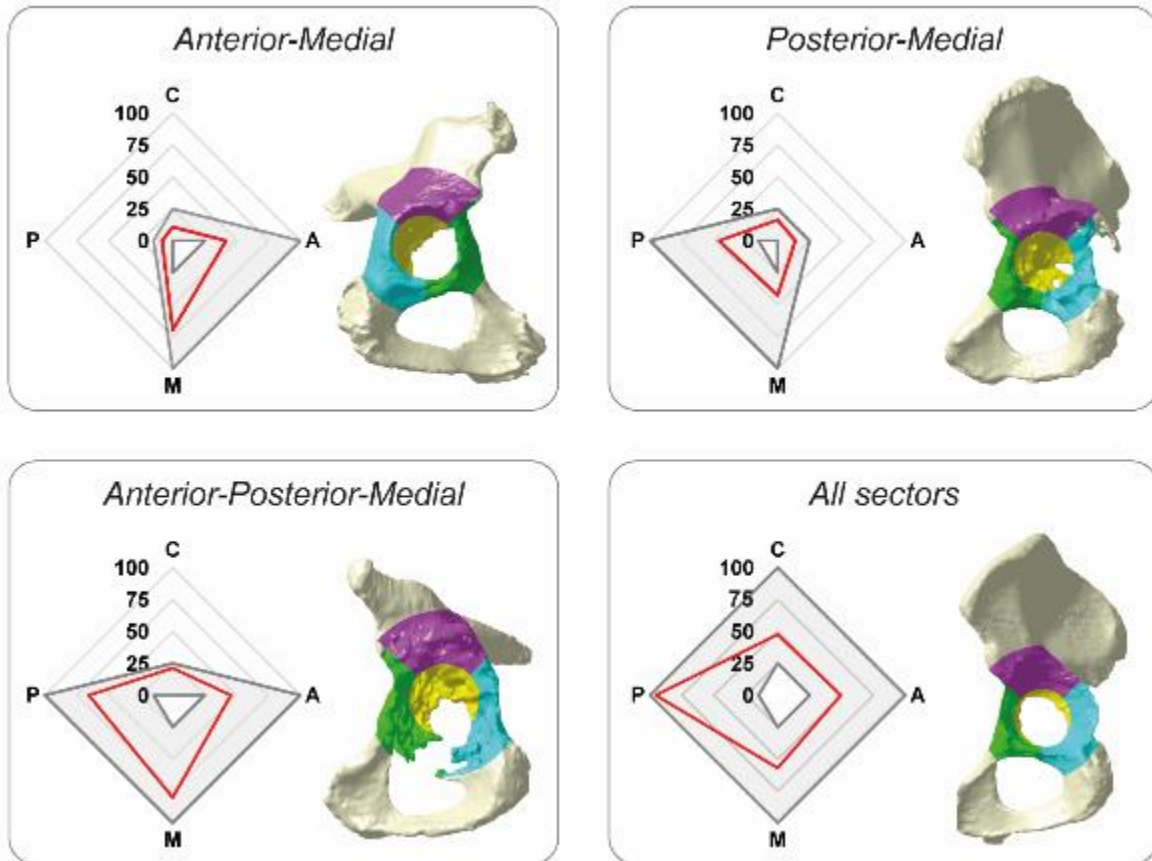


**Figure 2.** Abstract of derived bone defect groups based on the distribution of relative bone volume loss in % among the sectors Cranial roof (C), Anterior column (A), Posterior column (P) and Medial wall (M). Four defect groups with one case each are exemplarily shown (Anterior-Medial, Posterior-Medial, Anterior-Posterior-Medial, All sectors). The spider plots depict the definitions of the defect groups based on the thresholds for relative bone volume loss of 25% (C, A, M) and 15% (P) in gray and the distribution of relative bone volume loss of the individual cases (red lines). The 3D-models of the individual cases with color-coded defect sectors (C: purple, A: green, P: blue, M: yellow) are shown to the right. Adapted from Schierjott et al. [41].

## 1.4 Acetabular revision treatment

Acetabular revision surgeries aim to achieve stable implant fixation, reconstruction of the center of rotation (CoR) and functioning hip biomechanics, as well as restoration of bone stock [42]. Thereby, the revision situation is often associated with bone loss and variation in bone quality [43,44]. This requires, besides standard hemispherical press-fit cups, specific treatment options, such as jumbo or oblong revision cups, augments, reinforcement rings, reconstruction cages, cup-cage-constructs, or impaction bone grafting (IBG), to mention just a few of the applied techniques (Figure 3, Figure 4).

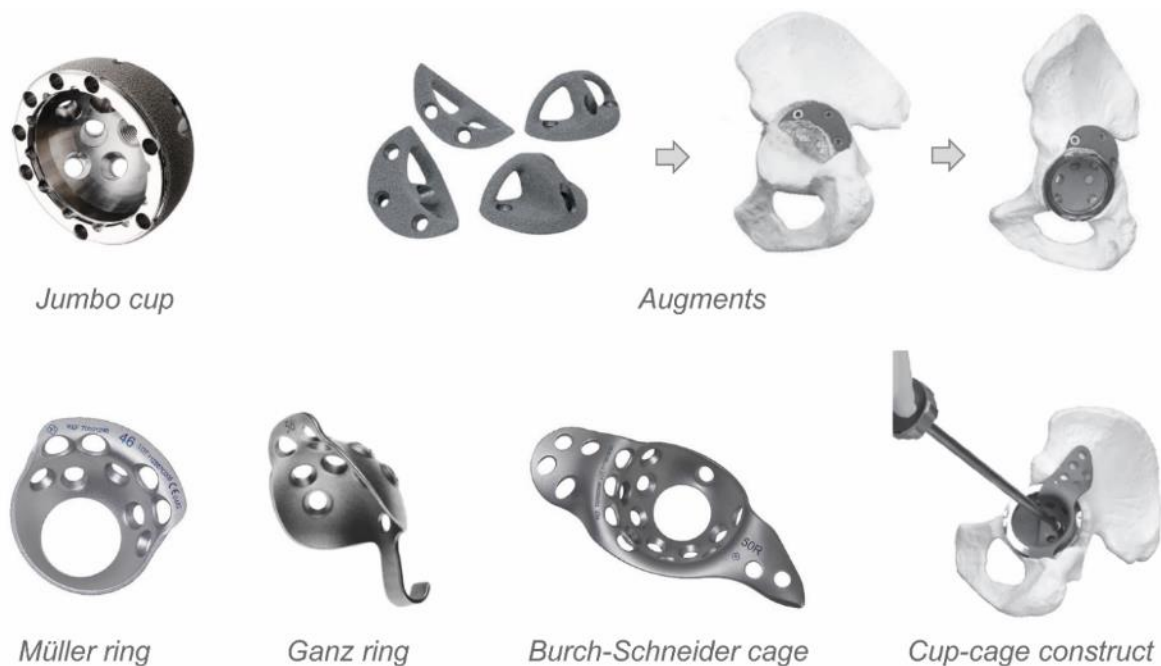


**Figure 3.** Overview of a few of the available acetabular revision implants. Images adapted from DePuy Synthes, Zimmer Biomet, implantcast and Kawanabe et al. 2011 [45–50].

Standard hemispherical press-fit cups can be used in mainly cavitory defects, in which more than 50% of host bone contact is still present and a stable press-fit fixation can be achieved by a 3-point-clamping [51]. Bone screws are often used for additional fixation [51].

In addition to the standard press-fit cups, so called jumbo cups with increased outer diameter and oblong cups with screw holes for fixation are available [52,53].

Augments are metallic structures in form of different spherical segments in different sizes which are combined with acetabular cups and which can provide stability in segmental, i.e. rim defects [54].

Reinforcement rings are available as Ganz type and Müller type and are typically used in cavitory defects, medium-sized defects of the medial wall or anterior column defects and can be combined with allograft defect filling [51]. Both types provide several screw holes for

fixation in the cranial roof / cranial rim and the Ganz type provides an additional caudal hook for fixation in the incisura acetabuli [51]. In these reinforcement rings, a polyethylene (PE) cup is fixed with bone cement [51].

Reconstruction cages (e.g. Burch-Schneider cages) have two flaps which can be bent to fit to the pelvic bone and can be used in larger defects with involvement of both columns [51]. The proximal flange is screwed on the iliac bone, and the distal flange is anchored into the ischium or, in few cases, fixed to it with screws [51]. As in the reinforcement rings, a PE cup is fixed in the cages to serve as articulation surface [51]. Reconstruction cages are often used in combination with allografts in larger acetabular defects [55–57]. Due to their concept of “bridging” the defect from host-bone to host-bone, they provide protection of the underlying bone graft from overload and hence potential for best possible osseointegration of the graft [42,51].

Allografts, i.e. grafts from human donors are provided via bone banks and are used in form of structural / bulk allografts, i.e. a part of the femoral head, acetabulum, distal femoral condyle or proximal tibia [58,59], or in form of morsellized allografts, i.e. bone chips [60,61]. Bulk allografts can be used as alternative to metallic augments [62,63], whereas bone chips are typically used for the impaction bone grafting technique [60,61,64]. For this purpose, primarily fresh-frozen human donor femoral heads are used [65,66]. After thawing, they are divided into several parts and using a bone rongeur or a bone mill, bone chips of different sizes are prepared [61,65]. Cancellous bone chips are preferred in revision arthroplasty due to their osteogenic features [67].

The chips are compacted in the defect acetabulum with hemispherical impactors and an orthopedic hammer [60,65]. In presence of uncontained defects, the bone grafts can be compacted on a metal mesh, a technique which was found to be successful for medial defects, but critical in case of segmental defects [66]. After compaction, a press-fit cup, cemented PE cup, reinforcement ring or reconstruction cage is implanted on the graft material (Figure 4) [61,64,68].

IBG enables the restoration of bone stock [61] as the bone graft is gradually incorporated and replaced by newly formed bone [69]. This is especially important to provide an improved situation for potential re-revisions, i.e. a so-called “defect downsizing” [70]. However, the applied bone chips are expensive and limited in supply. Moreover, they are time-consuming to produce in the operating room (OR) and differ in quality due to biological variation and the preparation technique used [71]. In addition, despite careful choice of donors and processing to limit infection risk, a risk of disease transmission remains [71].

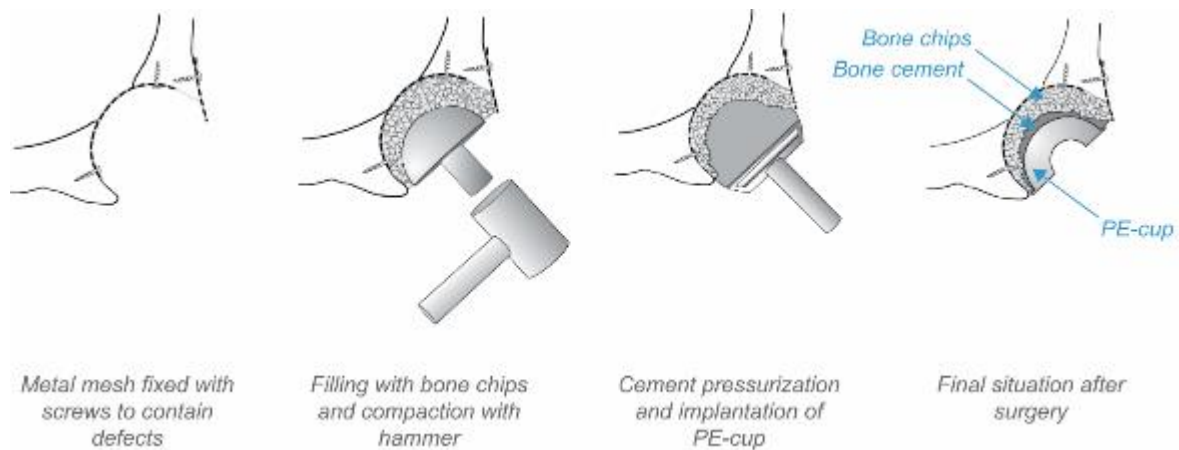


**Figure 4.** Impaction bone grafting technique, exemplarily shown with metal mesh and cemented PE-cup. Adapted from van Haaren [72].

Synthetic bone graft substitutes (BGS) may represent an attractive alternative and have to fulfill the following requirements to represent an ideal substitute for bone chips [73]:

- Biocompatibility
- Surface that supports cell adhesion, proliferation, and differentiation and hence osseointegration
- Be bioresorbable and ideally completely replaceable by endogenous bone
- Be sterilizable without change in properties
- Cost-effective production of 3D structures in different shapes and sizes
- Interconnecting porosity to enable cell ingrowth and vascularization
- Mechanical stability to allow weight bearing as soon as possible

During the last years, numerous BGS have been developed as supplement or alternative to allograft bone chips. These BGS are often based on hydroxyapatite (HA), tricalcium phosphate (TCP), TCP-HA mixtures, titanium (Ti) or bioactive glass (b.a.glass) and provided in form of granules [74–78], scaffolds [79] or cement [80].

However, clinical application in acetabular bone defects has yet only been reported for few of them [74,75]. This is most likely related to the fact that in load-bearing situations, such as in the acetabulum, it is difficult to achieve the required properties porosity, resorbability and mechanical stability as these are conflicting to a certain extent [73].

Some BGS have been tested in vitro concerning primary stability or mechanical properties in artificial acetabular defects [80–84]. These defects were applied in a variety of locations and their shape was strongly simplified to cylinders, hemispheres, or other spherical segments. Clinically existing defects on the other hand, have been found to have a rather complex shape with involvement of several acetabular areas [36,41,85], which demands a

less simplified defect implementation procedure. Moreover, in the previous in vitro studies, the defects were implemented at numerous different locations in different sizes, depending on the type of treatment to be tested. This limits comparability between the studies i.e. between the outcomes of the different treatment strategies.

This resulted in the **second publication** entitled “*A method to assess primary stability of acetabular components in association with bone defects*” with the following aims: (1) Development of a simplified acetabular bone defect model based on a clinically existing defect, (2) Derivation of three additional, less severe bone defect increments from the simplified defect in order to build up a stepwise testing procedure to test different treatment strategies in defects with increasing severity, and (3) Assessment of the influence of an acetabular bone defect and defect filling on the primary stability of a press-fit cup.

Based on the quantitative acetabular bone defect analysis [39,41], a representative clinical defect was chosen in consultation with five senior hip revision surgeons. The defect was described as common and likely to be treated (among others) with bone chips.

A simplified version of this defect was developed with the following aims: Implementation with hemispherical acetabular reamers to enable application of this procedure also in human donor specimens using simple tools; Possibility to derive several bone defect increments; Preservation of main characteristics of the defect including geometry and bone volume loss.

Under application of nine hemispherical reaming procedures, the defect could be simplified (increment 4) and showed an overall volume conformity of >99% with the original defect volume, a comparable bone volume loss distribution among the defect sectors and a comparable shape (more detailed information can be found in the additional content II). Three additional, less severe bone defect increments (increments 1-3) could be derived from the simplified defect (increment 4) by exclusion of specific reaming procedures (Figure 5).

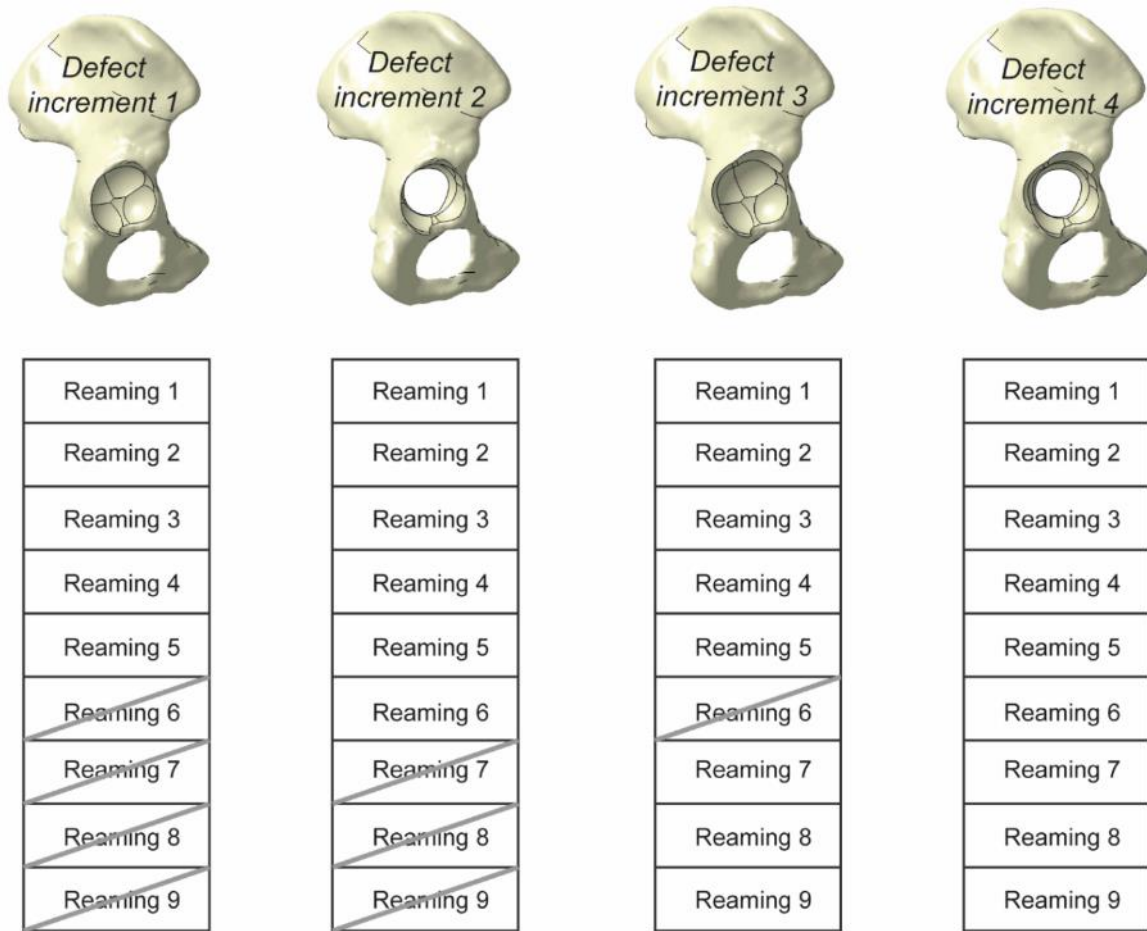


**Figure 5.** Overview of bone defect increments derived from the simplified defect (increment 4) by exclusion of specific reaming procedures as indicated in the tables. Adapted from Schierjott et al. [86].

The smallest bone defect increment (increment 1: Mainly medial, contained defect with posterior-inferior rim damage) was implemented in an especially therefore developed acetabular test model made of polyurethane foam.

In order to investigate the influence of bone defect and bone defect filling on the primary stability of a press-fit cup, three test groups (N = 6 each) were defined: *Primary* (acetabular test model without defect, treated with press-fit cup), *Defect* (acetabular test model with defect, treated with press-fit cup), and *Filled* (acetabular test model with defect, treated with BGS and press-fit cup). BGS in form of  $\beta$ -TCP-HA pyramid-shaped granules in a polyethylene glycol-glycerol (PEG) matrix was used.

The specimens were placed under a servo-hydraulic testing machine and loaded dynamically in a sinusoidal wave form in direction of the maximum resultant force during level walking. Relative motions between cup and acetabular test model were measured in 3D using tracking points and the optical measurement system GOM Pontos (GOM GmbH Braunschweig, Germany).

The test groups were compared concerning inducible displacement, migration, total motion and resultant cup tilt. It was found that the implemented acetabular bone defect had a detrimental effect on primary stability, but that primary stability could mostly be reestablished by defect filling.

In the future, the developed test model including the four bone defect increments could be used to test and compare different treatment strategies in defects with increasing severity.

The previously mentioned synthetic BGS could be an attractive alternative to bone chips to increase the reproducibility of the mechanical properties and to decrease the infection risk. However, it had to be assessed whether their performance is comparable (or maybe even superior) to the performance of bone chips, which represent the current gold standard in this application.

This resulted in the **third publication** entitled “*Primary stability of a press-fit cup in combination with impaction grafting in an acetabular defect model*” with the following aims: (1) Assessment of the primary stability of a press-fit cup in combination with compacted bone chips in the previously developed acetabular defect model, (2) Comparison with the primary stability achieved by defect filling with two different BGS ( $\beta$ -TCP tetrapods in a collagen matrix and bioactive glass granules in a PEG matrix).

As basis for this publication the acetabular test model with bone defect increment 1, developed in the second publication, was used, whereby the wall thickness was increased to enable compaction of the filling material similar to the techniques applied in the OR.

In order to compare the primary stability achieved by the BGS with bone chips, three test groups (N = 6 each) were defined: *Bone chips* (cancellous bone chips from donor femoral heads), *b.a.glass+PEG* (bioactive glass S53P4 granules in a PEG matrix) and *tetrapods+coll* ( $\beta$ -TCP tetrapods in a collagen matrix).

The specimens were loaded dynamically in direction of the maximum resultant force during level walking with stepwise increased maximum load. Relative motions between cup and acetabular test model were measured at the end of each load step using tracking points and the optical measurement system GOM Pontos.

It was found that the course of inducible displacement was comparable among the three test groups with highest values for *bone chips* and lowest values for *b.a.glass+PEG* at the last load step (3000 N). Migration was predominant in *b.a.glass+PEG* and lowest for *tetrapods+coll*.

It could be concluded that *tetrapods+coll* may represent an attractive alternative to *bone chips*, showing a comparable performance and even smaller relative motions towards higher loads than bone chips. However, this can yet only be concluded for this specific

defect used in this study and primary stability should be further assessed in additional / more severe defects.

## 1.5 Conclusions

Within this dissertation, 50 acetabular bone defects associated with revision surgery were successfully quantified. To the author's knowledge, it was the first study to analyze such a large number of defects under application of several parameters. The results showed a large variation among the defects, yet it was possible to identify correlations between several parameters and derive possible defect groups.

The large variation of bone defects and their complex shapes suggested that actual clinical defect cases should be used as basis for pre-clinical testing, rather than theoretical and strongly simplified defect shapes as in most previous in vitro studies.

A representative clinical bone defect case was simplified to a model defect while still preserving the main defect characteristics and defect increments were derived thereof. In the future, these could be used as part of a platform concept to test and compare different treatment strategies in defects with different severities.

Using the developed test model, it could be shown that the acetabular bone defect had a detrimental effect on the primary stability of a press-fit cup. However, defect filling with a BGS could mostly reestablish primary stability, i.e. reduce relative motions to a level at which osseointegration might still be possible.

By comparing the primary stability of a press-fit cup in combination with bone chips and two different bone graft substitutes, it was seen that the BGS consisting of  $\beta$ -TCP and collagen achieved results similar to the bone chips. This suggests that this BGS might be an attractive alternative to bone chips, providing more reproducible mechanical properties, lower infection risk and improved availability.

However, besides the assessed primary stability, other factors such as the potential for osseointegration are vital for the clinical long-term success of the material and should be further assessed in large-animal studies or mechano-biological models.

## 1.6 Author contribution

### **First publication:**

Within the first publication, the author of this dissertation (RS) contributed to the study design and definition of analysis parameters. She performed the analysis based on the 3D-models in the CAD-software, as well as the statistical evaluation and was responsible for the interpretation of results. In addition, she was responsible for drafting the manuscript, including the illustrations, as well as for the further submission and review process.

### **Second publication:**

Within the second publication, RS was responsible for the study design and the analysis methods used. She developed the acetabular test model and the simplified bone defect based on a clinical case. She performed preliminary tests and supervised the primary stability test series, which were performed by AR. RS further supervised the statistical analysis (AR) and was responsible for the interpretation of the results. In addition, RS was responsible for drafting the manuscript, including the illustrations, as well as for the further submission and review process.

### **Third publication:**

Within the third publication, RS was responsible for the study design and the analysis methods used. She prepared and performed the primary stability tests, as well as the relative motion analysis and statistical evaluation. Moreover, she was responsible for the interpretation of results, for drafting the manuscript, including illustrations, as well as for the following submission and review process.

## 2 Zusammenfassung (Deutsch)

### Zielformulierung

Ziel der vorliegenden Doktorarbeit war es, zu ermitteln, welche acetabulären Knochendefekte im Zusammenhang mit Revisionseingriffen vorliegen und diese zu quantifizieren. Des Weiteren sollte ein in vitro Testmodell entwickelt werden, um den Einfluss eines Defekts und einer Defektfüllung auf die Primärstabilität einer Press-fit-Pfanne zu untersuchen. Abschließend sollte untersucht werden, ob die Wahl des Füllmaterials einen Einfluss auf die Primärstabilität der Pfanne hat, bzw. ob durch synthetische Knochenersatzmaterialien (KEM) eine ähnliche Primärstabilität wie mit dem Goldstandard Knochenchips erzielt werden kann.

### Hintergrund

Die aseptische Lockerung ist einer der Hauptrevisionsgründe bei Hüft-Totalendoprothesen (Hüft-TEP). Diese kann, neben der häufiger ursächlichen partikelinduzierten Osteolyse, unter anderem auch durch zu große Relativbewegungen zwischen Implantat und Knochen bedingt sein, die zur Bildung einer Bindegewebsmembran, einer weiteren Lockerung und letzten Endes zur Revision des Implantats führen.

Revisions-Operationen sind häufig mit acetabulären Knochendefekten infolge periprothetischer Osteolysen verbunden, welche die darauffolgende Implantatfixierung erschweren. Für diese Knochendefekte existiert eine Vielzahl von Klassifikationsmethoden, welche jedoch größtenteils deskriptiv sind und deshalb nur schwer in die Implantatentwicklung und prä-klinische Prüfung übertragbar sind.

Für die Versorgung der Knochendefekte wird eine Vielzahl verschiedener Implantatsysteme und Methoden eingesetzt, unter anderem die „Impaction bone grafting“-Technik, bei der Knochenchips in einem Defekt komprimiert und mit einer Pfanne, einer Pfannendachschale oder Stützschale kombiniert werden. Knochenchips haben jedoch auch einige Nachteile wie beispielsweise ihre begrenzte Verfügbarkeit und das verbleibende Infektionsrisiko. Synthetische KEM könnten eine attraktive Alternative darstellen, jedoch wurde ihr Potential zur Wiederherstellung der Primärstabilität in Kombination mit Press-fit-Pfannen bisher kaum untersucht.

### Material und Methode

In einem ersten Schritt wurden 50 Computertomographie-Datensätze (CT-Datensätze) von Becken mit acetabulären Knochendefekten anhand von sechs Parametern ausgewertet und quantifiziert. Hierzu wurden virtuelle 3D-Modelle der Defektbecken erstellt und ihr jeweiliger „nativer“ Zustand über ein statistisches Formmodell rekonstruiert. Dadurch

konnten unter anderem der Knochenvolumenverlust und die Knochenneubildung in einzelnen Bereichen des Acetabulums bestimmt werden.

Basierend auf der Defektanalyse wurde gemeinsam mit den klinischen Beratern ein repräsentativer Fall als Grundlage für die darauffolgenden prä-klinischen Tests ausgewählt. Um den Defekt später mit einfachen Hilfsmitteln auch in humane Spenderbecken einbringen zu können, wurde seine Geometrie vereinfacht. Hierfür wurden neun Fräsoperationen mit hemispherischen Acetabulumfräsern definiert, um den Defekt mit seinen wichtigsten Charakteristiken zu reproduzieren.

Von dem so entstandenen „Gesamtdefekt“ (Defektstufe 4) wurden drei zusätzliche, weniger schwerwiegende Defektstufen (Defektstufe 1-3) abgeleitet, indem bestimmte Fräsoperationen ausgeschlossen wurden. Auf diese Weise wurde ein Plattformkonzept mit unterschiedlichen Defektstufen entwickelt, um zukünftig verschiedene Revisionsimplantate bzw. Versorgungsstrategien schrittweise in immer schwerwiegenderen Defektstufen testen zu können.

Es wurde ein vereinfachtes Acetabulummodell (AM) aus Polyurethan-Schaum entwickelt, in welches der Defekt (Defektstufe 1: Hauptsächlich medialer, umschlossener Defekt mit posterior-inferiorem Randdefekt) eingebracht wurde.

Insgesamt wurden sechs Testgruppen im Rahmen der Dissertation auf ihre Primärstabilität untersucht: Primärsituation (AM ohne Defekt, versorgt mit Press-fit-Pfanne), Defektsituation (AM mit Defekt, versorgt mit Press-fit-Pfanne) und vier Varianten von Defektfüllungen (AM mit Defekt, versorgt mit Press-fit-Pfanne und Knochenchips bzw. drei verschiedenen KEM). Die Proben wurden dynamisch belastet und die Primärstabilität wurde in Form von Relativbewegungen (reversible Bewegungen und Migration) zwischen Press-fit-Pfanne und AM mit Hilfe eines optischen Messsystems untersucht.

### **Ergebnisse**

Bei der Analyse der Defekte wiesen die Messwerte der untersuchten Parameter eine sehr große Bandbreite auf. Dennoch konnten Korrelationen zwischen einzelnen Analyseparametern ermittelt und eine erste Einteilung in mehrere Defektgruppen vorgenommen werden.

Der für die prä-klinischen Tests ausgewählte Defekt konnte mithilfe mehrerer Fräsoperationen in einer vereinfachten Weise reproduziert werden, wobei der artifizielle Defekt eine Übereinstimmung des Gesamtvolumens von >99% mit dem Originaldefekt und eine vergleichbare Geometrie zeigte.

Der in Publikation 2 implementierte Defekt (Defektstufe 1: Hauptsächlich medialer, umschlossener Defekt mit posterior-inferiorem Randdefekt) führte zu einem Anstieg der Relativbewegungen gegenüber der Primärsituation (1,9-fache reversible Bewegung und

8,2-fache Migration), welche sich durch die Defektfüllung wieder reduzieren ließen (1,1-fach bzw. 2,4-fach gegenüber Primärsituation).

Bei dem Vergleich der Defektfüllung mit Knochenchips und zwei verschiedenen KEM in Publikation 3 (bioaktives Glas in PEG-Matrix und  $\beta$ -TCP Tetrapoden in Collagen-Matrix) zeigte sich, dass sich  $\beta$ -TCP Tetrapoden in Collagen-Matrix unter Last ähnlich verhielten wie Knochenchips bzw. ähnliche Relativbewegungen aufwiesen und somit eine attraktive Alternative zum Goldstandard Knochenchips darstellen könnten.

### **Diskussion und Ausblick**

Im Rahmen dieser Doktorarbeit konnten acetabuläre Knochendefekte erfolgreich quantifiziert, und ein repräsentativer Defekt in einen in vitro Testaufbau übertragen werden. Die Defektanalysemethodik könnte zukünftig dazu verwendet werden, eine quantitative, vom jeweiligen Anwender unabhängige, reproduzierbare Defektklassifikation zu etablieren. Hierfür ist jedoch die Untersuchung einer noch größeren Anzahl von Defekten notwendig, wobei auch die jeweils gewählten Defektversorgungen und deren klinischer (Langzeit-) Erfolg analysiert werden sollten.

In den durchgeführten in vitro Tests wurde der negative Einfluss eines Defektes auf die Primärstabilität einer zementfreien Versorgung dargelegt und das Potential bestimmter KEM aufgezeigt, zukünftig Knochenchips als Füllmaterial zu ersetzen. Diesbezüglich vorteilhaft sind die zuverlässig reproduzierbaren mechanischen Eigenschaften, das verringerte Infektionsrisiko und die bessere Verfügbarkeit der KEM.

An dieser Stelle muss jedoch betont werden, dass die Fähigkeit bestimmter KEM, die Primärstabilität wiederherzustellen, bisher nur in einem spezifischen Defekt getestet wurde und nicht direkt auf alle Defekttypen übertragbar ist. Folglich sollte in Zukunft die Primärstabilität in weiteren bzw. größeren Modelldefekten untersucht werden, um zusätzliche Informationen über mögliche Limitationen des Materials und Voraussetzungen für dessen Einsatz zu erhalten. Zusätzlich zur Primärstabilität sollte außerdem untersucht werden, ob sich KEM bezüglich der Dauerfestigkeit und des Osseointegrationspotentials (Struktur und Oberflächeneigenschaften, die das Einwachsen von Knochensubstanz ermöglichen) als Ersatz für Knochenchips eignen, da diese Faktoren ebenfalls maßgeblich für den klinischen Langzeiterfolg der Versorgung sind.

### **3 Abstract (English)**

#### **Objectives**

The objectives of this dissertation were to assess which acetabular bone defects associated with revision surgery exist and to analyze these defects in a quantitative way. Furthermore, the aim was to develop an acetabular bone defect model to assess the influence of bone defect and bone defect filling on the primary stability of a press-fit cup, and to ascertain whether the type of filling material influences primary stability, i.e. if synthetic BGS can achieve primary stability comparable to the gold standard bone chips.

#### **Background**

Aseptic loosening is one of the main reasons for revision in THA. This is most commonly caused by particle-induced osteolysis but can, besides others, also be induced by excessive relative motion between implant and bone, which leads to the formation of fibrous tissue and further loosening, eventually resulting in revision surgery.

Revision surgery is often associated with acetabular bone defects due to periprosthetic osteolysis, which make the following implant fixation difficult. In order to categorize the defects, numerous classification schemes have been published. However, most of them are rather descriptive and hence difficult to transfer to implant development or pre-clinical testing.

To treat the defects, numerous implant systems and treatment strategies exist, besides others the impaction bone grafting technique (IBG), whereby bone chips are compacted into a defect and combined with a cup, reinforcement ring or reconstruction cage. However, the bone chips have some disadvantages such as limited supply and remaining infection risk. Synthetic bone graft substitutes (BGS) may represent an attractive alternative, but their potential to reestablish primary stability in combination with press-fit cups has yet hardly been assessed.

#### **Materials and methods**

First, 50 computed tomography (CT) data sets of pelvises with acetabular bone defects were analyzed and quantified using six parameters. In order to do so, virtual 3D models of the defect pelvises were created, and the corresponding “native” situation was reconstructed via a statistical shape model (SSM) for each pelvis individually. Based on these models, parameters such as bone volume loss and new bone formation in specific areas of the acetabulum could be assessed.

On the basis of the quantitative defect analysis, a representative defect was chosen in consultation with the clinical advisors for the following pre-clinical tests. In order to later on enable defect implementation with simple tools in human donor specimens, its geometry

was simplified. For this purpose, nine reaming procedures with hemispherical reamers were defined in order to reproduce the defect with its main characteristics.

From the resulting “complete defect” (defect increment 4), three additional, less severe bone defect increments were derived by exclusion of specific reaming procedures (defect increments 1-3). The resulting platform concept was developed to test different revision treatment strategies in defects with increasing severity in the future.

A surrogate acetabular model (AM) made of polyurethane foam was developed, in which the defect (increment 1: Mainly medial contained defect with damage of the posterior-inferior rim) was implemented.

Within this dissertation, a total of six test groups were investigated concerning their primary stability: Primary situation (AM without defect, treated with press-fit cup), defect situation (AM with defect, treated with press-fit cup), and four different types of defect filling (AM with defect, treated with press-fit cup and bone chips / three different types of BGS).

The specimens were loaded dynamically and primary stability in terms of relative motion between cup and AM (inducible displacement and migration) were assessed using an optical measurement system.

## **Results**

The defect analysis showed a large variation of values in all analyzed parameters. However, correlations between single analysis parameters could be observed and first defect groups could be established.

The representative defect chosen for the pre-clinical tests could be reproduced in a simplified way using several reaming procedures, whereby the simplified defect showed a total volume conformity of >99% with the original defect, as well as a comparable geometry. The defect implemented in publication 2 (increment 1: Mainly medial contained defect with damage of the posterior-inferior rim) led to an increase in relative motion compared to the primary situation without defect (1.9-fold increase of inducible displacement and 8.2-fold increase in migration). By filling the defect, this could be reduced again to 1.1-fold increase and 2.4-fold increase in comparison with the primary situation, respectively.

Within the comparison of bone chips with two BGS in publication 3 (bioactive glass in PEG and  $\beta$ -TCP tetrapods in collagen) it was seen that the  $\beta$ -TCP tetrapods in collagen matrix showed a behavior comparable to bone chips, i.e. comparable relative motions and could hence represent an attractive alternative to the gold standard bone chips.

## **Discussion and outlook**

Within this dissertation, acetabular bone defects could successfully be quantified, and one representative defect was transferred into a pre-clinical testing model.

In the future, the defect analysis method could potentially be used to establish a quantitative, impartial, reproducible defect classification. In order to do so, an even larger number of defects should be analyzed, also in association with the chosen defect treatment and clinical (long-term) treatment success.

In the performed in vitro tests, the negative influence of a defect on primary stability of a press-fit cup could be shown, as well as the potential of certain BGS to reestablish primary stability and hence to potentially substitute bone chips in the future. Benefits of the BGS would be the reproducible mechanical characteristics, the reduced infection risk and the improved availability.

However, it is important to point out that the ability of specific BGS to reestablish primary stability was so far assessed in one specific defect and the results may be different in another defect type. Hence, primary stability should further be investigated in additional and more severe defects to obtain additional information about potential limitations of the material or prerequisites for its application. Moreover, it should be assessed whether the durability and the potential for osseointegration (pore structure and surface properties to enable bone ingrowth) of the BGS are sufficient to substitute bone chips, as these factors also influence the clinical long-term success of the defect treatment.

## 4 Publications

### 4.1 Publication I: Quantitative assessment acetabular bone defects: A study of 50 computed tomography data sets

Authors: Ronja A Schierjott, Georg Hettich, Heiko Graichen, Volkmar Jansson, Maximilian Rudert, Francesco Traina, Patrick Weber, Thomas M Grupp

Journal: PLoS ONE

Volume: 14

Pages: 1-22

Year: 2019

DOI: <https://doi.org/10.1371/journal.pone.0222511>

Impact factor: 2.776 (according to InCites Journal Citation Reports 2018)

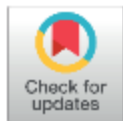
## RESEARCH ARTICLE

# Quantitative assessment of acetabular bone defects: A study of 50 computed tomography data sets

Ronja A. Schierjott<sup>1,2\*</sup>, Georg Hettich<sup>1</sup>, Heiko Graichen<sup>3</sup>, Volkmar Jansson<sup>2</sup>, Maximilian Rudert<sup>4</sup>, Francesco Traina<sup>5,6</sup>, Patrick Weber<sup>2</sup>, Thomas M. Grupp<sup>1,2</sup>

**1** Research & Development Department, B. Braun Aesculap AG, Tuttlingen, Germany, **2** Department of Orthopaedic Surgery, Physical Medicine & Rehabilitation, Ludwig-Maximilians-University Munich, Campus Grosshadern, Munich, Germany, **3** Department for Arthroplasty and General Orthopaedic Surgery, Orthopaedic Hospital Lindenlohe, Schwandorf, Germany, **4** Department of Orthopaedic Surgery, König-Ludwig-Haus, Julius-Maximilians-University Würzburg, Würzburg, Germany, **5** Ortopedia-Traumatologia e Chirurgia Protetica e dei Reimpianti d'Anca e di Ginocchio, Istituto Ortopedico Rizzoli di Bologna, Bologna, Italy, **6** Dipartimento di Scienze Biomediche, Odontoiatriche e delle Immagini Morfologiche e Funzionali, Università Degli Studi Di Messina, Messina, Italy

\* [ronja\\_alissa.schierjott@aesculap.de](mailto:ronja_alissa.schierjott@aesculap.de)



## OPEN ACCESS

**Citation:** Schierjott RA, Hettich G, Graichen H, Jansson V, Rudert M, Traina F, et al. (2019) Quantitative assessment of acetabular bone defects: A study of 50 computed tomography data sets. *PLOS ONE* 14(10): e0222511. <https://doi.org/10.1371/journal.pone.0222511>

**Editor:** Stuart Barry Goodman, Stanford University, UNITED STATES

**Received:** March 18, 2019

**Accepted:** August 31, 2019

**Published:** October 17, 2019

**Copyright:** © 2019 Schierjott et al. This is an open access article distributed under the terms of the [Creative Commons Attribution License](https://creativecommons.org/licenses/by/4.0/), which permits unrestricted use, distribution, and reproduction in any medium, provided the original author and source are credited.

**Data Availability Statement:** All relevant data are within the manuscript and its Supporting Information files.

**Funding:** Three of the authors (RS, GH, TG) were funded by B. Braun Aesculap AG, Tuttlingen (<https://www.bbraun.com/en/company/organization-facts-figures/bbraun-aesculap-partner-for-surgery.html>). The funder provided support in the form of salaries for authors RS, GH, and TG, but did not have any additional role in the study design, data collection and analysis, decision

## Abstract

### Objectives

Acetabular bone defect quantification and classification is still challenging. The objectives of this study were to suggest and define parameters for the quantification of acetabular bone defects, to analyze 50 bone defects and to present the results and correlations between the defined parameters.

### Methods

The analysis was based on CT-data of pelvises with acetabular bone defects and their reconstruction via a statistical shape model. Based on this data, bone volume loss and new bone formation were analyzed in four sectors (cranial roof, anterior column, posterior column, and medial wall). In addition, ovality of the acetabulum, lateral center-edge angle, implant migration, and presence of wall defects were analyzed and correlations between the different parameters were assessed.

### Results

Bone volume loss was found in all sectors and was multidirectional in most cases. Highest relative bone volume loss was found in the medial wall with median and [25, 75]—percentile values of 72.8 [50.6, 95.0] %. Ovality, given as the length to width ratio of the acetabulum, was 1.3 [1.1, 1.4] with a maximum of 2.0, which indicated an oval shape of the defect acetabulum. Lateral center-edge angle was 30.4° [21.5°, 40.4°], which indicated a wide range of roof coverage in the defect acetabulum. Total implant migration was 25.3 [14.8, 32.7] mm, whereby cranial was the most common direction. 49/50 cases showed a wall defect in at

to publish, or preparation of the manuscript. The specific roles of these authors are articulated in the 'author contributions' section.

**Competing Interests:** We have read the journal's policy and the authors of this manuscript have the following competing interests: Three of the authors (RS, GH, TG) are employees of B. Braun Aesculap AG Tuttlingen, a manufacturer of orthopedic implants. Four of the authors (HG, WJ, MR, FT) are advising surgeons in Aesculap R&D projects and three authors (WJ, MR, PW) are getting institutional support. This does not alter our adherence to PLOS ONE policies on sharing data and materials.

least one sector. It was observed that implant migration in cranial direction was associated with relative bone volume loss in cranial roof ( $R = 0.74$ ) and ovality ( $R = 0.67$ ).

## Conclusion

Within this study, 50 pelvises with acetabular bone defects were successfully analyzed using six parameters. This could provide the basis for a novel classification concept which would represent a quantitative, objective, unambiguous, and reproducible classification approach for acetabular bone defects.

## Introduction

Revision hip surgery is often associated with acetabular bone defects, which are challenging to quantify. Numerous classification systems have been published in order to categorize those defects [1–3]. However, most of these classification systems are based on plane radiographs and mainly rely on the interpretation of anatomical landmarks, which may lead to poor reliability and repeatability [4–6]. Furthermore, as they are mainly descriptive, it remains difficult to transfer them into pre-clinical testing, implant development, and pre-operative planning. An ideal classification system would provide an objective, unambiguous, surgically relevant and reproducible categorization of bone defects, while being easy to apply. This would ease communication between surgeons, determination of treatment strategy and would also facilitate the prediction and comparison of surgical outcomes.

The application of three-dimensional (3D) imaging such as Computed-tomography (CT) may help to overcome the drawbacks associated with conservative radiograph-based defect classifications [7]. Recently, some approaches towards a more quantitative defect analysis based on 3D-imaging techniques were made, including the analysis of total radial bone loss [7–9], volume loss [7, 10] and remaining bone thickness [7]. Total radial bone loss (TrABL) was among others assessed by Gelaude et al., who conducted the analysis based on segmented CT-data of the defect acetabulum and its anatomic reconstruction [8]. The possibilities to analyze volume loss and remaining bone thickness were mentioned by Horas et al. [7]. Recently, Hettich et al. validated a method to analyze acetabular bone defects in terms of bone volume loss and new bone formation [10]. The study was based on CT-data of defect pelvises and their anatomic reconstructions which were obtained via a statistical shape model (SSM). The bone volumes of defect and native pelvises in four defect sectors were assessed. Bone volume loss and new bone formation were obtained in each sector as absolute value and relative to the native bone volume. These studies pointed out possibilities to analyze acetabular bone defects in a quantitative way. However, these studies using anatomic reconstructions were focused on the analysis of one single parameter (e.g. bone volume loss) and the methods were only applied to a limited number of cases.

In order to evaluate the severity of acetabular bone defects, numerous parameters are of interest, such as bone volume loss, new bone formation, shape of the acetabulum (ovality), support by the cranial roof (lateral center-edge angle, LCE angle), migration of the existing implant, and presence of wall defects. This information could be beneficial in clinical practice for pre-operative planning, prediction and comparison of surgical outcomes, as well as in research and development for implant design and pre-clinical testing.

The objectives of this study were to (1) suggest and define parameters for acetabular bone defect analysis, (2) quantify 50 clinical cases with acetabular bone defects, and (3) present the results and correlations between the parameters.

## Materials and methods

### CT-data

In order to conduct this study, a total of 90 clinical CT-data sets related to acetabular bone defects were kindly provided by the senior hip surgeons HG, VJ, MR, FT and PW from all four involved clinical centers, which was approved by the LMU Munich ethics committee (project no. 18–108 UE). Patients of all age groups with acetabular bone defects of Paprosky type 2A to 3B, including pelvic discontinuity, were selected for this study, whereby CT scans were conducted within pre-operative planning. Patients with existing primary THA, revision THA, infection-related cement spacers, and without implants were included. In accordance with the ethics committee, anonymized CT-data was provided, and patient information was restricted to age and gender. The data sets were screened and the following exclusion criteria were applied to allow successful reconstruction with the SSM [10]: (1) Unilateral scans of the pelvis, (2) data sets with poor image quality, and (3) scans with a distinctive tilted position of the pelvis. After the application of the exclusion criteria, 50 defect hemi-pelvises were included in this study with CT scans conducted between May 2014 and November 2018. 34 were female, 16 male and mean age was  $70.02 \pm 11.39$  (Table 1), average slice thickness and pixel size were  $2.37 \pm 0.86$  mm and  $0.79 \pm 0.20$  mm, respectively.

### Image processing

The analysis was based on solid models of the defect pelvis and the corresponding native pelvis (Fig 1), as previously described and validated [10]. The CT-data set of the defect pelvis was segmented in Mimics 19.0 (Materialise NV, Leuven, Belgium) (Fig 1A). For the reconstruction of the native pelvis corresponding to each defect pelvis, the pathological areas of the segmented CT-data sets were masked and excluded for each defect pelvis individually (Fig 1B). A SSM was trained based on the CT-data sets of 66 healthy pelvises [10]. The SSM is a deformable model that describes the typical 3D shape variation occurring in the training population by so called modes of shape variation that are sorted by their geometric significance. The SSM was fitted only onto the remaining healthy bone structures of each defect pelvis individually by using the first 20 modes of shape variation and the excluded pathological areas could be extrapolated. This resulted in a statistically probable native pelvis model individually for each defect pelvis. After showing promising validation results, comparable to previously applied SSMs, this method was considered to be well suited for the quantitative assessment of acetabular bone defects within the present study. The resulting 3D-models of native pelvis and defect pelvis were exported as Standard-Tessellated-Language (STL) surfaces and mesh correction algorithms were applied in 3-matic (Materialise NV, Leuven, Belgium) and Geomagic Design X (3Dsystems, Rock Hill, USA). In order to process the defect and native pelvis in the CAD-software CATIA V5 (Dassault Systèmes, Vélizy-Villacoublay Cedex, France), both models were transformed into solids using the auto surfacing function in Geomagic Design X (Fig 1C and 1D).

### Quantitative analysis

The quantitative analysis was performed in CATIA V5 and included six parameters (Fig 2): (1) bone volume loss, (2) new bone formation, (3) ovality of the acetabulum, (4) LCE angle, (5) implant migration, and (6) wall defects. In order to perform a detailed analysis of the defects, four different sectors were defined [10]: Cranial roof (Cranial), anterior column (Anterior), posterior column (Posterior), and medial wall (Medial). To take defects into account, which

Table 1. Details of the 50 CT data sets included in the study.

Data set	Age [years]	Gender [F/M]	Clinic	Implant type	Data set	Age [years]	Gender [F/M]	Clinic	Implant type
01	63	F	Rizzoli	Muller ring <sup>a</sup>	26	78	F	LMU	Cement spacer
02	62	F	Rizzoli	Muller ring <sup>a</sup>	27	49	F	LMU	Cemented PE cup <sup>b</sup>
03	78	F	LJ	Cage <sup>c</sup>	28	54	M	LMU	Screw cup
04	78	M	LMU	Cage <sup>c</sup>	29	47	M	LMU	Cement spacer
05	52	F	LMU	Press-fit cup <sup>d</sup>	30	78	F	LMU	No implant
06	57	M	Rizzoli	Press-fit cup <sup>d</sup>	31	74	M	LMU	Cement spacer
07	65	F	LMU	Cage <sup>c</sup>	32	72	F	LMU	Press-fit cup
08	65	F	LMU	Muller ring <sup>a</sup>	33	69	F	LMU	Cement spacer <sup>e</sup>
09	84	F	Rizzoli	Press-fit cup <sup>d</sup>	34	75	F	LMU	Cemented PE cup
10	84	F	Rizzoli	Cemented PE cup	35	69	F	Wrzb	Cage and metal cup <sup>f</sup>
11	55	M	LJ	Muller ring with metal cup <sup>f</sup>	36	79	F	LMU	Press-fit cup
12	72	M	Rizzoli	Press-fit cup <sup>d</sup>	37	82	M	Wrzb	Cemented PE-cup <sup>b</sup>
13	76	F	LMU	Cemented PE-cup	38	86	F	LMU	No implant
14	56	F	LJ	Press-fit cup	39	80	F	Wrzb	Press-fit cup
15	73	F	LMU	Screw cup	40	82	M	Wrzb	Cement spacer
16	77	F	Rizzoli	Cemented PE-cup	41	75	M	LMU	Screw cup
17	56	M	Wrzb	Press-fit cup and plate <sup>g</sup>	42	52	M	LMU	Press-fit cup
18	77	F	Wrzb	Screw cup	43	75	M	LMU	Press-fit cup
19	83	F	LMU	Screw cup	44	83	F	LMU	No implant
20	59	M	Rizzoli	Press-fit cup <sup>d</sup>	45	57	F	LMU	Screw cup <sup>h</sup>
21	57	F	Wrzb	Screw cup	46	67	F	Wrzb	No implant
22	68	M	LMU	Cement spacer	47	76	F	LMU	Cemented PE-cup <sup>b</sup>
23	67	F	Wrzb	Screw cup	48	81	F	Wrzb	Press-fit cup <sup>i</sup>
24	68	M	LMU	Cage <sup>c</sup>	49	91	F	LMU	Press-fit cup
25	85	F	LMU	Screw cup	50	54	F	LMU	Cage and metal cup <sup>f</sup>

Clinic names are abbreviated (LJ = Orthopaedic Hospital Lindenlohe; LMU = Orthopaedic Surgery LMU Munich; Rizzoli = Istituto Ortopedico Rizzoli di Bologna; Wrzb = König-Ludwig-Haus Würzburg). Cages and Muller rings were combined with Polyethylene (PE) cups if not otherwise indicated.

<sup>a</sup>with screws for acetabular component fixation

<sup>b</sup>with screws for bone fixation

<sup>c</sup>Metal on metal

<https://doi.org/10.1371/journal.pone.0222511.t001>

expand beyond the defined sectors around the acetabulum, bone volume loss in the os ilium, os pubis and os ischii was additionally considered where applicable.

Bone volume loss was analyzed by Boolean operations, whereby the defect pelvis was subtracted from the native pelvis (Fig 2A). New bone formation was also analyzed by Boolean operations, whereby the native pelvis was subtracted from the defect pelvis [10] (Fig 2B). Boolean operations were applied in each defect sector individually. Bone volume loss and new bone formation were calculated as absolute values for each defect sector, and as relative values in relation to the native bone volume in each sector.

Ovality of the acetabulum was measured by fitting an ellipse in the defect acetabulum with the native acetabular plane as basis. Ovality was defined as the ratio of length to width, whereby the ratio 1 represents a circular acetabulum (Fig 2C).

LCF angle was measured based on a technique also used with plane radiographs [11]. The most lateral edge of the cranial roof was marked and a line connecting the native center of rotation (CoR) with the lateral edge was defined. The LCF angle was measured as the angle

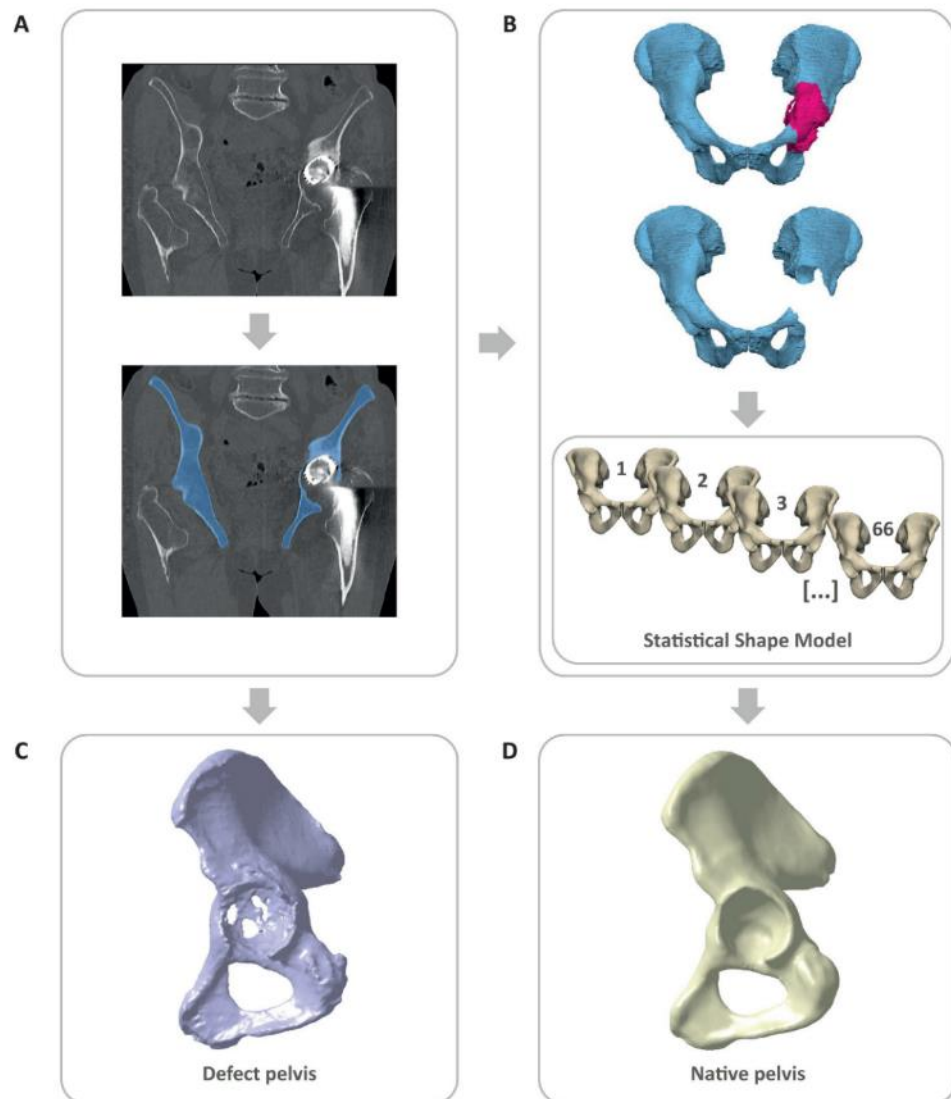


**Fig 1. Workflow to obtain defect and native pelvis for the analysis.** (A) Segmentation of clinical CT-data set. (B) Masking of the pathological area and application of a statistical shape model to reconstruct the native pelvis. (C) Transformation of CT-data set into solid model of defect pelvis. (D) Transformation of SSM-based reconstruction into solid model of native pelvis.

<https://doi.org/10.1371/journal.pone.0222511.g001>

between the connection line and the body Z-axis, projected on the anterior pelvic plane (Fig 2D).

Implant migration was measured as the difference between the native CoR and the actual implant CoR which was derived by a sphere fitting on the implant surface. Implant migration

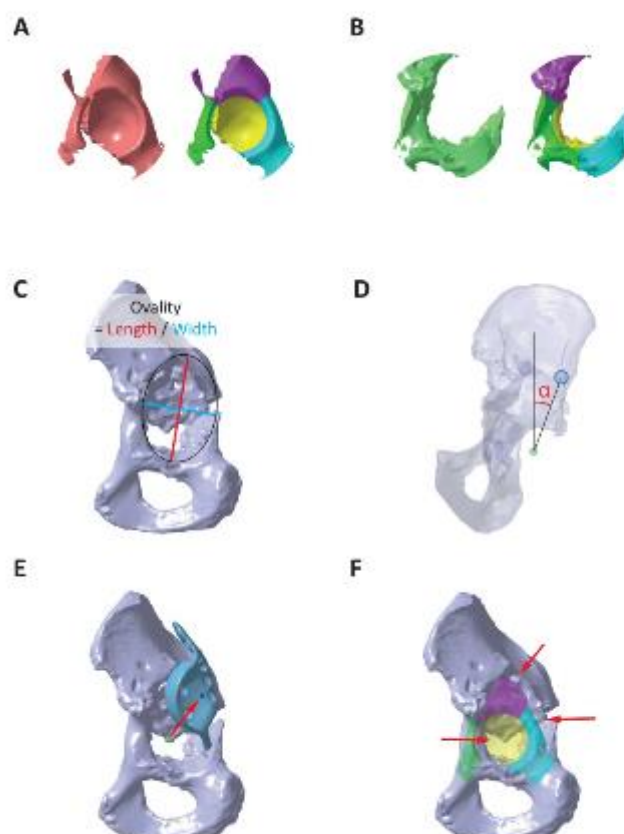


**Fig 2. Defect analysis parameters.** (A) Bone volume loss in total and in each defect sector calculated using Itolstein operations. (B) New bone formation in total and in each defect sector. (C) Ovality of the defect acetabulum given by the ratio of length to width. (D) Lateral center-edge angle defined by the line connecting the most lateral point in the cranial roof with the center of rotation (CoR) and the body Z-axis. (E) Implant migration defined by the distance and direction between the native CoR and the CoR of the existing implant. (F) Wall defect defined by holes and absent bone structures at the acetabular rim (grey = defect pelvis, color transparent = native bone volume in each sector).

<https://doi.org/10.1371/journal.pone.0222511.g002>

was analyzed in terms of total distance and distance in medial-lateral, anterior-posterior, and cranial-caudal direction (Fig 2E).

Wall defects were defined as holes with a dimension of 5 mm or larger in length and width or completely absent bone structures at the acetabular rim, indicated by a distance between native and defect rim of 5 mm or larger (Fig 2F).

### Statistical analysis

Statistical analysis included a test for normal distribution of data (Shapiro-Wilk test) and a test for statistical significance between relative bone volume loss in the single sectors (Mann-Whitney-U test). Level of significance was set to  $p < 0.05$ . Correlation analysis between the different parameters was performed where applicable. Correlation coefficients were interpreted as

moderate correlation ( $0.5 < R < 0.7$ ), high correlation ( $0.7 < R < 0.9$ ), and very high correlation ( $0.9 < R < 1.0$ ) [12].

## Results

Bone volume loss, new bone formation, ovality, LCE angle and implant migration in cranial and medial direction are exemplary shown for eight cases (Fig 3).

As most data was found to have a non-normal distribution, the results are presented using the median and [25th, 75th]—percentile values. For better comparison with results reported in literature, mean values  $\pm$  standard deviations are additionally summarized (Table 2).

### Bone volume loss

Median absolute bone volume loss was 20.5 [10.8, 29.8] ml in Cranial, 6.8 [5.1, 10.5] ml in Anterior, 12.5 [5.7, 20.3] ml in Posterior, and 14.3 [9.7, 19.3] ml in Medial (Fig 4A). Minimum was 4.8 ml in Cranial, 1.5 ml in Anterior, 1.9 ml in Posterior, and 2.8 ml in Medial. Maximum was 46.0 ml in Cranial, 14.8 ml in Anterior, 33.2 ml in Posterior, and 26.4 ml in Medial. In 13/50 cases, bone volume loss in Cranial was accompanied by bone loss in the os ilium and in 4/50 cases, bone loss in Posterior was accompanied by bone loss in the os ischii. In 5/50 cases, pelvic discontinuity was present. Median relative bone volume loss was 45.3 [24.8, 70.2] % in Cranial, 42.1 [27.0, 61.2] % in Anterior, 41.7 [17.7, 60.5] % in Posterior, and 72.8 [50.6, 95.0] % in Medial (Fig 4B). Minimum was 10.7% in Cranial, 8.7% in Anterior, 7.0% in Posterior, and 14.6% in Medial. Maximum was 97.9% in Cranial (case with 97.7% presented in Fig 3A, 97.9% corresponds to case presented in Fig 3E), 87.8% in Anterior, 93.5% in Posterior, and 100.0% in Medial (case presented in Fig 3B). Difference between the groups was significant for Medial and Cranial ( $p < 0.001$ ), Medial and Anterior ( $p < 0.001$ ), and Medial and Posterior ( $p < 0.001$ ). Median and percentile values of absolute bone volume loss were highest in Cranial, whereas median and percentile values of relative bone volume loss were highest in Medial. This difference is related to unequal sizes the defect sectors.

### New bone formation

Median absolute bone formation was 4.5 [3.0, 6.3] ml in Cranial, 2.9 [1.8, 5.3] ml in Anterior, 4.5 [2.8, 6.7] ml in Posterior, and 2.2 [0.7, 3.4] ml in Medial (Fig 5A). Minimum was 0.3 ml in Cranial, 0.3 ml in Anterior, 0.6 ml in Posterior, and 0.0 ml in Medial. Maximum was 14.2 ml in Cranial, 12.7 ml in Anterior, 16.4 ml in Posterior, and 21.3 ml in Medial. Median relative new bone formation was 10.0 [6.4, 14.3] % in Cranial, 19.2 [8.6, 29.2] % in Anterior, 12.5 [9.0, 19.1] % in Posterior, and 11.5 [3.2, 22.4] % in Medial (Fig 5B). Minimum was 0.8% in Cranial, 2.1% in Anterior, 1.6% in Posterior, and 0.0% in Medial. Maximum was 31.2% in Cranial (case presented in Fig 3C), 67.6% in Anterior, 54.1% in Posterior (case presented in Fig 3D) and 99.1% in Medial.

### Ovality of the acetabulum

Ovality was defined as the ratio of length to width of the acetabulum. Median ovality was 1.3 [1.1, 1.4] (Fig 6A). Maximum value was 2.0 and minimum value was 1.0 (case presented in Fig 3F).

### Lateral center-edge angle

Median LCE angle was 30.4° [21.5°, 40.4°] (Fig 6B). Smallest LCE angle was 11.6° (case presented in Fig 3E), and largest LCE angle was 63.0° (case presented in Fig 3F). In a study

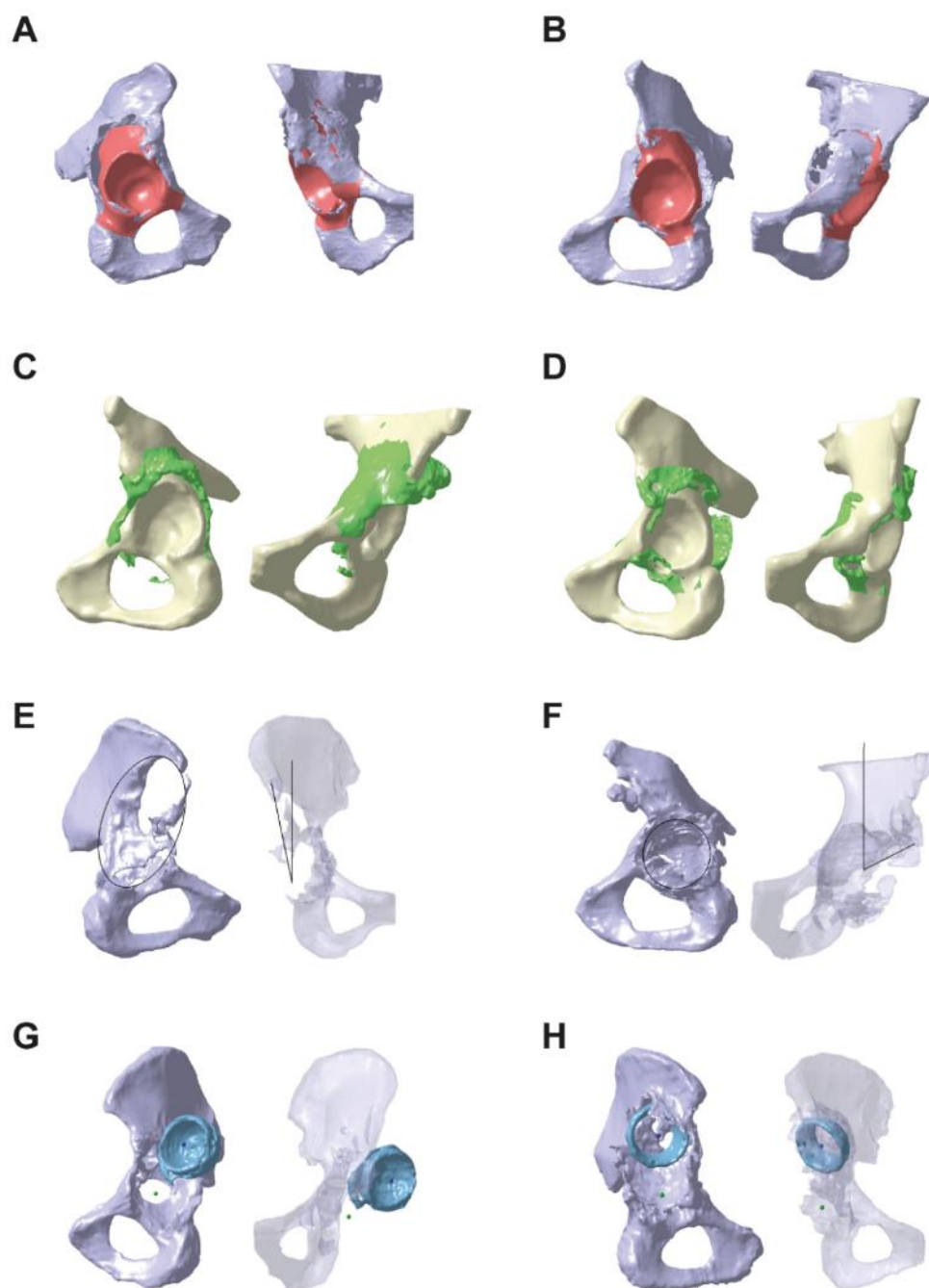


**Fig 3. Exemplary defect data sets.** (A) Defect pelvis (grey) superimposed with bone volume loss (red) of the case with second-highest relative bone volume loss in Cranial (97.7%). (B) Case with maximum relative bone volume loss in Medial (100.0%). (C) Native pelvis (yellow) superimposed with new bone formation (green) of the case with maximum relative new bone formation in Cranial (31.2%). (D) Case with maximum new bone formation in Posterior (54.1%). (E) Defect pelvis superimposed with ovality and LCE angle of the case with smallest LCE angle (11.6°) and large ovality (1.8). (F) Case with largest LCE angle (63.0°) and smallest ovality (1.0). (G) Defect pelvis superimposed with existing implant (blue) of the case with largest implant migration in lateral direction (39.6 mm). (H) Case with the largest implant migration in cranial direction (52.7 mm).

<https://doi.org/10.1371/journal.pone.0222511.g003>

about hip dysplasia, LCE angles between 25° and 39° were considered as normal [11]. Applying this to the data of the present study, 18/50 cases showed a normal LCE angle, whereas the remaining cases either showed a reduced (17 cases) or increased angle (15 cases).

### Implant migration

Implant migration was analyzed in terms of total distance, as well as distance in medial-lateral, anterior-posterior, and cranial-caudal direction (Fig 7). Only cases with segmentable metal implants could be included in this analysis which applied to 32/50 cases. Median total distance was 25.3 [14.8, 32.7] mm with a minimum value of 5.4 mm and a maximum value of 53.5 mm. Median distance in medial direction was 8.9 [4.2, 13.8] mm, in lateral direction 6.5 [2.1, 11.8] mm, in anterior direction 1.6 [0.7, 7.9] mm, in posterior direction 13.2 [4.3, 19.4] mm, in cranial direction 16.6 [11.2, 26.8] mm, and in distal direction 3.6 [N/A, N/A] mm. The maximum distance in medial direction was 20.3 mm, in lateral direction 39.6 mm (case presented in Fig 3G), in anterior direction 17.4 mm, in posterior direction 37.9 mm, in cranial direction 52.7 mm (case presented in Fig 3H), and in distal direction 4.8 mm. 30/32 cases showed a migration in cranial direction. The predominant direction of migration was cranial in 14/32 cases, posterior in 7/32, medial in 7/32 and lateral in 4/32 cases.

### Wall defects

Wall defects, defined as holes with 5 mm or larger in length/width or uncovered rim areas with a distance of 5 mm or more between native and defect pelvis, were present in 49/50 cases (Fig 8). In one case, only Cranial was concerned, whereas the remaining 48 cases showed wall defects in at least two sectors in combination: In three cases, Cranial and Anterior were concerned, in six cases Cranial and Posterior, in one case Cranial and Medial, in two cases Anterior and Medial, in twelve cases Cranial, Anterior and Posterior, in four cases Cranial, Anterior and Medial, in three cases Cranial, Posterior and Medial and in 17 cases, wall defects were present in all four sectors.

### Correlation analysis

Correlation analysis was performed between the different parameters. High correlation was found between total implant migration and migration in cranial-caudal direction ( $R = 0.89$ ).

**Table 2. Mean values ± standard deviations for comparison with values given in literature.**

	Bone volume loss		Bone formation		Ovality	LCE angle	Implant migration
	[ml]	[%]	[ml]	[%]			
Cranial	21.2 ± 11.2	47.6 ± 26.3	5.0 ± 3.0	11.2 ± 7.1	1.3 ± 0.2	31.9 ± 11.5	25.1 ± 13.2
Anterior	7.5 ± 3.6	42.6 ± 20.5	3.8 ± 2.8	21.3 ± 13.3			
Posterior	13.8 ± 8.4	41.4 ± 24.9	5.1 ± 3.5	15.5 ± 10.5			
Medial	14.4 ± 5.7	69.2 ± 24.8	2.9 ± 3.4	15.7 ± 16.8			
Total	56.8 ± 21.6	48.7 ± 18.6	16.9 ± 8.1	14.7 ± 7.2			

<https://doi.org/10.1371/journal.pone.0222511.t002>

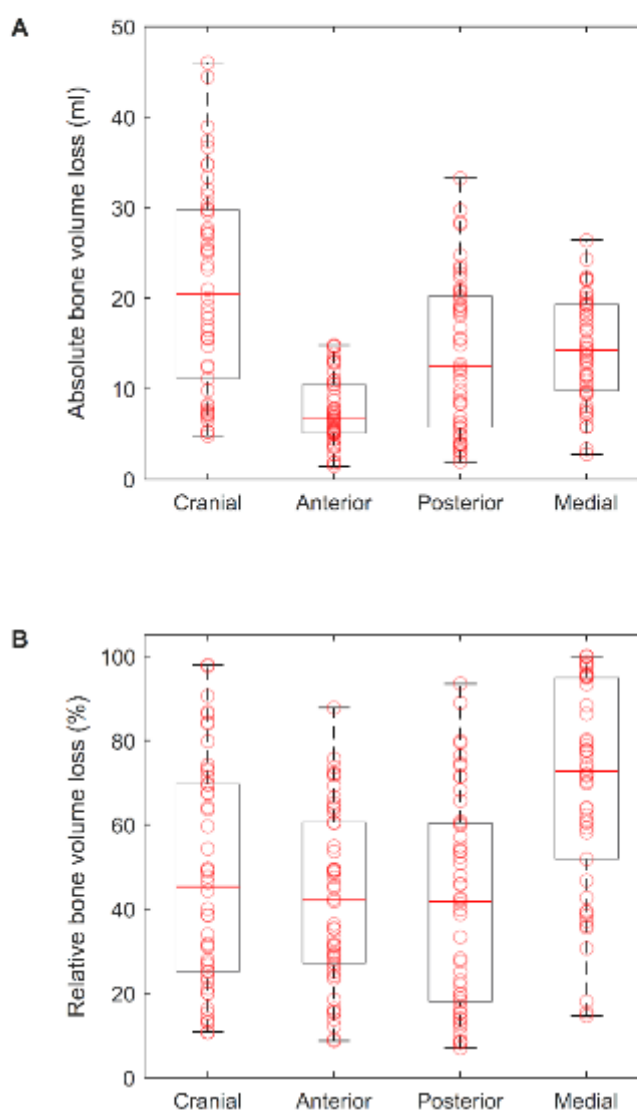


**Fig 4. Bone volume loss in each sector.** (A) Boxplots of absolute bone volume loss, superimposed with scatter plots of single values. (B) Boxplots of relative bone volume loss with respect to native bone volume, superimposed with scatter plots of single values.

<https://doi.org/10.1371/journal.pone.0222511.g004>

between implant migration in cranial direction and absolute bone volume loss in Cranial ( $R = 0.76$ ), and for implant migration in cranial direction and relative bone volume loss in Cranial ( $R = 0.74$ ). Moderate correlation was found between implant migration in cranial

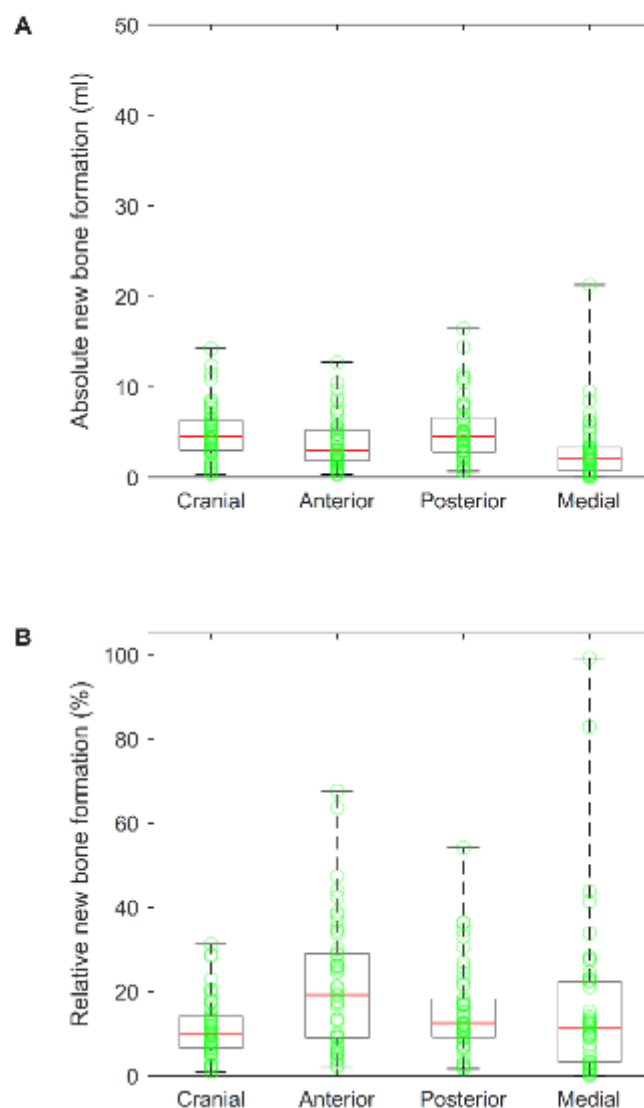


**Fig 5. New bone formation in each sector.** (A) Boxplots of absolute new bone formation, superimposed with scatter-plots of single values. (B) Boxplots of relative new bone formation with respect to native bone volume, superimposed with scatter-plots of single values.

<https://doi.org/10.1371/journal.pone.0222511.g005>

direction and ovality ( $R = 0.67$ ), for total implant migration and ovality ( $R = 0.69$ ), for relative bone volume loss in Cranial and ovality ( $R = 0.64$ ), for relative bone volume loss in Cranial and I.C.E. angle ( $R = -0.61$ ), and for relative bone volume loss in Cranial and total implant

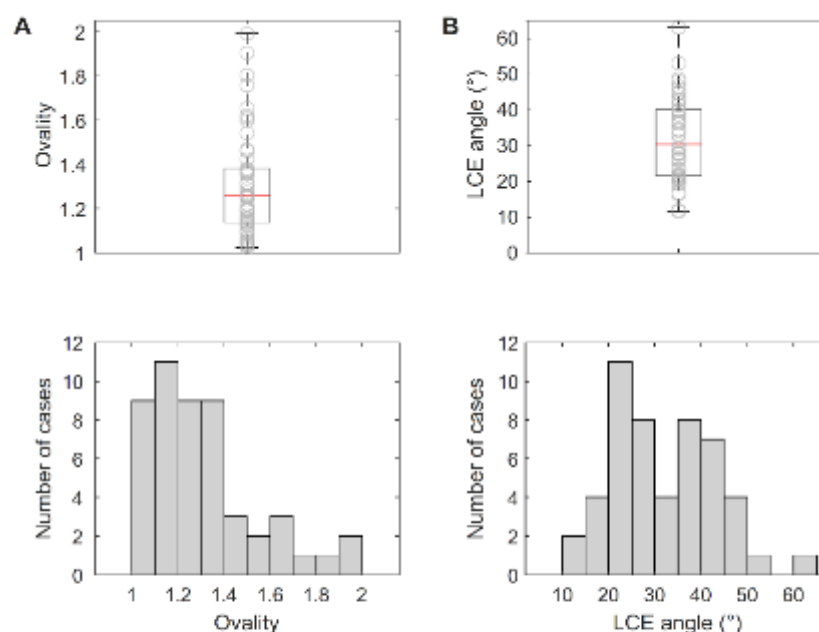


**Fig 6. Ovality and lateral center-edge angle (LCE angle).** (A) Boxplot of ovality values, superimposed with scatter-plot of single values and histogram of ovality values. Ovality is given as the length to width ratio of the defect acetabulum. (B) Boxplot of LCE angles, superimposed with scatter-plot of single values and histogram of LCE angles.

<https://doi.org/10.1371/journal.pone.0222511.g006>

migration ( $R = 0.65$ ). Moderate correlation was also found for absolute bone volume loss in Cranial and total implant migration ( $R = 0.66$ ), and for relative bone volume loss in Posterior and implant migration in posterior direction ( $R = 0.66$ ).

### Derivation of defect groups

Based on relative bone volume loss in each sector, defect groups could be derived. Thereby, thresholds of 15% and 25% were applied to separate clinically relevant bone loss from uncritical bone loss or bone loss caused by measurement inaccuracies. The threshold values were inspired by a study of Gelaude et al. 2011 who defined bone loss greater 15% as slight and greater 25% as moderate [8]. In combination with the assumption that the posterior column is critical for implant stability, a threshold of greater 15% in Posterior and a threshold of greater 25% in Cranial, Anterior and Medial was defined to identify clinically relevant bone loss. Applying these thresholds to the data of the present study, it was found that relevant bone loss was most frequent in Medial (47/50 cases) and Posterior (41/50 cases). Interestingly, relevant bone volume loss in Posterior was in 40/41 cases accompanied by relevant bone volume loss in Medial.

Based on the relative bone volume loss and the applied thresholds, each clinical case could be assigned to a specific group according to the sectors concerned with relevant bone volume loss (Fig 9). Defect groups are visualized as areas within spider plots (Fig 9). The extent of the areas in the four directions Cranial (C), Anterior (A), Posterior (P), and Medial (M) represents the amount of the corresponding relative bone volume loss. As an example, a case with relative

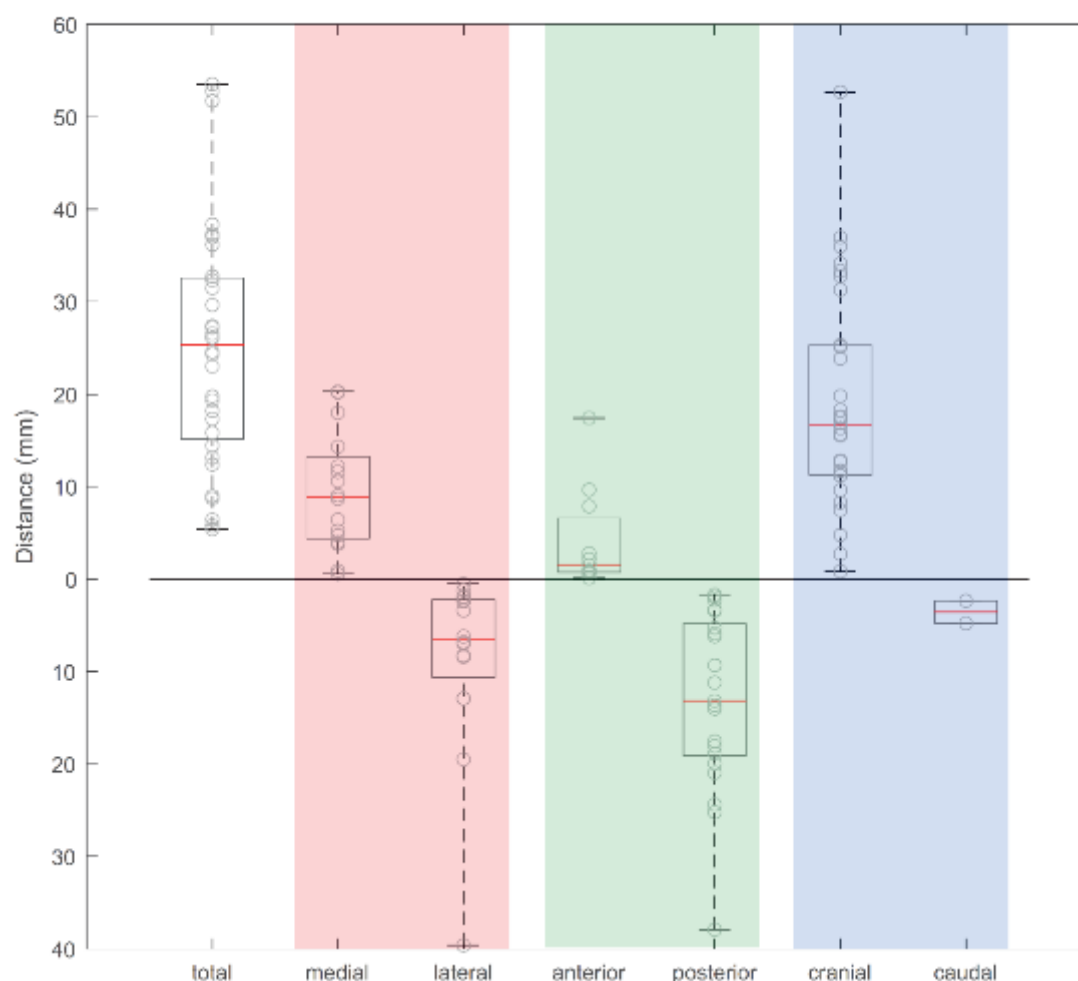


**Fig 7. Implant migration.** Boxplots superimposed with scatter plots of single values showing total migration and migration in medial lateral direction (body X axis), anterior-posterior direction (body Y-axis), and cranial-caudal direction (body Z-axis).

<https://doi.org/10.1371/journal.pone.0222511.g007>

bone volume loss in Cranial of 34.0%, in Anterior of 12.2%, in Posterior of 7.0% and in Medial of 14.6% would be assigned to group *Cranial* (Fig 9A), a case with relative bone volume loss in Cranial of 86.4%, in Anterior of 23.5%, in Posterior of 14.0% and in Medial of 35.5% to group *Cranial-Medial* (Fig 9B), a case with relative bone volume loss in Cranial of 23.7%, in Anterior of 75.7%, in Posterior of 10.5% and in Medial of 62.3% to group *Anterior-Medial* (Fig 9C), a case with relative bone volume loss in Cranial of 73.3%, in Anterior of 31.1%, in Posterior of 13.8% and in Medial of 37.2% to group *Cranial-Anterior-Medial* (Fig 9D), a case with relative bone volume loss in Cranial of 67.5%, in Anterior of 9.0%, in Posterior of 68.3% and in Medial of 95.3% to group *Cranial-Posterior-Medial* (Fig 9E), and a case with relative bone volume loss

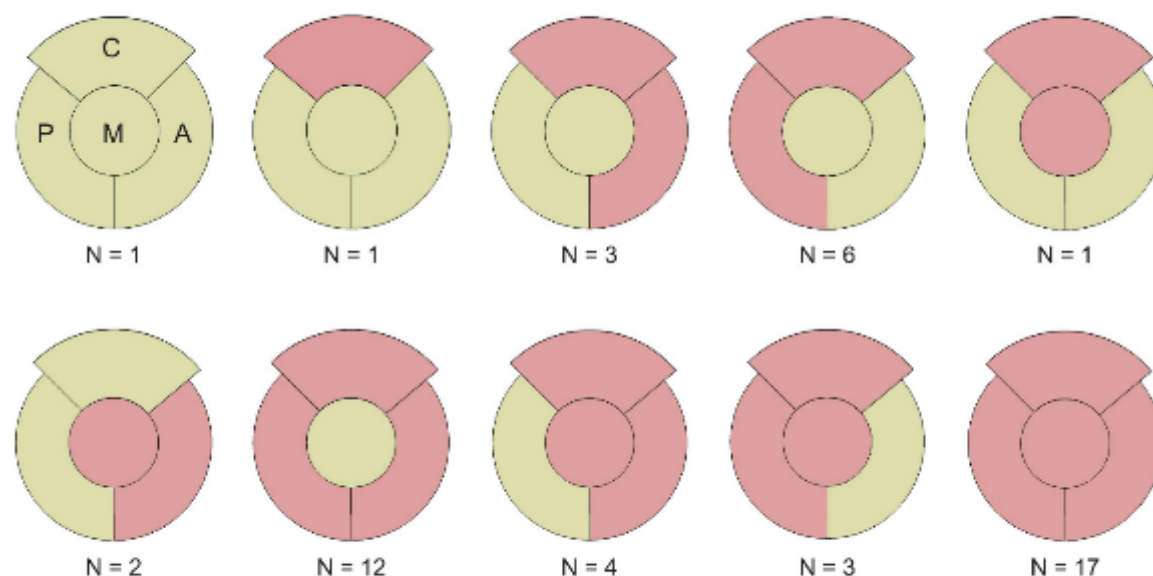


**Fig 8. Wall defects.** Red color indicates wall defects in the corresponding sectors. Number of concerned cases within this study are indicated below each wall defect combination (C = Cranial, A = Anterior, P = Posterior, M = Medial).

<https://doi.org/10.1371/journal.pone.0222511.g008>

in Cranial of 31.8%, in Anterior of 65.2%, in Posterior of 53.7% and in Medial of 73.5% to group *AB* sectors (Fig 9F). Since a pelvic discontinuity cannot be identified by bone volume loss alone, these cases could be assigned to a separate group based on the CT-images (Fig 9G).

Based on the proposed assignment principle, 17 separate defect groups could be derived (Fig 10). Applying this grouping to the data presented in this study, each defect could be unambiguously assigned to a specific defect group. The number of cases within each group is indicated below each spider plot (Fig 10).

## Discussion

The objectives of this study were to (1) suggest and define parameters for acetabular bone defect analysis, (2) quantify 50 clinical cases with acetabular bone defects, and (3) present the results and correlations between the parameters.

Highest relative bone volume loss was found in the medial wall with median and [25, 75]—percentile values of 72.8 [50.6, 95.0] %. Ovality was 1.3 [1.1, 1.4], lateral center-edge angle was 30.4° [21.5°, 40.4°], and total implant migration was 25.3 [14.8, 32.7] mm. Correlation was, besides others, found between implant migration in cranial direction and relative bone volume loss in cranial roof ( $R = 0.74$ ), as well as ovality ( $R = 0.67$ ).

Numerous studies have been conducted to quantify bone volume loss of osteolytic lesions in the acetabulum [13–21]. These studies identified a mean bone volume loss between 4.9 ml [13] and 37.9 ml [16], which is lower than the mean bone volume loss observed in the present study (56.8 ± 21.6 ml, Table 2). This difference could be attributed to the fact that the patients included in the previous studies often had a well-functioning total hip arthroplasty (THA). In contrast, the CT data analyzed in the present study was obtained within pre-operative planning and hence often associated with implant migration and large acetabular bone loss. Gelaude

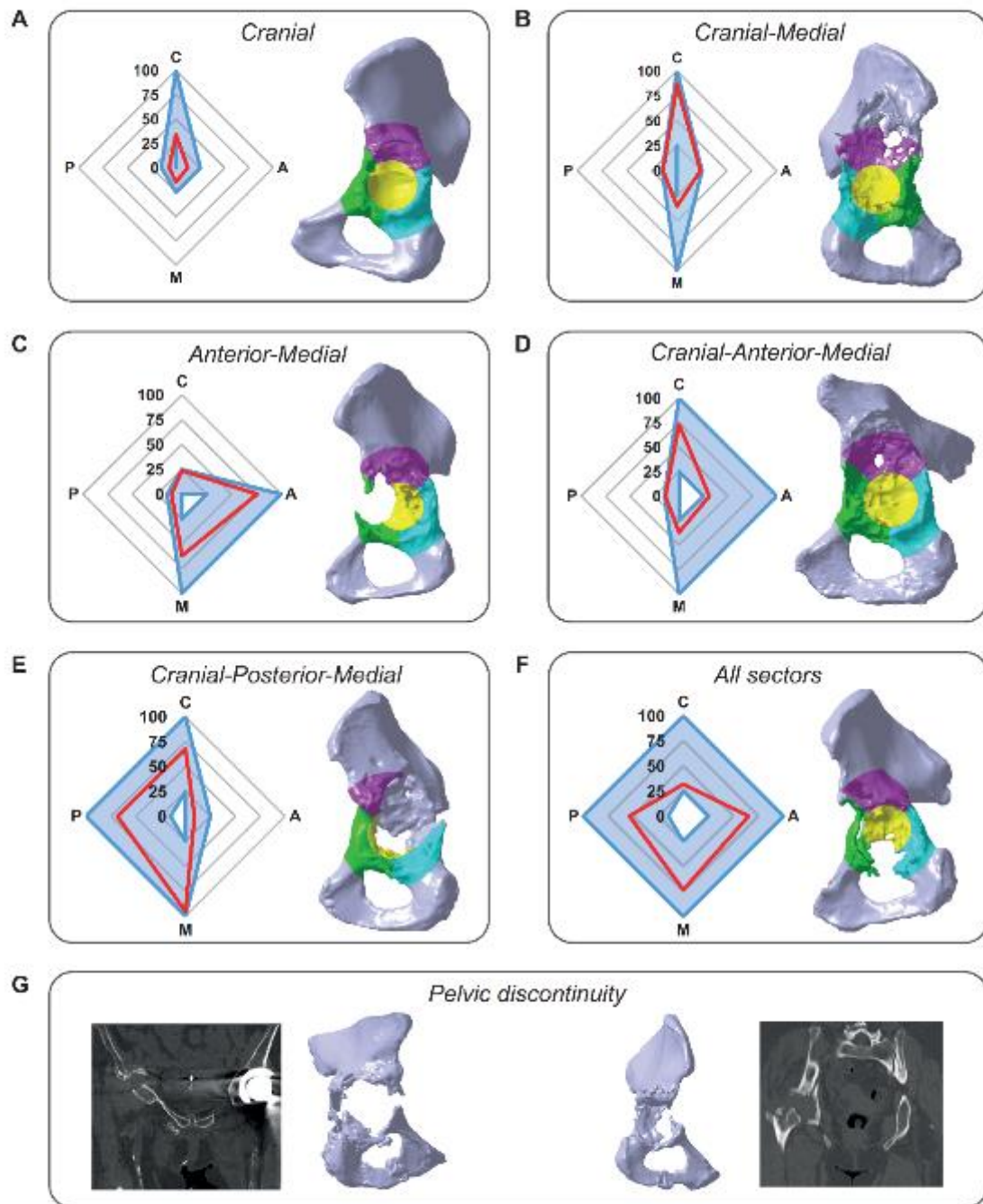


**Fig 9. Exemplary application of defect groups.** Eight exemplary cases were assigned to the corresponding defect groups. Shown are defect pelvises with defect sectors visualized by different colors and spider plots which show the individual relative bone volume loss (red line) and the corresponding defect group (blue area). Directions in the spider plots are given by Cranial (C), Anterior (A), Posterior (P), and Medial (M). Assignment to *Pelvic discontinuity* was based on 3D-models and CT-images. Group (A) *Cranial* defect, (B) *Cranial-Medial* defect, (C) *Anterior-Medial* defect, (D) *Cranial-Anterior-Medial* defect, (E) *Cranial-Posterior-Medial* defect, (F) *All sectors* defect, (G) *Pelvic discontinuity*.

<https://doi.org/10.1371/journal.pone.0222511.g009>

et al. published a method to assess the total radial bone loss around the acetabulum [8,9]. In a study of 30 acetabular bone defects, they found highest bone loss in the posterosuperior region [9]. In the present study, relative bone volume loss was highest in Cranial and Medial. However, comparison with the results of Gelaude et al. 2013 is limited due to the different sector definitions and different calculation methods for bone loss. In the present study, relative bone volume loss of at least 7.0% was observed in the four sectors of all 50 cases, which indicates multidirectional bone loss. This is in good accordance with previous studies which also found combined defects [8, 22, 23]. Implant migration of more than 5 mm was observed in all 32 analyzed cases in this study. This is in contrast to a recent study of Villatte et al., 2017, who assessed the 5.9-year radiological survival rate of acetabular revision treatments with bone allografts and reinforcement ring in 71 patients and found such high migration rates in only 9 patients [24]. A high correlation between implant migration in cranial direction and relative bone volume loss in Cranial ( $R = 0.74$ ), as well as a moderate correlation between implant migration in posterior direction and relative bone volume loss in Posterior was found ( $R = 0.66$ ). Wright and Paprosky already pointed out the influence of migration direction on the involvement of acetabular columns [22], whereby they reported that superior and lateral migration is an indication for a stronger involvement of the posterior column.

Based on the relative bone volume loss in each sector and the application of thresholds, a theoretical total of 17 defect groups could be derived (Fig 10). Comparing the defect groups with the Paprosky classification, group *All intact* would correspond to a Paprosky 1 and 2A defect, group *Cranial* would correspond to Paprosky 2B, group *Medial* would correspond to Paprosky 2C, and group *Cranial-Medial* would correspond to Paprosky 3A. Group *All sectors* would correspond to Paprosky 3B (grey boxes in Fig 10). Hence, the presented quantitative approach could establish a link to the widely used classification system while providing objective, and reproducible information on each defect.

Sandgren et al. 2013 already suggested a quantitative classification system for osteolytic lesions based on the analysis of 206 hips using length measurements [25]. However, since a prerequisite for the application of this method is a clearly defined border around the bone loss, its application to large acetabular bone defects in association with implant migration is limited. The present study quantified acetabular bone defects based on an anatomical reconstruction of the pelvis such that the analysis could also be applied to bone defects without clearly defined borders. Essentially, defect groups could be established based on any of the herein described parameters or based on a combination thereof. The approach based on bone volume loss would enable an unambiguous assignment of defects into groups which is straightforward and unsophisticated. Alternatively, a combination of several parameters could be applied, resulting in a defect characterization matrix. This option would enable a more detailed defect description, which might be helpful to determine treatment strategy, but which would also be more complex and time consuming to apply.

### Limitations

This study has some limitations. First, the metal implants caused artefacts in the CT-images which may have a detrimental effect on segmentation, and which required manual segmentation under supervision of an experienced radiologist. Second, the assessment of bone volume

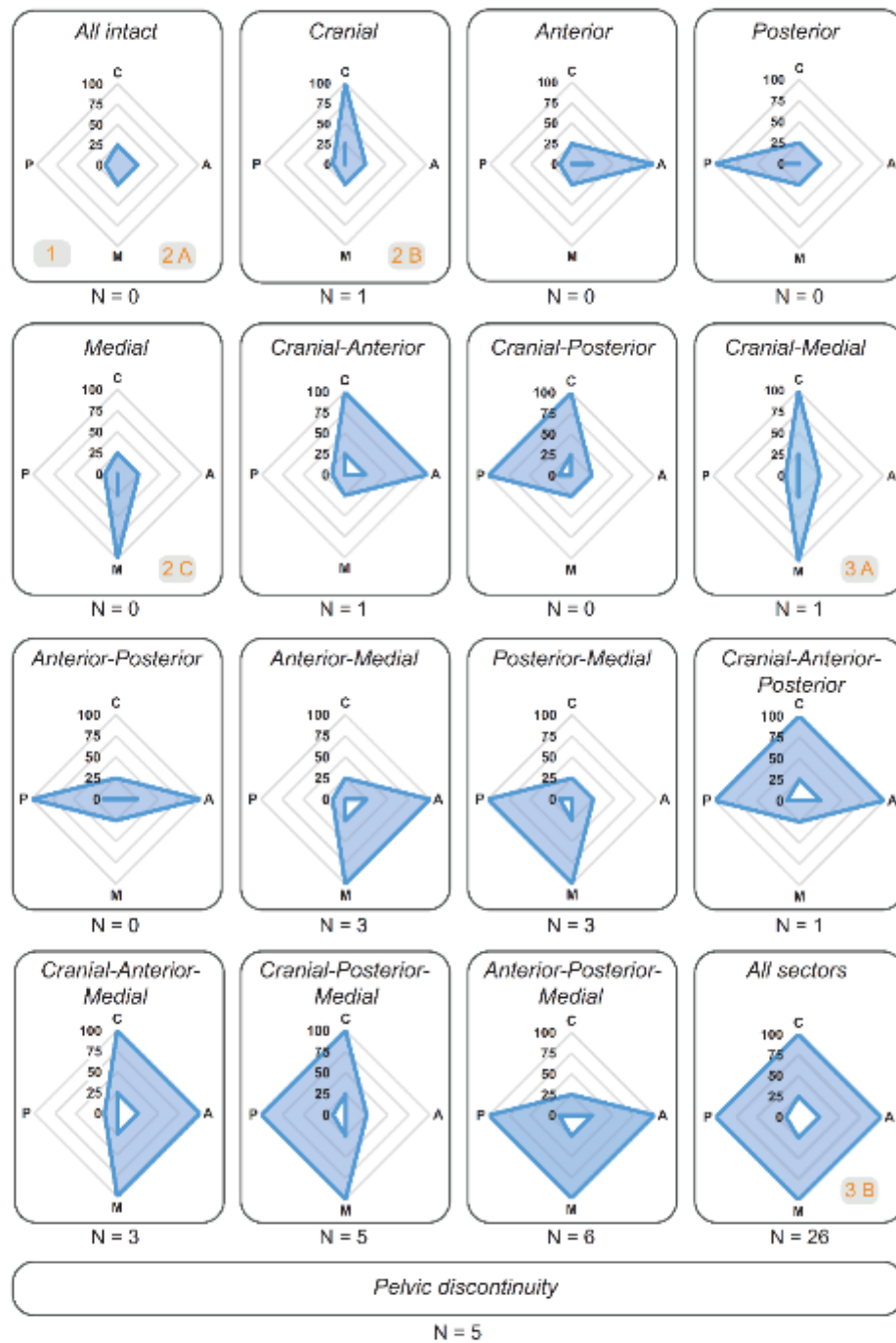


**Fig 10. Derived defect groups.** Individual cases are assigned to defect groups based on the combination of sectors concerned with relevant bone loss (blue areas). Relative bone volume loss is presented as spider plot with the directions Cranial (C), Anterior (A), Posterior (P), and Medial (M). Number of cases within this study assigned to each defect group is indicated below each plot. Comparison with Paprosky classification is shown in grey boxes in the corresponding group.

<https://doi.org/10.1371/journal.pone.0222511.g010>

loss and new bone formation relies on the accuracy of the SSM-based reconstruction of the native pelvis. Reconstruction errors may produce shell-like volumes when subtracting defect pelvis from native pelvis, which are also counted as bone volume loss. This may lead to an over-estimation of bone volume loss. The same applies to the calculation of new bone formation. Third, the proposed defect groups depend on the threshold definition for clinically relevant bone loss. The thresholds of 15% and 25% suggested within this study were defined in consultation with the senior hip revision surgeons HG, VJ, MR, FT and PW and refer to the definitions for slight and moderate bone loss by Gelaude et al. 2011 [8]. These thresholds were used to show the grouping concept and do not represent an exact definition of clinically relevant bone loss. In order to define these threshold values, further studies should be conducted which bring bone loss in relation with treatment strategy and treatment success. Fourth, the proposed defect grouping was based on relative bone volume loss only. However, other clinical parameters were indirectly included due to their correlations with relative bone volume loss and the grouping concept is not restricted to using this parameter. Fifth, it is questionable if 50 cases are enough to capture the whole range of acetabular defects. Nevertheless, to the authors knowledge, there is no study yet about the quantification of acetabular bone defects using several parameters which involves a higher number of cases. Sixth, in order to apply the presented analysis method, a CT scan is required. CT has already been mentioned as promising basis for defect classification [7] and has been widely used during the last years, for example for pre-clinical testing in terms of finite element analysis [26]. This indicates the increasing availability of this imaging technique. Nevertheless, CT is associated with increased irradiation dose and cost in comparison with radiographs as required for previously established classification schemes such as Paprosky [27]. This should be taken into account and the decision whether or not a CT scan is necessary to plan revision surgery should be made carefully and individually for each patient. Seventh, there is no direct clinical consequence in terms of treatment suggestion yet. In order to achieve this, an even larger number of defects should be assessed, also including a follow-up of chosen treatments and treatment success in short- to long-term. Based on this data, defect stages could be defined, and treatment options could be derived thereof.

### Conclusion and outlook

In this study, 50 acetabular bone defects were successfully quantified using six parameters. Based on the results for relative bone volume loss and on the application of thresholds for clinically relevant bone volume loss (Posterior > 15%; Cranial, Anterior, Medial > 25%), defect groups for acetabular bone loss could be derived. This would provide a quantitative, impartial, unambiguous, and reproducible assignment of acetabular bone defects and could also be applied in cases of large bone defects and implant migration.

The quantitative analysis and the assignment to groups could be beneficial in clinical, scientific and engineering applications. In clinical practice, it could ease communication between the surgeons and could provide important information to determine treatment options and to conduct pre-operative planning. Furthermore, using this concept, fully automated assignment of acetabular bone defects to specific defect groups would be possible. In science, it could facilitate the comparison of surgical outcomes due to unambiguous assignment of bone defects. In

engineering applications, the data could be used for the development of novel implant concepts and treatment strategies, such as patient-specific implants. Furthermore, it could also enable the transfer of clinically existing defects into pre-clinical in-vitro and in-silico testing, as quantitative data for bone volume loss and defect shape information are now available. Further studies should be conducted in order to enlarge the number of cases to obtain more information on the range of acetabular bone defects and to verify the applied parameters and thresholds for defect grouping. By including the analysis of chosen treatments and treatment success, a link between defect parameters and successful treatment strategies could be established. This would enable the development of a novel quantitative and impartial defect classification which also provides the suggestion of treatment strategies.

### Supporting information

**S1 File. Summary of the raw data of bone volume for each defect pelvis and corresponding native pelvis.** In columns A and B, the case numbers (1 to 50) alongside with the internal identifiers are listed. In columns C to F, the volume of the native pelvis in each sector is listed in  $\text{mm}^3$  for each case. In columns G to J, the volume of the defect pelvis in each sector is listed in  $\text{mm}^3$  for each case. In columns K to N, absolute bone volume loss in each sector in  $\text{mm}^3$  is listed. In columns O to R, relative bone volume loss in each sector (in relation to the native volume in each sector) in % is listed. In columns S to V, absolute new bone formation in each sector in  $\text{mm}^3$  is listed. In columns W to Z, relative new bone formation in each sector (in relation to the native volume in each sector) in % is listed.  
(XLSX)

**S2 File. Summary of the raw data of the analysis of additional parameters (ovality, lateral center-edge (LCE) angle, implant migration, wall defects).** In columns A and B, the case numbers (1 to 50) alongside with the internal identifiers are listed. In column C to D, the length and width of the defect acetabulum are listed, which is transferred to a ratio representing the ovality in columns E and F. In column G, the LCE angles are listed. In columns H to N, the total implant migration, migration in medial-lateral, anterior-posterior, and cranial-distal direction in mm are listed. Grey filling indicates that it was not possible to measure implant migration due to the fact that there was no segmentable implant present in the corresponding CT data. In columns O to R, the existence of wall defects in each sector is indicated by "1" in the corresponding column, whereas an intact wall is indicated by "0".  
(XLSX)

**S3 File. Results of the analysis of bone volume loss as absolute values in ml (sheet 1: Bone - Vol. Loss Absolute) and as relative values (in relation to native bone volume in each sector) in % (sheet 2: Bone Vol. Loss Relative).** In both sheets, in columns A and B, the case numbers (1 to 50) alongside with the internal identifiers are listed. In sheet 1, columns C to G, the bone volume loss (ml) in each sector, and in total is listed in ml for each case. Below the single measurement values, the median, 25<sup>th</sup> percentile, 75<sup>th</sup> percentile, minimum and maximum values are shown, as well as the mean and standard deviations for bone volume loss each sector and for overall bone volume loss. In sheet 2, columns C to F, the bone volume loss (%) in each sector relative to the native bone volume in each sector is listed. Below the single measurement values, the median, 25<sup>th</sup> percentile, 75<sup>th</sup> percentile, minimum and maximum values are shown, as well as the mean and standard deviations for bone volume loss in each sector. Columns H to R show the defect groups based on the applied thresholds 25% (Cranial, Anterior, Medial) and 15% (Posterior) which were present within the 50 analyzed cases. An "x" indicates the group the corresponding case is assigned to. The number of cases in each group

is shown below.

(XLSX)

**S4 File. Results of the analysis of new bone formation in absolute values in ml (sheet 1: Bone\_Form\_Abs) and relative values (in relation to the native bone volume in each sector) in % (sheet 2: Bone\_Form\_Rel).** In both sheets, in columns A and B, the case numbers (1 to 50) alongside with the internal identifiers are listed. In sheet 1, columns C to G, the new bone formation (ml) in each sector and in total is listed in ml for each case. Below the single measurement values, the median, 25<sup>th</sup> percentile, 75<sup>th</sup> percentile, minimum and maximum values are shown, as well as the mean and standard deviations for new bone formation in each sector and for overall new bone loss. In sheet 2, columns C to F, the bone volume loss (%) in each sector relative to the native bone volume in each sector is listed. Below the single measurement values, the median, 25<sup>th</sup> percentile, 75<sup>th</sup> percentile, minimum and maximum values are shown, as well as the mean and standard deviations for new bone formation in each sector. (XLSX)

**S5 File. Results of the additional parameter analysis, including ovality (sheet 1), LCE angle (sheet 2), implant migration (sheet 3), and wall defects (sheet 4).** In all sheets, in columns A and B, the case numbers (1 to 50) alongside with the internal identifiers are listed. In sheet 1 column C, the ovality for each case is listed. Below the single measurement values, the median, 25<sup>th</sup> percentile, 75<sup>th</sup> percentile, minimum and maximum values are shown, as well as the mean and standard deviations. In sheet 2, column C, the LCE angle is listed for each case. Below the single measurement values, the median, 25<sup>th</sup> percentile, 75<sup>th</sup> percentile, minimum and maximum values are shown, as well as the mean and standard deviations. In columns F to H, the assignment to the groups according to Wiberg et al. is shown. In sheet 3, implant migration is listed as total distance in mm (column C) and distance in medial-lateral, anterior-posterior, cranial-distal direction (column D to I). Below the single measurement values, the median, 25<sup>th</sup> percentile, 75<sup>th</sup> percentile, minimum and maximum values, as well as the mean and standard deviations are shown. In column J, the implant type is listed and in column K to M, the predominant directions based on the values in column D to I are listed. Based on the predominant migration direction, the defect cases could be grouped, as shown in column L and M. In sheet 4, column C to E, the existence of wall defects in each sector is indicated by "1", whereas an intact wall is indicated by "0". Based on the combination of concerned sectors, the cases could be grouped (column G). A description of the groups and the number of cases in each group is shown in columns I to K. (XLSX)

**S6 File. Summary of the correlation coefficients (R-values) between the single analysis parameters (Variable 1 and Variable 2).** Correlations with  $0.5 \leq R < 0.7$  are color-coded in green, correlations with  $0.7 \leq R < 0.9$  in yellow, and correlations with  $0.9 \leq R$  in pink, whereby obvious correlations between absolute and relative bone loss, as well as between absolute and relative new bone formation are grayed out. (XLS)

**S7 File. Results of the Mann-Whitney test for statistical significance between bone volume loss in the single sectors and new bone formation in the single sectors.** Variable 1 and Variable 2 represent the parameters and the table is sub-divided into the four sections absolute bone volume loss, relative bone volume loss, absolute new bone formation, and relative new bone formation. Statistical significance is indicated by a p value  $< 0.05$  in column D and description "TRUE" in column E (hypothesis). (XLS)

## Acknowledgments

The authors would like to thank Dr. med. Rudolf Schierjott for his support in the segmentation of the CT-data sets, Jessica Stübler for her work on segmentation and image data processing.

## Author Contributions

**Conceptualization:** Ronja A. Schierjott, Georg Hettich, Heiko Graichen, Volkmar Jansson, Maximilian Rudert, Francesco Traina, Patrick Weber, Thomas M. Grupp.

**Formal analysis:** Ronja A. Schierjott.

**Methodology:** Ronja A. Schierjott, Georg Hettich, Thomas M. Grupp.

**Project administration:** Thomas M. Grupp.

**Resources:** Heiko Graichen, Volkmar Jansson, Maximilian Rudert, Francesco Traina, Patrick Weber.

**Supervision:** Thomas M. Grupp.

**Validation:** Ronja A. Schierjott, Georg Hettich, Heiko Graichen, Volkmar Jansson, Maximilian Rudert, Francesco Traina, Patrick Weber, Thomas M. Grupp.

**Visualization:** Ronja A. Schierjott.

**Writing – original draft:** Ronja A. Schierjott.

**Writing – review & editing:** Georg Hettich, Heiko Graichen, Volkmar Jansson, Maximilian Rudert, Francesco Traina, Patrick Weber, Thomas M. Grupp.

## References

1. Paprosky WG, Perona PG, Lawrence JM. Acetabular defect classification and surgical reconstruction in revision arthroplasty. A 6-year follow-up evaluation. *J Arthroplasty*. 1994; 9: 33–44. [https://doi.org/10.1016/0883-5403\(94\)90135-x](https://doi.org/10.1016/0883-5403(94)90135-x) PMID: 8163974
2. D'Antonio JA, Capello WN, Borden LS, Bargar WL, Bierbaum BF, Boetticher WG, et al. Classification and management of acetabular abnormalities in total hip arthroplasty. *Clinical Orthopaedics and Related Research*. 1989; 126–137.
3. Saleh KJ, Holtzman J, Gafni A, Saleh L, Jaroszynski G, Wong P, et al. Development, test reliability and validation of a classification for revision hip arthroplasty. *J. Orthop. Res.* 2001; 19: 50–56. [https://doi.org/10.1016/S0736-0266\(00\)00021-8](https://doi.org/10.1016/S0736-0266(00)00021-8) PMID: 11332620
4. Johanson NA, Drittmier KR, Cerynik DL, Stehman CC. Grading acetabular defects. The need for a universal and valid system. *J Arthroplasty*. 2010; 25: 425–431. <https://doi.org/10.1016/j.arth.2009.02.021> PMID: 19375688
5. Engh CA, Sychterz CJ, Young AM, Pollock DC, Toomey SD, Engh CA. Interobserver and intraobserver variability in radiographic assessment of osteolysis. *J Arthroplasty*. 2002; 17: 752–759. <https://doi.org/10.1054/arth.2002.33554> PMID: 12216030
6. Safir O, Lin C, Kosashvili Y, Masne IP, Gross AE, Backstein D. Limitations of conventional radiographs in the assessment of acetabular defects following total hip arthroplasty. *Can J Surg*. 2012; 55: 401–407. <https://doi.org/10.1503/cjcs.000511> PMID: 22992397
7. Horas K, Arnold J, Steiner AF, Hoberg M, Rudert M, Holzapfel BM. Acetabular defect classification in times of 3D imaging and patient-specific treatment protocols. *Der Orthopäde*. 2017; 46: 168–178. <https://doi.org/10.1007/s00132-016-3378-y> PMID: 28073371
8. Gelaude F, Clijmans T, Delpont H. Quantitative computerized assessment of the degree of acetabular bone deficiency: Total radial Acetabular Bone Loss (TrABL). *Adv Orthop*. 2011; 1–12. <https://doi.org/10.4061/2011/494382> PMID: 22013539
9. Gelaude F, Demol J, Clijmans T, Delpont H. CT-based quantification of bone loss for refined classification of acetabular deficiencies: comparison of 30 Paprosky type IIIA–B cases. *Orthopaedic Proceedings*. 2013; 95-B: 26.

10. Hetlich G, Schierjott RA, Ramm H, Graichen H, Jansson V, Rudert M, et al. Method for quantitative assessment of acetabular bone defects. *J. Orthop. Res.* 2018; 1–9. <https://doi.org/10.1002/jor.24165> PMID: 30345568
11. Henle P, Tannast M, Siebenrock KA. Imaging in developmental dysplasia of the hip. *Der Orthopäde.* 2008; 37: 525–531. <https://doi.org/10.1007/s00132-008-1205-3> PMID: 18496670
12. Calkins KG. *Applied Statistics—Lesson 5. Correlation coefficients*, 2005. Available: <https://www.andrews.edu/~calkins/math/edsm611/edsm05.htm>. Accessed 7 June 2019.
13. Puri L, Wixson RL, Stern SH, Kohli J, Hendrix RW, David SS. Use of helical computed tomography for the assessment of acetabular osteolysis after total hip arthroplasty. *J Bone Joint Surg Am.* 2002; 84: 609–614. <https://doi.org/10.2106/00004623-200204000-00016> PMID: 11940623
14. Leung S, Naudie D, Kitamura N, Walde T, Engh CA. Computed tomography in the assessment of periacetabular osteolysis. *J Bone Joint Surg Am.* 2005; 87: 592–597. <https://doi.org/10.2106/JBJS.D.02116> PMID: 15741627
15. Garcia-Cimbrelo E, Tapia M, Hervas CM. Assessment of bone defects around the acetabular cup with use of multislice computed tomography in total hip replacement. *Orthopaedic Proceedings.* 2006; 88-B: 49–50.
16. Garcia-Cimbrelo E, Tapia M, Martin-Hervas C. Multislice Computed Tomography for Evaluating Acetabular Defects in Revision THA. *Clinical Orthopaedics and Related Research.* 2007; 136–143.
17. Garcia-Rey E, Garcia-Cimbrelo E, Martin-Hervas C. Assessment of bone defects around the acetabular cup with use of multislice computed tomography in total hip replacement. *Orthopaedic Proceedings.* 2006; 88-B: 64–65.
18. Tapia M, Garcia-Cimbrelo E, Martin-Hervas C. Assessment of acetabular defects through the use of multislice-CT in total hip prostheses. *Orthopaedic Proceedings.* 2005; 87-B: 83.
19. Egawa H, Ho H, Huynh C, Hooper RH, Engh CA, Engh CA. A three-dimensional method for evaluating changes in acetabular osteolytic lesions in response to treatment. *Clinical Orthopaedics and Related Research.* 2010; 468: 480–490. <https://doi.org/10.1007/s11999-009-1050-0> PMID: 19701674
20. Howie DW, Neale SD, Martin W, Costi K, Kane T, Stamenkov R, et al. Progression of periacetabular osteolytic lesions. *J Bone Joint Surg Am.* 2012; 94: e1171–6. <https://doi.org/10.2106/JBJS.K.00877> PMID: 22992823
21. Stamenkov RB, Howie DW, Neale SD, McGee MA, Taylor DJ, Findlay DM. Distribution of periacetabular osteolytic lesions varies according to component design. *J Arthroplasty.* 2010; 25: 913–919. <https://doi.org/10.1016/j.arth.2009.08.003> PMID: 19775854
22. Wright G, Paprosky WG. *Acetabular Reconstruction: Classification of Bone Defects and Treatment Options*; 2016. Available: <https://musculoskeletalkey.com/acetabular-reconstruction-classification-of-bone-defects-and-treatment-options/>. Accessed 12 December 2018.
23. Wasiliew GI, Janz V, Perka C, Mueller M. Treatment of acetabular defects with the trabecular metal revision system. *Der Orthopäde.* 2017; 46: 148–157. <https://doi.org/10.1007/s00132-016-3381-3> PMID: 29093681
24. Villatte G, Erivan R, Salles G, Pereira B, Galvin M, Descamps S, et al. Acetabular bone defects in THA revision: Reconstruction using morsellised virus-inactivated bone allograft and reinforcement ring. Seven-year outcomes in 85 patients. *Orthop Traumatol Surg Res.* 2017; 103: 543–548. <https://doi.org/10.1016/j.otsr.2017.03.008> PMID: 28366746
25. Sandgren B, Crafoord J, Garrellick G, Carlsson L, Weidenhielm L, Olivecrona H. Computed tomography vs. digital radiography assessment for detection of osteolysis in asymptomatic patients with uncemented cups. A proposal for a new classification system based on computer tomography. *J Arthroplasty.* 2013; 28: 1608–1613. <https://doi.org/10.1016/j.arth.2013.01.029> PMID: 23618751
26. Amirouche F, Solitro GF, Wala A, Gonzalez M, Bobko A. Segmental acetabular rim defects, bone loss, oversizing, and press fit cup in total hip arthroplasty evaluated with a probabilistic finite element analysis. *Int Orthop.* 2017; 41: 1527–1533. <https://doi.org/10.1007/s00264-016-3309-y> PMID: 28012048
27. Paprosky WG, Cross MB. *CORR Insights®: Validity and reliability of the Paprosky acetabular defect classification.* *Clinical Orthopaedics and Related Research.* 2013; 471: 2266. <https://doi.org/10.1007/s11999-013-2938-2> PMID: 23613087

#### **4.2 Publication II: A method to assess primary stability of acetabular components in association with bone defects**

Authors: Ronja A Schierjott, Georg Hettich, Alexandra Ringkamp,  
Marc Baxmann, Federico Morosato, Philipp Damm,  
Thomas M Grupp

Journal: Journal of Orthopaedic Research

Volume: 38

Pages: 1769-1778

Year: 2020

DOI: <https://doi.org/10.1002/jor.24591>

Impact factor: 2.728 (according to InCites Journal Citation Reports 2019)

## RESEARCH ARTICLE

# A method to assess primary stability of acetabular components in association with bone defects

Ronja A. Schierjott<sup>1,2</sup>  | Georg Hettich<sup>1</sup> | Alexandra Ringkamp<sup>3</sup> | Marc Baxmann<sup>1</sup> | Federico Morosato<sup>4</sup> | Philipp Damm<sup>5</sup> | Thomas M. Grupp<sup>1,2</sup>

<sup>1</sup>Research & Development, Aesculap AG, Am Aesculap Platz, Tuttlingen, Germany

<sup>2</sup>Department of Orthopaedic Surgery, Physical Medicine & Rehabilitation, Ludwig-Maximilians-University Munich, Munich, Germany

<sup>3</sup>Department of Biomechanics, Faculty of Mechanical Engineering, Technische Universität Ilmenau, Ilmenau, Germany

<sup>4</sup>Department of Industrial Engineering, School of Engineering and Architecture, Università di Bologna, Bologna, Italy

<sup>5</sup>Julius Wolff Institute, Joint Loading & Musculoskeletal Analysis, Charité-Universitätsmedizin Berlin, Berlin, Germany

## Correspondence

Ronja A. Schierjott, Am Aesculap Platz, 78532 Tuttlingen, Germany  
Email: ronja\_alissaschierjott@aesculap.de

## Abstract

The objectives of this study were to develop a simplified acetabular bone defect model based on a representative clinical case, derive four bone defect increments from the simplified defect to establish a step-wise testing procedure, and analyze the impact of bone defect and bone defect filling on primary stability of a press-fit cup in the smallest defined bone defect increment. The original bone defect was approximated with nine reaming procedures and by exclusion of specific procedures, four defect increments were derived. The smallest increment was used in an artificial acetabular test model to test primary stability of a press-fit cup in combination with bone graft substitute (BGS). A primary acetabular test model and a defect model without filling were used as reference. Load was applied in direction of level walking in sinusoidal waveform with an incrementally increasing maximum load (300 N/1000 cycles from 600 to 3000 N). Relative motions (inducible displacement, migration, and total motion) between cup and test model were assessed with an optical measurement system. Original and simplified bone defect volume showed a conformity of 99%. Maximum total motion in the primary setup at 600 N ( $45.7 \pm 5.6 \mu\text{m}$ ) was in a range comparable to tests in human donor specimens ( $36.0 \pm 16.8 \mu\text{m}$ ). Primary stability was reduced by the bone defect, but could mostly be reestablished by BGS-filling. The presented method could be used as platform to test and compare different treatment strategies for increasing bone defect severity in a standardized way.

## KEYWORDS

acetabular bone defect model, bone graft substitute, optical measurement, primary stability

## 1 | INTRODUCTION

Aseptic loosening is one of the main reasons for revision in total hip arthroplasty (THA).<sup>1</sup> Among others, it can be caused by excessive relative motion between implant and bone. It has been shown that relative motions above  $150 \mu\text{m}$  prevent bone ingrowth and cause fibrous tissue formation, whereas relative motions below  $40 \mu\text{m}$  enable osseointegration.<sup>2,3</sup> Absence of

osseointegration eventually results in implant loosening and revision surgery, which is often accompanied by bone loss. This makes subsequent implant fixation even more challenging, and may require specific treatment strategies, such as bone grafts or bone graft substitutes (BGS) in combination with cemented or press-fit cups, as well as augments or revision implants. However, there are no standardized test methods yet available to test such specific treatment strategies.

This is an open access article under the terms of the Creative Commons Attribution-NonCommercial license, which permits use, distribution and reproduction in any medium, provided the original work is properly cited and is not used for commercial purposes.

© 2020 The Authors. *Journal of Orthopaedic Research* published by Wiley Periodicals, Inc. on behalf of Orthopaedic Research Society

Previous *in vitro* studies concerning primary implant stability were often focused on the assessment of different hemispherical cups for primary THA.<sup>4–10</sup> Typically, primary stability was assessed by lever-out, pull-/push-out, rotational tests, or in some cases under axial loading with relative motion measurement by linear variable differential transformers (LVDTs) or optical markers.

In revision THA, primary stability was so far analyzed by a limited number of studies in which a simplified acetabular defect was implemented in human donor specimens, Sawbone composite pelvises or surrogate models to test press-fit cups,<sup>11,12</sup> press-fit cups with augments,<sup>13</sup> reconstruction shells,<sup>14,15</sup> or cemented cups in combination with bone grafts or BGS.<sup>16–19</sup> To the authors' knowledge, no study has yet assessed primary stability of press-fit cups in combination with BGS defect filling in a surrogate acetabular test model.

More importantly, in the previous studies, defect shape was implemented by simplified procedures, often by using one acetabular reamer. This leads to simple defect shapes limited to a hemisphere in the acetabular ground<sup>12</sup> or other single spherical segments at the rim of the acetabulum.<sup>13,20</sup> However, clinical cases often show an irregular shape, which requires a less simplified defect implementation.

There is a large variation of acetabular bone defects, and in the previous *in vitro* testing studies different defect locations and sizes were used depending on the treatment strategy to be tested. This makes the comparison between treatment strategies difficult.

In studies about acetabular bone defects, it was found that bone loss is multidirectional in most cases<sup>21–23</sup> and that bone volume loss in the posterior column and the medial area often appear in combination.<sup>24</sup> Bone loss in the medial area can be present as cavemous defect (AAOS type II)<sup>24</sup> or with the destruction of the medial wall (Paprosky type 2C).<sup>23</sup> Beyond those defects, the cranial roof can be affected, either combined with an intact medial wall (Paprosky type 2B) or with a destroyed medial wall (Paprosky type 3A).<sup>25</sup> In order to improve comparability of *in vitro* tests and transfer to clinical defect situations, it would be beneficial to use a standardized and realistic defect, which could be enlarged incrementally to test different treatment strategies for increasing bone defect severity.

The aims of this study were to (a) develop a simplified bone defect model based on computed tomography (CT) data of a clinically existing acetabular bone defect, (b) derive four different bone defect increments from the simplified defect to build up a step-wise testing procedure for increasing bone defect severity, and (c) assess the influence of defect and BGS filling on primary stability of a press-fit cup in the smallest defined bone defect increment.

## 2 | MATERIALS AND METHODS

### 2.1 | Acetabular test model

An artificial acetabular test model was developed, replicating the main support structures os ilium, os pubis, and os ischii, as well as the incisura acetabuli, oriented towards a previously developed surrogate model<sup>25</sup> (Figure 1A). Dimensions of the acetabulum were based

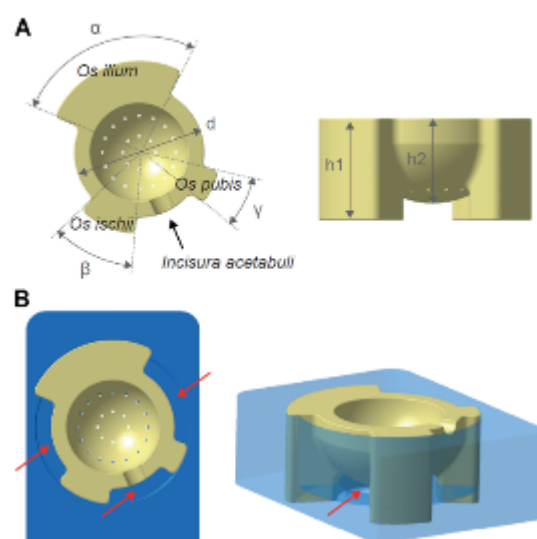


**FIGURE 1** Acetabular test model. A, Acetabular model made of 20 PCF polyurethane foam with top and lateral view. Dimensions of os ilium, os pubis, and os ischii ( $\alpha = 95^\circ$ ,  $\beta = 26^\circ$ ,  $\gamma = 43^\circ$ ,  $h_1 = 40$  mm) and acetabulum ( $d = 64$  mm,  $h_2 = 33.5$  mm) based on the representative clinical computed tomography-data set, and holes in the acetabular ground to allow matrix dissolution in the test series with bone graft substitute. B, Acetabular test model in fixation block made of acrylic resin. Recess areas of 8 mm around the acetabular rim and behind the acetabulum (indicated by red arrows) allow for displacement under load [Color figure can be viewed at [wileyonlinelibrary.com](http://wileyonlinelibrary.com)]

on a clinical CT-data set (Figure 2A), whose use was approved by the Ludwig-Maximilians-University Munich ethics committee (project no. 18-108 UE) and incisura diameter was set to 10 mm.<sup>25</sup> The present model was made of 20 pounds per cubic foot (PCF) (0.32 g/cm<sup>3</sup>) solid rigid polyurethane (PU) foam (Sawbones, Malmö, Sweden) with a compressive strength of 8.4 MPa and Young's modulus of 210 MPa to represent slightly weakened bone as expected in revision surgeries, referring to a study of Crosnier et al.<sup>26</sup> who used 30 PCF (0.48 g/cm<sup>3</sup>) and 15 PCF (0.24 g/cm<sup>3</sup>) foams to simulate two different bone qualities. The test model was placed in an additively manufactured fixation block made of acrylic resin. Recess areas around the test model of 8 mm allowed displacement under load (Figure 1B).

### 2.2 | Development of simplified bone defect model and derivation of defect increments

On the basis of the clinically existing defect (Figure 2A), a simplified bone defect model was developed and four defect increments were derived thereof (Figures 3 and S2).

The defect has been quantitatively analyzed based on CT data, alongside with 49 other CT-data sets,<sup>21,27</sup> which was approved by the Ludwig-Maximilians-University Munich ethics committee (project no. 18-108 UE).

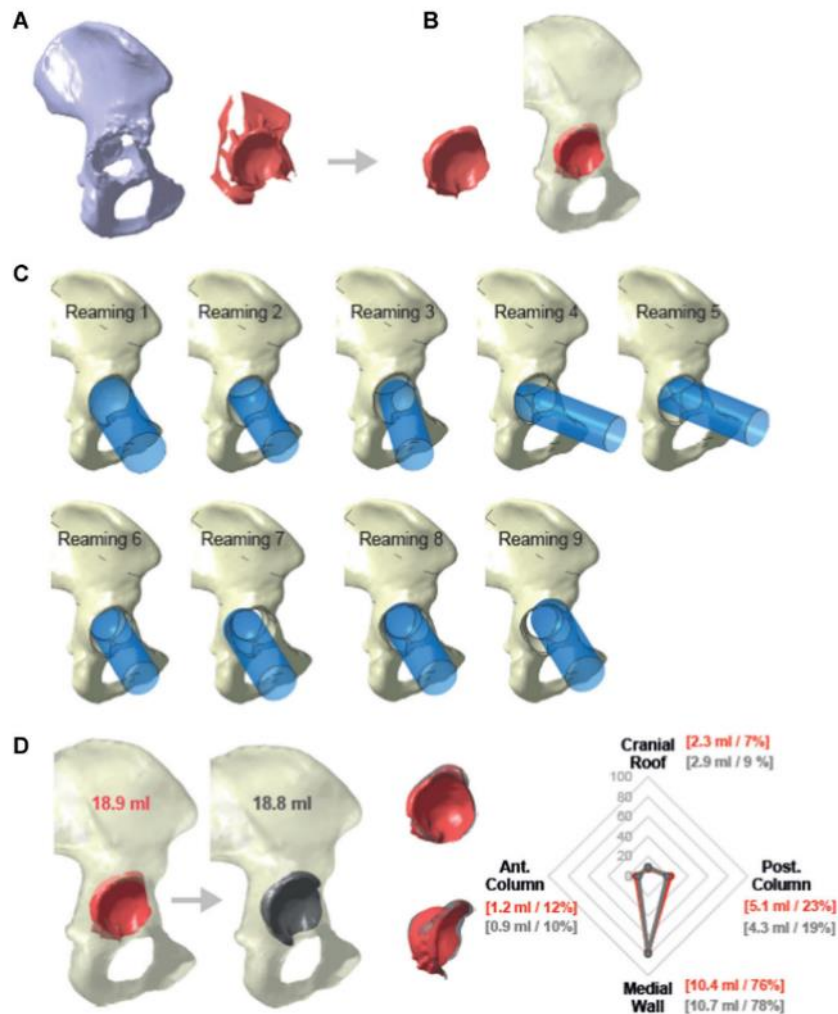


**FIGURE 2** Development of simplified bone defect model. A, Three-dimensional model of defect pelvis (light gray) and defect volume (red). B, Defect volume after removal of screw holes and reconstruction inaccuracies. C, Virtual reaming procedures to approximate defect volume with hemispherical reamers. D, Resulting simplified defect volume (dark gray) in comparison with original defect volume (red) presented as spider-plot showing volume loss in the pre-defined defect sectors cranial roof, anterior column, posterior column, and medial wall [Color figure can be viewed at [wileyonlinelibrary.com](http://wileyonlinelibrary.com)]



**FIGURE 3** Derivation of bone defect increment 1 as a mainly medial contained defect with rim defect in the inferior aspect of the posterior column. Application with reaming procedures 1 to 5 [Color figure can be viewed at [wileyonlinelibrary.com](http://wileyonlinelibrary.com)]

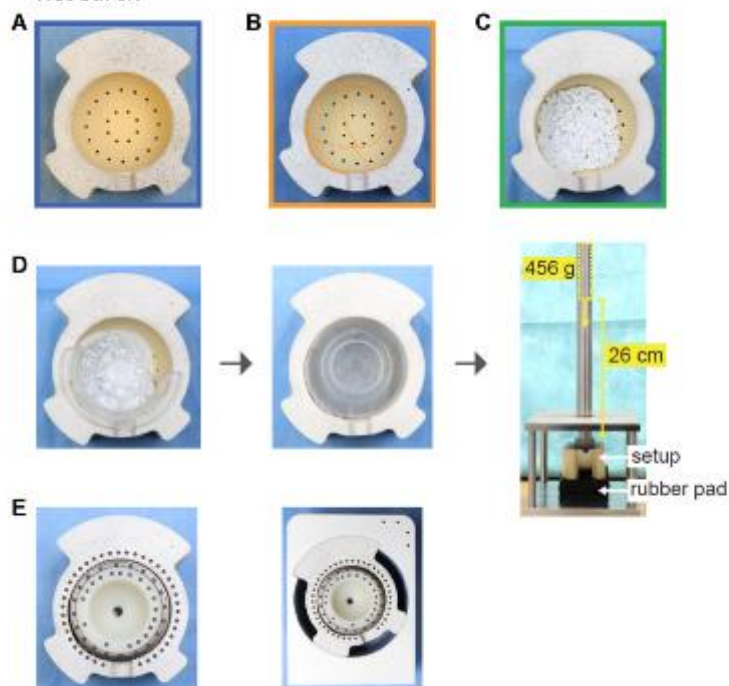


**FIGURE 4** The three test series and their preparation. A, Exemplary acetabular test model for test series Primary. B, Exemplary model for test series Empty with defect contour shown with orange lines. C, Exemplary model for test series Filled. D, Preparation of test series Filled with implantation of bone graft substitute using a filling template, an impactor, and a drop-weight impactation device. E, Specimen preparation with marker points and positioning in fixation block, exemplary shown for test series Filled [Color figure can be viewed at [wileyonlinelibrary.com](http://wileyonlinelibrary.com)]

Within the data of the quantitative analysis of 50 CT-data sets with acetabular bone defects, it was found that the herein presented defect showed relative bone volume loss close to the 25th percentile in the sectors cranial roof, anterior column and posterior column, and close to the median in the sector medial wall.<sup>21,27</sup> Hence, it represented a comparatively small defect within the 50 analyzed revision cases, which could be treated with bone graft (substitutes), medial and segmental containments, making it a suitable basis for the herein developed acetabular test model. Four senior hip revision surgeons from four different European clinical centers were consulted concerning the choice of a representative defect and confirmed the frequency of this defect type in revision surgery.

After bone volume loss analysis (Figure 2A), shell like reconstruction inaccuracies were removed, as well as the screw holes, assuming that these were not essential for stability (Figure 2B). In an iterative approach, nine virtual reaming procedures were defined to approximate volume and shape of the original defect with hemispherical acetabular reamers (Figure 2C), which would also enable defect implementation in donor specimens. The resulting simplified defect showed a shape comparable with the original defect (Figure 2D). Total defect volume (bone volume loss) showed a conformity of 99% and distribution of bone volume loss among the four defect sectors cranial roof, anterior column, posterior column, and medial wall<sup>27</sup> was also comparable between original and simplified defect (Figure 2D, spider plot). Detailed information on reamer size, position, and orientation can be found in Figure S1. On the basis of this simplified defect, three additional defect increments were derived by excluding specific reaming procedures (Figure S2) in order to build up a step-wise testing procedure for reconstruction strategies. The first bone defect increment (Figure 3) could be treated with BGS and was used as

basis for the acetabular test model in this study. It represents a mainly medial, contained defect with rim damage in the posterior-inferior aspect of approximately one-third of the circumference.

### 2.3 | Test series and specimen preparation

In the present study, defect Increment 1 was used in order to test BGS in combination with a press-fit cup. Three test series with  $N = 6$  each were conducted (Figure 4A-C): Acetabular test model without defect, treated with press-fit cup (Primary), test model with defect, treated with press-fit cup (Empty), test model with defect, treated with BGS and press fit cup (Filled). Specimen preparation included application of a random pattern on the acetabular test models to enable later analysis of deformations. A Plasmafit press-fit cup (Aesculap AG, Tuttlingen, Germany) size 48 mm was chosen for all three test series based on virtual planning on the original three-dimensional [3D] defect model in consultation with the clinical advisors. The resulting press-fit with a 48 mm diameter hemispherical reaming was 1.2 mm in relation to the diameter. In the series Primary there was circumferential contact between cup and foam, whereas in series Empty and Filled, rim contact was reduced to 2/3 of the circumference due to the defect in the inferior aspect of the posterior column (Figure 4B). The BGS were  $\beta$ -tricalcium phosphate-hydroxyapatite prototype granules with an edge length of 3.5 mm, which were mixed with polyethylene glycol and glycerin in a ratio of 4:1 by weight. A template was used to fill the defect with the correct and reproducible amount of BGS and a custom-made impactor and a drop-weight-device were used to impact the material. The weight (456 g) was dropped five times from a height of 26 cm (corresponding to an impulse

of 1.0N-s) to simulate impaction with a standard orthopedic hammer, whereby the acetabular test model was placed on a rubber pad to simulate soft tissue reaction (Figure 4D).

Cups were pressed-in displacement controlled with the material testing machine ZwickRoell Z010 (ZwickRoell GmbH & Co. KG, Ulm, Germany). Specimens were conditioned in purified water for 45 minutes, followed by 24 hours air-cure, and application of marker points on cup and acetabular test model (Figure 4E).

## 2.4 | Load protocol and stop criteria

The acetabular test model was placed under the servo-hydraulic testing machine MTS 858 Mini Bionix II (MTS, Minneapolis) such that the maximum resultant force during level walking, that is, during contralateral toe-off (Figure 5A) could be applied vertically (Figure 5B). Resultant force direction with respect to the acetabular cup was derived from data provided on [www.orthoload.com/orthoload-dub/](http://www.orthoload.com/orthoload-dub/) (OrthoLoad club, Julius-Wolff-Institute Berlin). All basic data have been obtained in a

previous study on in vivo loads measured in the femoral prosthesis, which has been independently conducted, funded and ethically approved (IEA2/057/09).<sup>28</sup> The data transformed to the acetabular cup coordinate system used within the present study have not yet been published. They are available in an internal database, with access restricted to OrthoLoad club members. Ten patients with instrumented hip implants performed daily activities such as level walking twelve months postoperatively, whereby motion was tracked via an optical tracking system and load in the femoral prosthesis was measured in vivo.<sup>28</sup> In vivo load data and motion data, given in the femoral coordinate system and the lab coordinate system, were transformed to an acetabular cup related coordinate system. Trials were averaged using the "Dynamic time wrapping" approach<sup>27</sup> and scaled.<sup>30</sup>

Mean cup-inclination and anteversion of the 10 patients were  $35^\circ \pm 6^\circ$  and  $28^\circ \pm 7^\circ$ , respectively. However, with the aim to use a standardized cup position within the Lowinneck safe zone, inclination of  $45^\circ$  and anteversion of  $20^\circ$  were assumed within this study.<sup>31</sup>

Force was applied in a sinusoidal waveform (2 Hz) via a 28 mm ceramic head, with a minimum load of 300 N.<sup>32</sup> Maximum load was

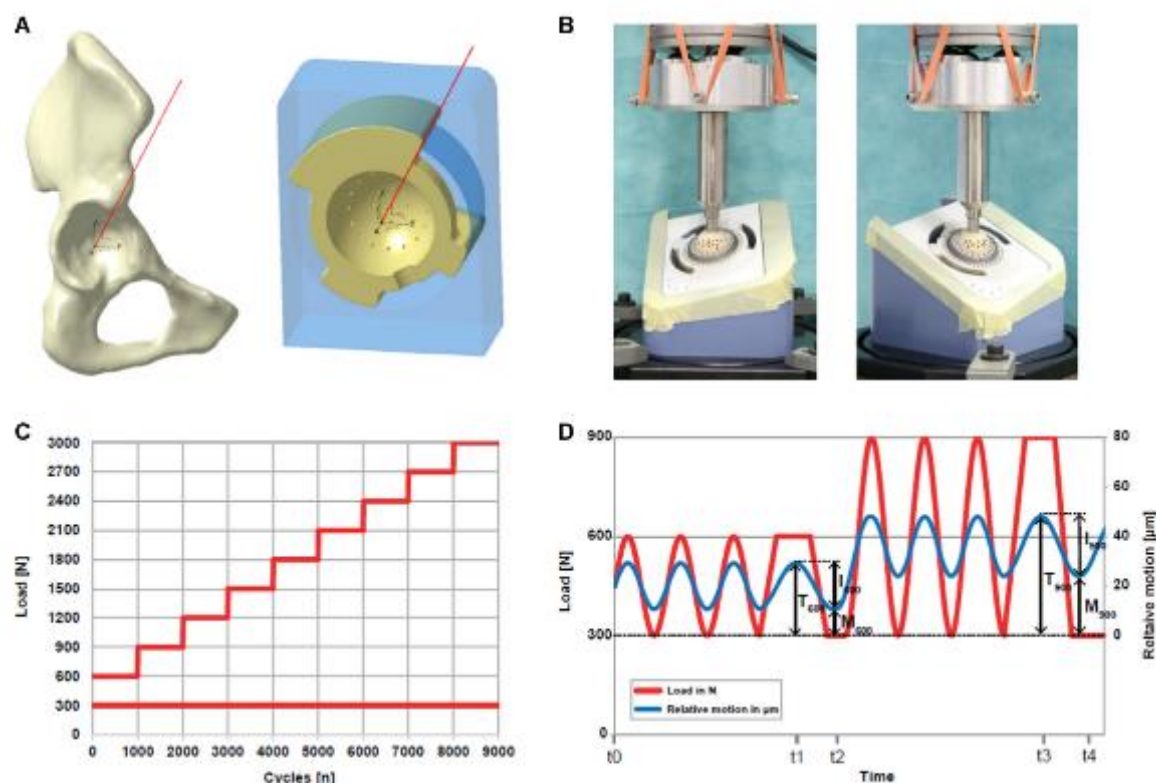


**FIGURE 5** Load application and relative motion measurement. A, Direction of load given by the maximum resultant force during level walking, indicated by red line in a native hemipelvis and the acetabular test model. B, Orientation and fixation under the servo-hydraulic testing machine for axial load application. C, Load protocol with nine load stages. Minimum load was 300 N for all load stages and maximum load was increased incrementally with 300 N/1000 cycles from 600 N (load stage 1) to 3000 N (load stage 9). D, Relative motion measurement, schematically shown for the first two load stages (600 and 900 N) with four exemplary load cycles. Load curve (red) overlaid with relative motion curve (blue). Measurements, that is, images were taken at static preload of 300 N ( $t_0$ ) and at the end of each load stage at maximum load (here  $t_1$  and  $t_3$ ) and minimum load (here  $t_2$  and  $t_4$ ). Inducible displacement was measured between the minimum and maximum load at each load stage (here indicated as  $M_{600}$  and  $M_{900}$ ). Migration was measured between the preload and the minimum load at each load stage (here indicated as  $T_{600}$  and  $T_{900}$ ) [Color figure can be viewed at [wileyonlinelibrary.com](http://wileyonlinelibrary.com)]

increased incrementally from 600 N (load stage 1) to 3000 N (load stage 9) with 300 N/1000 cycles<sup>33</sup> (Figure 5C).

Stop criteria was defined as structural failure of the acetabular test model or displacement of the MTS actuator of more than 2.5 mm, which was defined as conservative threshold based on migration values critical for long-term fixation of acetabular cups.<sup>34–36</sup>

## 2.5 | Relative motion measurement

Relative motions between cup and acetabular test model were assessed in 3D using the optical measurement system GOM Pontos 5M with two 5MP cameras with 50 mm lenses and the software Aramis Professional 2017 (GOM GmbH, Braunschweig, Germany). Marker points size 0.4 mm (ID 35231) with  $N = 20$  on the cup and  $N = 38$  on the test model were used, whereof  $N = 33$  were visible throughout the tests. Images were taken statically in the beginning at 300 N ( $t_0$ ) and at the end of each load stage at the corresponding maximum ( $t_1, t_3$ , etc.) and minimum ( $t_2, t_4$ , etc.) load (Figure 5D). It was distinguished between inducible displacement, migration, and total motion. Inducible displacement was defined as the displacement between maximum and minimum load in each load stage, migration as the displacement between the preload of 300 N and the minimum load at each load stage, and total motion as the displacement between the preload and the maximum load at each load stage (Figure 5D). Relative motion is given as mean value of all 33 marker points (Figure 6) and as maximum value (highest motion value within all 33 marker points) in Table 1.

## 2.6 | Resulting cup position measurement

Resulting cup position was measured after dynamic testing as angle between cup surface and acetabular test model surface with the tactile measurement system Prismo Navigator (Carl Zeiss Industrielle Messtechnik GmbH, Oberkochen, Germany) with a measurement inaccuracy of  $(0.9 + L/350) \mu\text{m}$ .

## 2.7 | Statistical analysis

Statistical analysis was performed using nonparametric tests, as the sample size ( $N = 6$ ) was too small to confirm normality. Test for statistical significance between the three test series was performed (Mann Whitney U test) with level of significance set to  $P < .05$ .

## 3 | RESULTS

### 3.1 | Relative motions

Inducible displacement, migration, and total motion increased with increasing load in all specimens (Figure 6). Series Empty was only

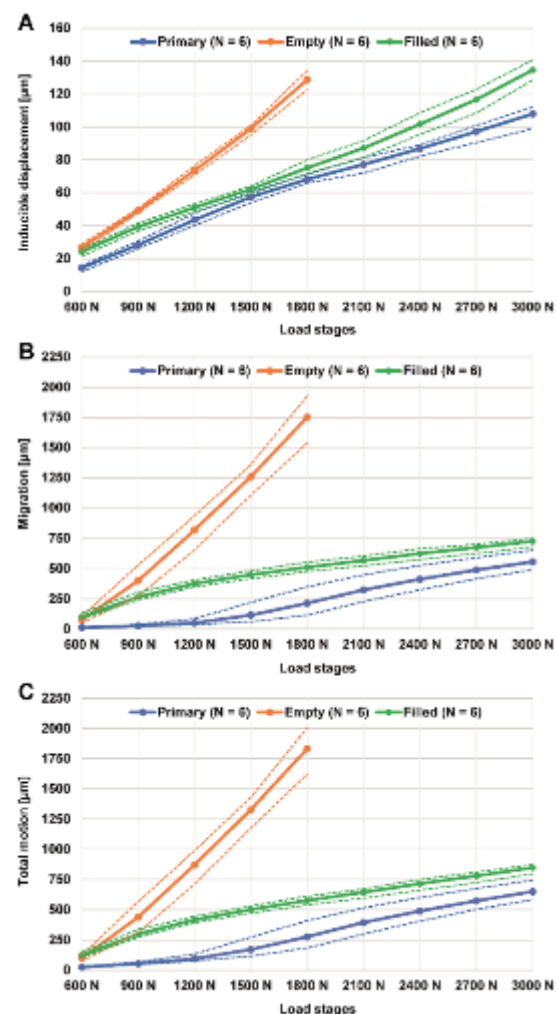


**FIGURE 6** Mean relative motions between cup and test model given as mean of  $N = 6$  in each test series (solid line) and as minimum and maximum within each test series (dashed lines). A, Inducible displacement. B, Migration. C, Total motion [Color figure can be viewed at [wileyonlinelibrary.com](http://wileyonlinelibrary.com)]

recorded until load stage 1800 N, as four out of six specimens reached the displacement stop criteria at the following load stage.

Mean inducible displacement was highest for Empty and lowest for Primary in all load stages (Figure 6A). At the last comparable load stage, 1800 N, mean inducible displacement of Empty ( $128.6 \pm 4.9 \mu\text{m}$ ) was increased 1.9-fold with respect to Primary ( $68.1 \pm 1.9 \mu\text{m}$ ) and in Filled ( $75.1 \pm 3.0 \mu\text{m}$ ), it was increased 1.1-fold with respect to Primary. Differences between all groups were statistically significant with  $P = .002$ . Furthermore, Primary and Filled were comparable in terms of curve.

Mean migration was highest for Empty and lowest for Primary in all load stages, except the first one (Figure 6B). At the last comparable load stage, 1800 N, mean migration of Empty

**TABLE 1** Inducible displacement, migration, and total motion in each load stage for the three test series, given as maximum motion in the 33 tracking points

	600 N	900 N	1200 N	1500 N	1800 N	2100 N	2400 N	2700 N	3000 N
Maximum inducible displacement in 33 tracking points (mean ± SD) in $\mu\text{m}$									
Primary	26 ± 3	48 ± 2	71 ± 3	93 ± 5	110 ± 3	127 ± 7	147 ± 5	167 ± 8	186 ± 9
Empty	64 ± 6	128 ± 7	188 ± 6	242 ± 7	292 ± 4	N/A	N/A	N/A	N/A
Filled	50 ± 3	75 ± 9	91 ± 9	106 ± 10	127 ± 7	146 ± 7	171 ± 10	199 ± 11	239 ± 12
Maximum migration in 33 tracking points (mean ± SD) in $\mu\text{m}$									
Primary	23 ± 4	45 ± 8	79 ± 22	213 ± 161	441 ± 279	730 ± 261	955 ± 239	1138 ± 212	1296 ± 195
Empty	192 ± 54	1077 ± 271	2149 ± 303	3212 ± 279	4311 ± 353	N/A	N/A	N/A	N/A
Filled	271 ± 48	712 ± 66	986 ± 86	1155 ± 120	1279 ± 138	1383 ± 141	1478 ± 146	1563 ± 141	1650 ± 145
Maximum total motion in 33 tracking points (mean ± SD) in $\mu\text{m}$									
Primary	46 ± 6	90 ± 9	144 ± 18	282 ± 148	500 ± 267	790 ± 257	1022 ± 235	1212 ± 214	1379 ± 199
Empty	252 ± 58	1205 ± 273	2337 ± 301	3451 ± 278	4599 ± 350	N/A	N/A	N/A	N/A
Filled	319 ± 45	787 ± 64	1073 ± 93	1253 ± 128	1390 ± 146	1508 ± 146	1619 ± 154	1727 ± 152	1837 ± 150

Note: Mean values and standard deviations of  $N = 6$  in each test series are shown.

( $1751.1 \pm 154.8 \mu\text{m}$ ) was increased 8.2-fold with respect to Primary ( $213.6 \pm 91.7 \mu\text{m}$ ), and in *Filled* ( $511.4 \pm 30.8 \mu\text{m}$ ), it was increased 2.4-fold with respect to Primary. Differences between all groups were statistically significant with  $P = .002$ . Empty showed a very steep migration curve, whereas *Filled* showed a steep curve in the beginning with flattening in the following load stages. Primary showed almost no migration in the beginning, but started to migrate in load stages 1500 to 1800 N which corresponded to the force applied to press the cups into the Primary setups ( $1841 \pm 205 \text{ N}$ ).

Mean total motion showed characteristics comparable to mean migration with highest values for Empty and lowest for Primary in load stages 900 to 3000 N (Figure 6C).

### 3.2 | Resulting cup position

Resulting cup position, measured after dynamic testing, was  $1.4^\circ \pm 0.3^\circ$  for Primary,  $7.3^\circ \pm 0.3^\circ$  for Empty, and  $1.6^\circ \pm 0.3^\circ$  for *Filled* (Figure 7), which corresponded to a 5.3-fold increase of resulting cup angle in Empty, and a 1.1-fold increase in *Filled* in comparison to Primary, respectively. Difference was statistically significant between Primary and Empty, and *Filled* and Empty with  $P = .002$  each.

## 4 | DISCUSSION

The objectives of this study were to (a) develop a simplified bone defect model based on a clinically existing acetabular bone defect, (b) build up a procedure to test different treatment strategies in one bone defect model whose severity can be increased incrementally, and (c) compare the stability of a press-fit cup in a primary situation with a revision situation with and without defect filling.

Pre-clinical testing of THA revision treatment strategies has been conducted using donor specimens,<sup>13,15,37,38</sup> Sawbone hemipelvises,<sup>20</sup> and foam models, either as block<sup>32</sup> or with an approximated acetabular shape.<sup>17,25,39</sup> PU foam has been widely used as surrogate for cancellous bone, as it provides more reproducible mechanical properties and can

be machined more easily than human cadaver specimens, which both reduces interspecimen variability. It is more readily available, of lower cost and test duration is not critical. Mechanical properties of PU foam are within the range of properties found for cancellous bone,<sup>40,41</sup> although these properties strongly depend on the individual donor, probe extraction site,<sup>42</sup> testing method and specimen preparation used.<sup>43</sup> The trabecular structure of cancellous bone is quite unique and can hardly be replicated by PU foam. The same applies to the anisotropic bone properties prescribed by Wolff's law.<sup>44</sup> Hence, PU foam represents an accepted surrogate material with a lot of advantages over cadaver specimens, but cannot replicate all their unique properties.

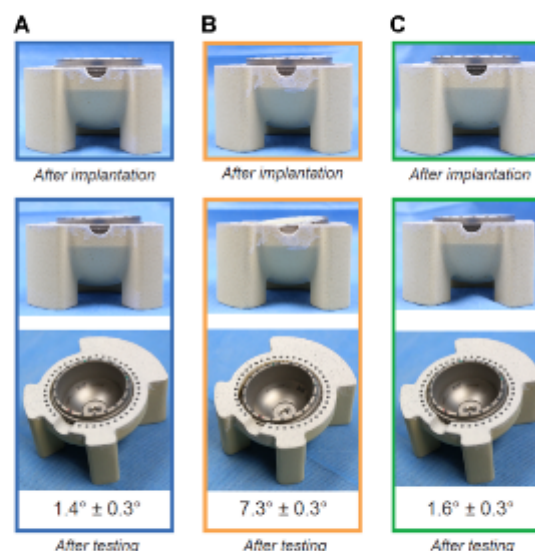


**FIGURE 7** Cup positions after implantation and after testing, exemplary shown for one specimen of each test series and with mean ± standard deviation of  $N = 6$  each, measured after dynamic testing. A, Primary series. B, Empty series. C, Filled series [Color figure can be viewed at [wileyonlinelibrary.com](http://wileyonlinelibrary.com)]

In the previous studies, load was applied torsional/tangential (lever-out), dynamically uniaxial, or dynamically with combined axial and rotational load (Table S1). In studies with dynamic load, 20 to 3600 motion cycles were applied, minimum load was 0 to 180 N, maximum load 490 to 3800 N, whereby maximum load was constant throughout the tests in most studies with some exceptions.<sup>17,20,45</sup> In studies with bone defects, these were applied at different locations, either centrally,<sup>15,19,37,45,46</sup> cranially,<sup>11,15</sup> posterior-cranially,<sup>13,25,39</sup> or posteriorly<sup>29</sup> and were implemented in a simplified way, often using only one acetabular reamer.<sup>19,45</sup> Relative motion consists of inducible displacement, migration, and total motion.<sup>47</sup> However, the previously mentioned studies did often not clearly differentiate between these components. Relative motion was measured using LVDTs,<sup>15,22,27</sup> or optical measurement systems.<sup>13,22,30</sup> LVDT measurements are limited to spot checks at the interface<sup>48,49</sup> and the sensor fixation can damage the bone or setup<sup>49,50</sup> and can hence influence its mechanical properties. Using optical measurement systems, a larger amount of measurement points can be used and due to the fact that the tracking points are only stacked to the surface, the properties of the bone/setup are not influenced. However, this also means that this type of measurement only provides information about relative motions at the surface of the specimen.

In the existing studies, comparison between the treatment strategies is difficult due to the variety of test models (donor specimens, foam models, etc.), load protocols (different directions and magnitudes), types of bone defects (different sizes and locations), interpretations of relative motion (inducible displacement, migration, etc.), and measurement techniques (optical, electromagnetic, etc.) used (Table S1).

Within the present study these points were addressed with the aim to suggest a simplified, but realistic acetabular bone defect, which can be increased incrementally to test different revision treatment strategies based on one defect model. The bone defect was derived from a representative clinical case. It was simplified by nine reaming procedures with standard acetabular reamers such that this method could also be applied in donor specimens. The simplified defect showed a shape comparable to the original defect and a high overall volume conformity of 99% (Figure 2). Four defect increments were derived such that defect severity could be modified by the number of reaming procedures (Figures 3 and S2). Due to the implementation with several reaming procedures, defect shape was irregular and hence close to the clinical case. An acetabular test model, similar to a setup already applied in lever-out studies,<sup>29,37</sup> was used to provide best possible reproducibility and comparability between the test series. The anatomical structure around the acetabulum was mimicked by the main support structures os ilium, os ischii, and os pubis to provide behavior under load as realistic as possible. Dynamic uniaxial loading in direction of level walking was chosen, comparable with other dynamic loading studies.<sup>9,20,51</sup> Load was increased incrementally to investigate the relation of load and relative motion.<sup>9,18–20,45,46</sup> Relative motion between cup and acetabular test model was measured in terms of inducible displacement, migration, and total motion, which has yet only been done by a limited number of studies.<sup>9,52</sup> This enables the distinction between different motion mechanisms and the estimation of their clinical

consequence. The smallest defined bone defect increment was implemented in the acetabular test model, representing a mainly contained, medial defect that could be filled by bone graft or BGS. Three test series were conducted comparing the primary situation with a revision situation with and without BGS filling.

Within the test series, it could be seen that mean total relative motion in Primary at the first load stage was  $24.5 \pm 3.8 \mu\text{m}$ , and the maximum was  $45.7 \pm 5.6 \mu\text{m}$ , which was in a range comparable to the relative motions of a press-fit cup measured in human donor specimens with  $36.03 \pm 16.83 \mu\text{m}$ .<sup>30</sup> Lowest mean total relative motion was found in Primary, as previously documented by Pitto and Schmidt,<sup>15</sup> who assessed primary stability of a Müller, Ganz, and Burch-Schneider cage in a primary and numerous defect situations. In the present study, mean and maximum relative motion increased with increasing load, which is in agreement with cyclic axial loading tests in Sawbone hemipelvises.<sup>22</sup>

This study has several limitations. First, an artificial acetabular model made of PU foam was used to approximate bone structure instead of human donor specimens. Donor specimens represent the most realistic bone model, but are associated with restricted reproducibility and test duration. Second, the presented acetabular bone defect model was based on one individual defect case. The defect was chosen based on a quantitative defect analysis in consultation with four senior hip revision surgeons as a common and rather small defect with main damage in the medial and posterior aspect. There is a wide variation of acetabular bone defects and the herein presented defect model cannot cover the whole range encountered in revision patients, but is rather a first building block for a standardized testing procedure. Depending on the amount and distribution of bone loss in the different sectors of the acetabulum, results for relative motion may be different for other defects, for example, when the cranial roof is concerned with a larger amount of bone loss. Hence, conclusions derived from the specific bone defect model presented in this study do not necessarily apply to all individuals with bone loss. Third, uniaxial loading was applied although most daily activities represent multiaxial loading scenarios and relative motion was found to be higher under multiaxial, than under uniaxial loading.<sup>53</sup> However, application of uniaxial load does not jeopardize comparability between the different test series and multiaxial loading is sophisticated to simulate in vitro, especially when motion tracking is required during the tests. In addition, uniaxial loading does not simulate friction moments. However, during contralateral toe-off, moments are limited to 0.17% BWm<sup>28</sup> and were therefore considered to have only little impact on relative motion. Fourth, relative motion measurement was performed under static load at the end of each load stage such that the temporal course of relative motion within the single load stages could not be investigated. Fifth, angles between cup and acetabular model were measured only after the tests and values on cup orientation before testing could not be provided.

To the authors' knowledge, this is the first study to suggest a bone defect model based on a representative CT-data set of an acetabular bone defect. The defect was simplified with nine reamings

with standard acetabular reamers, such that it could be also implemented in human donor specimens. From the simplified defect, four defect increments were derived such that different treatment strategies could be tested based on one model. Relative motion in terms of inducible displacement, migration, and total motion was measured in the three test series *Primary*, *Empty*, and *Filled* such that the influence of bone defect and defect filling on stability of a press-fit cup could be assessed. The presented method provides a platform to test stability of different treatment strategies based on one simplified, but realistic bone defect model in a standardized way.

Future studies should include validation of the acetabular test model by comparison with human donor specimens, the comparison of BGS with bone grafts, testing of other treatment strategies in higher bone defect increments, and the application of additional directions of load. Furthermore, the acetabular bone defect model should be extended with additional bone defects to cover a broader range of bone defects encountered in revision patients.

#### ACKNOWLEDGMENTS

The authors would like to thank the senior hip revision surgeons Prof. Dr. med. Heiko Graichen, Prof. Dr. med. Dipl.-Ing. Volkmar Jansson, Prof. Dr. med. Maximilian Rudert, and Prof. Francesco Traina for their input concerning choice of representative defect and cup size, Josef-Benedikt Weiß and Sven Krüger for their input concerning relative motion measurement.

#### CONFLICT OF INTERESTS

RS, GH, MB, and TG are employees of Aesculap AG Tuttlingen, a manufacturer of orthopedic implants. FM and PD receive institutional support by Aesculap AG. Aesculap AG provided support in the form of salaries for RS, GH, MB, and TG, but did not have any role in design of the study, data analysis, decision to publish or manuscript preparation.

#### AUTHOR CONTRIBUTIONS

All authors worked on research design, or acquisition, analysis or interpretation of data. RS worked on drafting the paper and GH, AR, MB, FM, PD, and TG critically revised it. All authors have read and approved the final submitted manuscript.

#### ORCID

Ronja A. Schierjell  <http://orcid.org/0000-0002-0624-1978>

#### REFERENCES

- Sadoghi P, Liebensteiner M, Agreiter M, Leithner A, Böhler N, Labek G. Revision surgery after total joint arthroplasty: a complication-based analysis using worldwide arthroplasty registers. *J Arthroplasty*. 2013;28:1329-1332.
- Pilliar RM, Lee JM, Maniopoulos C. Observations on the effect of movement on bone ingrowth into porous-surfaced implants. *Clin Orthop Relat Res*. 1986;208:108-113.
- Bragdon CR, Burke D, Lowenstein JD, et al. Differences in stiffness of the interface between a cementless porous implant and cancellous bone in vivo in dogs due to varying amounts of implant motion. *J Arthroplasty*. 1996;11:945-951.
- Zietz C, Fritsche A, Klues D, Mittelmeier W, Bader R. Influence of acetabular cup design on the primary implant stability. An experimental and numerical analysis. *Orthopade*. 2009;38:1097-1105.
- Jahnke A, Schroeder S, Fonseca Ulloa CA, Ahmed GA, Ishaque BA, Rickert M. Effect of bearing friction torques on the primary stability of press fit acetabular cups: a novel in vitro method. *J Orthop Res*. 2018;36:2745-2753.
- Le Cann S, Galland A, Rosa B, et al. Does surface roughness influence the primary stability of acetabular cups? A numerical and experimental biomechanical evaluation. *Med Eng Phys*. 2014;36:1185-1190.
- Tabata T, Kaku N, Hara K, Tsunura H. Initial stability of cementless acetabular cups: press-fit and screw fixation interaction-an in vitro biomechanical study. *Eur J Orthop Surg Traumatol*. 2015;25:497-502.
- Jahnke A, Bott CC, Fonseca Ulloa CA, et al. In vitro examination of the primary stability of three press-fit acetabular cups under consideration of two different bearing couples. *Med Eng Phys*. 2019;67:49-54.
- Morosato F, Traina F, Cristofolini L. A reliable in vitro approach to assess the stability of acetabular implants using digital image correlation. *Strain*. 2019;55:1-12.
- Weißmann V, Ramskogler T, Schulze C, et al. Influence of synthetic bone substitutes on the anchorage behavior of open-porous acetabular cup. *Materials (Basel, Switzerland)*. 12, 2019:1-16.
- Meneghini RM, Meyer C, Buckley CA, Hanssen AD, Lewallen DG. Mechanical stability of novel highly porous metal acetabular components in revision total hip arthroplasty. *J Arthroplasty*. 2010;25:337-341.
- Adler E, Stuchin SA, Kummer FJ. Stability of press-fit acetabular cups. *J Arthroplasty*. 1992;7:295-301.
- Beckmann NA, Bitsch RC, Janoszka MB, Klotz MC, Bruckner T, Jaeger S. Treatment of high-grade acetabular defects: Do porous titanium cups provide better stability than traditional titanium cups when combined with an augment? *J Arthroplasty*. 2018;33:1838-1843.
- Wu H, Ma C, Ran J, et al. Biomechanical research on contour cage with transacetabular screws fixation in revision total hip arthroplasty. *Clin Biomech*. 2017;47:117-122.
- Pitto RP, Schmidt R. Primary mechanical stability of three acetabular reinforcement implants. Influence of bone stock defects. *Biomed Tech*. 1998;43:210-215.
- Arts JJC, Schreurs BW, Buma P, Verdonschot N. Cemented cup stability during lever-out testing after acetabular bone impaction grafting with bone graft substitutes mixes containing morsellized cancellous bone and tricalcium phosphate-hydroxyapatite granules. *Proc Inst Mech Eng [H]*. 2005;219:257-263.
- Arts JJC, Verdonschot N, Buma P, Schreurs BW. Larger bone graft size and washing of bone grafts prior to impaction enhances the initial stability of cemented cups. Experiments using a synthetic acetabular model. *Acta Orthop*. 2006;77:227-233.
- Bolder SBT, Verdonschot N, Schreurs BW, Buma P. The initial stability of cemented acetabular cups can be augmented by mixing morsellized bone grafts with tricalciumphosphate/hydroxyapatite particles in bone impaction grafting. *J Arthroplasty*. 2003;18:1056-1063.
- Bolder SBT, Verdonschot N, Schreurs BW, Buma P. Acetabular defect reconstruction with impacted morsellized bone grafts or TCP/HA particles. A study on the mechanical stability of cemented cups in an artificial acetabulum model. *Biomaterials*. 2002;23:659-666.

20. Beckmann NA, Bitsch RG, Condan M, Schonhoff M, Jaeger S. Comparison of the stability of three fixation techniques between porous metal acetabular components and augments. *Bone Joint Res.* 2018;7:282-288.
21. Schierjott RA, Hettich G, Graichen H, et al. Quantitative assessment of acetabular bone defects: a study of 50 computed tomography data sets. *PLoS One.* 2019;14:e0222511.
22. Gelaude F, Clijmans T, Delport H. Quantitative computerized assessment of the degree of acetabular bone deficiency: total radial acetabular bone loss (TrABL). *Adv Orthop.* 2011;2011:1-12.
23. Wright G, Paprosky WG 2016. Acetabular reconstruction: classification of bone defects and treatment options. <https://musculoskeletalkey.com/acetabular-reconstruction-classification-of-bone-defects-and-treatment-options/>. Accessed December 12, 2019.
24. D'Antonio JA, Capello WN, Borden LS, et al. Classification and management of acetabular abnormalities in total hip arthroplasty. *Clin Orthop Relat Res.* 1989;243:126-137.
25. Jamieson ML, Russell RD, Incavo SJ, Noble PC. Does an enhanced surface finish improve acetabular fixation in revision total hip arthroplasty? *J Arthroplasty.* 2011;26:644-648.
26. Crosnier EA, Keogh PS, Miles AW. A novel method to assess primary stability of press-fit acetabular cups. *Proc Inst Mech Eng [H].* 2014;228:1126-1134.
27. Hettich G, Schierjott RA, Ramm H, et al. Method for quantitative assessment of acetabular bone defects. *J Orthop Res.* 2019;37:181-189.
28. Damm P, Bender A, Bergmann G. Postoperative changes in in vivo measured friction in total hip joint prosthesis during walking. *PLoS One.* 2015;10:e0120438.
29. Bender A, Bergmann G. Determination of typical patterns from strongly varying signals. *Comput Methods Biomech Biomed Eng.* 2012;15:761-769.
30. Bergmann G, Bender A, Dymke J, Duda G, Damm P. Standardized loads acting in hip implants. *PLoS One.* 2016;11:e0155612.
31. Morosato F, Traina F, Cristofolini L. Standardization of hemipelvis alignment for in vitro biomechanical testing. *J Orthop Res.* 2018;36:1645-1652.
32. Bürkner A, Fottner A, Lichtinger T, et al. Primary stability of cementless threaded acetabular cups at first implantation and in the case of revision regarding micromotions as indicators. *Biomed Tech (Berl).* 2012;57:169-174.
33. Grupp TM, Saleh KJ, Holderied M, et al. Primary stability of tibial plateaus under dynamic compression-shear loading in human tibiae – influence of keel length, cementation area and tibial stem. *J Biomech.* 2017;59:9-22.
34. Ng T-P, Chiu K-Y. Acetabular revision without cement. *J Arthroplasty.* 2003;18:435-441.
35. Pijls BG, Nieuwenhuijse MJ, Flocco M, et al. Early proximal migration of cups is associated with late revision in THA. A systematic review and meta-analysis of 26 RSA studies and 49 survival studies. *Acta Orthop.* 2012;83:583-591.
36. Delaunay CP, Kasandji AI. Survivorship of rough surfaced threaded acetabular cups. 382 consecutive primary Zweymüller cups followed for 0.2-12 years. *Acta Orthop Scand.* 1998;69:379-383.
37. Hadjari MH, Hollis JM, Hofmann OE, et al. Initial stability of porous coated acetabular implants. The effect of screw placement, screw tightness, defect type, and oversize implants. *Clin Orthop Relat Res.* 1994;307:117-123.
38. Beckmann NA, Jaeger S, Janoszka MB, Klotz MC, Bruckner T, Bitsch RG. Comparison of the primary stability of a porous coated acetabular revision cup with a standard cup. *J Arthroplasty.* 2018;33:580-585.
39. Huber WO, Noble PC. Effect of design on the initial stability of press-fit cups in the presence of acetabular rim defects: experimental evaluation of the effect of adding circumferential fins. *Int Orthop.* 2014;38:725-731.
40. Sawbones USA. Biomechanical materials for precise, repeatable testing. <https://www.sawbones.com/biomechanical-product-info>. Accessed December 12, 2019.
41. Li B, Aspden RM. Composition and mechanical properties of cancellous bone from the femoral head of patients with osteoporosis or osteoarthritis. *J Bone Miner Res.* 1997;12:641-651.
42. van Ladebeijn R, Leslie H, Manning WA, et al. Mechanical properties of cancellous bone from the acetabulum in relation to acetabular shell fixation and compared with the corresponding femoral head. *Med Eng Phys.* 2018;53:75-81.
43. Linde F, Sorenson HCF. The effect of different storage methods on the mechanical properties of trabecular bone. *J Biomech.* 1993;26:1249-1252.
44. Frost HM. Wolff's law and bone's structural adaptations to mechanical usage: an overview for clinicians. *Angle Orthod.* 1994;64:175-188.
45. Bolder SB, Schreurs BW, Verdonschot N, van Unen JM, Gardeniers JW, Slooff TJ. Particle size of bone graft and method of impaction affect initial stability of cemented cups: human cadaveric and synthetic pelvic specimen studies. *Acta Orthop Scand.* 2003;74:652-657.
46. Walschot LH, Aquarius R, Schreurs BW, Buma P, Verdonschot N. Better primary stability with porous titanium particles than with bone particles in cemented impaction grafting. An in vitro study in synthetic acetabula. *J Biomed Mater Res B Appl Biomater.* 2013;101:1243-1250.
47. Britton JR, Lyons CG, Prendergast PJ. Measurement of the relative motion between an implant and bone under cyclic loading. *Strain.* 2004;40:193-202.
48. Gortchacow M, Wettstein M, Pioletti DP, Terrier A. A new technique to measure micromotion distribution around a cementless femoral stem. *J Biomech.* 2011;44:557-560.
49. Sukjamsri C, Geraldus DM, Gregory T, et al. Digital volume correlation and micro-CT: an in-vitro technique for measuring full-field interface micromotion around polyethylene implants. *J Biomech.* 2015;48:3447-3454.
50. Gao X, Fraulob M, Haiat G. Biomechanical behaviours of the bone-implant interface: a review. *J R Soc Interface.* 2019;16:20190259.
51. Crosnier EA, Keogh PS, Miles AW. The effect of dynamic hip motion on the micromotion of press-fit acetabular cups in six degrees of freedom. *Med Eng Phys.* 2016;38:717-724.
52. Pitto RP, Böhrer J, Hofmeister V. Factors influencing initial stability of uncemented acetabular components. An in-vitro study. *Biomed Tech.* 1997;12:363-368.

#### SUPPORTING INFORMATION

Additional supporting information may be found online in the Supporting Information section.

**How to cite this article:** Schierjott RA, Hettich G, Ringkamp A, et al. A method to assess primary stability of acetabular components in association with bone defects. *J Orthop Res.* 2020;1-10. <https://doi.org/10.1002/jor.24591>

**4.3 Publication III: Primary stability of a press-fit cup in combination with impaction grafting in an acetabular defect model**

Authors: Ronja A Schierjott, Georg Hettich, Marc Baxmann,  
Federico Morosato, Luca Cristofolini, Thomas M Grupp

Journal: Journal of Orthopaedic Research

Volume: Epub ahead of print

Pages: 1-12

Year: 2020

DOI: <https://doi.org/10.1002/jor.24810>

Impact factor: 2.728 (according to InCites Journal Citation Reports 2019)

Received: 2 March 2020 | Accepted: 13 July 2020

DOI: 10.1002/jor.24810

## RESEARCH ARTICLE

Journal of  
Orthopaedic  
Research®

# Primary stability of a press-fit cup in combination with impaction grafting in an acetabular defect model

Ronja A. Schierjott<sup>1,2</sup>  | Georg Hettich<sup>1</sup> | Marc Baxmann<sup>1</sup> | Federico Morosato<sup>3</sup> | Luca Cristofolini<sup>3</sup>  | Thomas M. Grupp<sup>1,2</sup>

<sup>1</sup>Research & Development Department, Aesculap AG, Tuttlingen, Germany

<sup>2</sup>Department of Orthopaedic Surgery, Physical Medicine & Rehabilitation, Campus Grosshadern, Ludwig-Maximilians University Munich, Munich, Germany

<sup>3</sup>Department of Industrial Engineering, Alma Mater Studiorum-Università di Bologna, Bologna, Italy

## Correspondence

Ronja A. Schierjott, Am Aesculap Platz, 78532 Tuttlingen, Germany.  
Email: ronja\_elissa.schierjott@aesculap.de

## Abstract

The objectives of this study were to (a) assess primary stability of a press-fit cup in a simplified acetabular defect model, filled with compacted cancellous bone chips, and (b) to compare the results with primary stability of a press-fit cup combined with two different types of bone graft substitute in the same defect model. A previously developed acetabular test model made of polyurethane foam was used, in which a mainly medial contained defect was implemented. Three test groups (N = 6 each) were prepared: Cancellous bone chips (*bone chips*), tricalciumphosphate tetrapods + collagen matrix (*tetrapods + coll*), bioactive glass S53P4 + polyethylene glycol-glycerol matrix (*b.a.glass + PEG*). Each material was compacted into the acetabulum and a press-fit cup was implanted. The specimens were loaded dynamically in the direction of the maximum resultant force during level walking. Relative motion between cup and test model was assessed with an optical measurement system. At the last load step (3000 N), inducible displacement was highest for bone chips with median [25th percentile; 75th percentile] value of 113 [110; 114]  $\mu\text{m}$  and lowest for *b.a.glass + PEG* with 91 [89; 93]  $\mu\text{m}$ . Migration at this load step was highest for *b.a.glass + PEG* with 868 [845; 936]  $\mu\text{m}$  and lowest for *tetrapods + coll* with 491 [487; 497]  $\mu\text{m}$ . The results show a comparable behavior under load of *tetrapods + coll* and bone chips and suggest that *tetrapods + coll* could be an attractive alternative to bone chips. However, so far, this was found for one specific defect type and primary stability should be further investigated in additional/more severe defects.

## KEYWORDS

acetabular bone defect model, impaction grafting, optical measurement, press-fit cup, primary stability, synthetic bone graft substitute

## 1 | INTRODUCTION

Revision hip surgery is still challenging and often associated with acetabular bone defects which make subsequent implant fixation even more difficult. The large variation in bone defects<sup>1,2</sup> requires a

broad range of specific treatment options, such as revision cups, reconstruction shells or impaction bone grafting (IBG). Using IBG, cancellous bone chips are compacted into a defect and combined with cemented polyethylene (PE) cups, press fit cups or reconstruction shells.<sup>3-5</sup> This technique enables bone stock reconstruction<sup>6</sup> and

This is an open access article under the terms of the Creative Commons Attribution-NonCommercial License, which permits use, distribution and reproduction in any medium, provided the original work is properly cited and is not used for commercial purposes.

© 2020 The Authors. Journal of Orthopaedic Research® published by Wiley Periodicals LLC on behalf of Orthopaedic Research Society

has shown satisfying clinical results in acetabular and femoral hip revision surgery.<sup>6,7</sup>

However, supply of donor bone is limited and very expensive. Furthermore, the preparation of bone chips in the operating room is time consuming and the quality of the produced bone chips differs widely due to biological variation and preparation technique.<sup>8</sup> Finally, an infection risk remains.<sup>9</sup>

Synthetic bone graft substitutes (BGS) may represent an attractive alternative or supplement to bone chips to increase reproducibility of mechanical properties and to decrease infection risk. Numerous BGS have been developed and tested. Most previous *in vitro* studies focused on mechanical properties in a simplified setup or primary stability of bone chips and BGS in combination with a cemented cup.<sup>9-12</sup> Primary stability is an important prerequisite for clinical long-term success and to the authors' knowledge, primary stability of these defect filling materials has yet hardly been assessed in combination with a press-fit cup.<sup>13,14</sup>

The objectives of this study were to (a) assess primary stability of compacted bone chips with a press-fit cup using a previously presented reproducible acetabular test model, and to (b) compare the results with two BGS materials.

## 2 | MATERIALS AND METHODS

### 2.1 | Acetabular test model and test setup

An artificial acetabular test model made of polyurethane (PU) foam was used, which replicated the main support structures of the pelvis *os ilium*, *os pubis* and *os ischii*.

This model was oriented towards a previously developed surrogate model<sup>15,16</sup> with the basic idea of mimicking the main support structures, while reducing the support in the remaining areas, especially in the *incisura acetabuli* (Figure 1A-D).<sup>14-16</sup> In the herein applied acetabular test model, a diameter of 10 mm was chosen for the *incisura acetabuli*, as described by Jamieson et al., 2011.<sup>15</sup> In order to represent a real pelvis as well as possible, the dimensions of the *os ilium*, *os pubis* and *os ischii* were derived from a clinical computed tomography (CT)-data set of a pelvis with acetabular bone defect. The latter was obtained within a previously conducted study in which 50 acetabular bone defects were quantitatively analyzed based on CT-data,<sup>2</sup> whereby use of the CT-data was approved by the Ludwig-Maximilians-University Munich ethics committee (project no. 18-108 UE).

20 pounds per cubic foot (PCF) (0.32 g/cm<sup>3</sup>) solid rigid PU foam (Sawbones Malmö, Sweden) with Young's modulus of 210 MPa and compressive strength of 8.4 MPa was chosen<sup>14</sup> to simulate slightly weakened bone as expected in revision surgery. This was oriented towards a study by Crosnier et al.,<sup>17</sup> who used 30 PCF and 15 PCF PU foam to simulate two different kinds of bone quality.

In the herein used acetabular test model, medial wall thickness of 5.6 mm was chosen to enable compaction of the defect filling materials with impacts similar to those applied during surgery.

A standardized, mainly medial contained defect with rim damage in the posterior-inferior aspect of approximately 1/3 of the

circumference was created.<sup>14</sup> This defect could be categorized as a variant of Paprosky 1 with some aspects of Paprosky 3A, that is, rim damage of 1/3 of the circumference.<sup>1</sup> Paprosky 1 is among the most commonly observed defect types based on studies analyzing radiographs in association with acetabular revision surgery.<sup>18,19</sup>

The acetabular test models were prepared with a random spray pattern for strain analysis and were fixed in an acrylic resin block (Figure 1D). The latter was placed in an orientation block aligning the specimen with the load axis for dynamic testing (Figure 1E).

In order to ensure that the herein applied artificial test model showed a behavior under load comparable to a real pelvis, total relative motion between a press fit cup and the artificial test model without defect, measured within a previous study of our research group,<sup>14</sup> was compared with relative motion between a press-fit cup and the surrounding bone in human donor specimens, relating to a study of Beckmann et al., 2018.<sup>20</sup>

Beckmann et al. compared relative motion between two different types of press-fit cups and the surrounding bone in 10 fresh-frozen human donor specimens.<sup>20</sup> Using a multi axial testing machine, they simulated 1000 repetitions of a normal gait cycle, whereby minimum and maximum load were restricted to 8.71% body weight (BW) and 69.93% BW, respectively. Based on the average donor weight, this corresponded to approximately 54 and 437 N, respectively. Relative motion was assessed using the optical measurement system GOM Pontos (GOM GmbH Braunschweig, Germany) and was found to be 36.03 ± 16.83 µm (Gription cup) and 29.27 ± 14.97 µm (Porocoat cup) after 1000 load cycles.<sup>20</sup>

In a previous study of our research group, relative motion between a press-fit cup and the artificial test setup without defect was assessed under dynamic loading in direction of the maximum resultant force during level walking. At the lowest defined load increment (600 N), mean (maximum) relative motion were found to be 24.5 ± 3.8 µm (45.7 ± 5.6 µm) and were hence in a range comparable to the relative motion measured in human donor specimens.<sup>14,20</sup>

### 2.2 | Test groups and specimen preparation

Three test groups were defined for this study: Morzellized allografts (bone chips), bioactive glass in a polyethylene glycol and glycerol matrix (*b.o.glass*+PEG), and ceramic tetrapods in a collagen matrix (*tetrapods*+coll) (Figure 1A-C). Cancellous bone chips were prepared from eight fresh frozen human donor femoral heads, retrieved within the ethics vote 5-170/2016 (University of Heidelberg, Germany). They were first sawed into slices. Using a bone nibbler, the cortical bone was removed and bone chips were nipped from the remaining cancellous bone.<sup>4</sup> A bone nibbler was used in order to produce relatively large bone chips which are most suitable for acetabular impaction grafting.<sup>9,11,21</sup> Bone chips size and variation were assessed by measuring the maximum edge length of 100 exemplary chips with a ruler.<sup>21</sup> Mean bone chips size was 7 ± 2 mm (range: 3 to 12 mm). Bone chips of all eight femoral heads were mixed to reduce inter-specimen variability (Figure 1A).

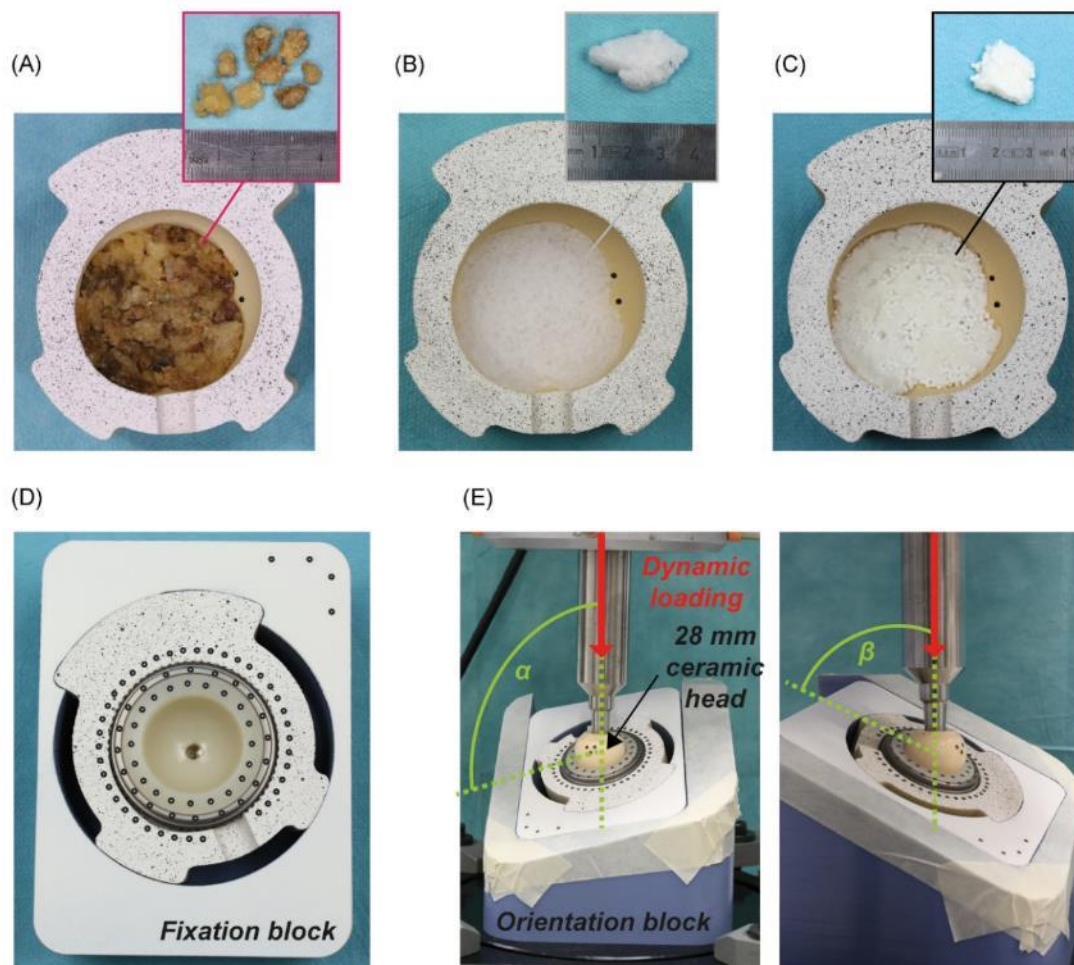


**FIGURE 1** Test groups in acetabular test model and final test setup. A, Test group allograft (*bone chips*). B, Test group bioactive glass and polyethylene glycol-glycerol matrix (*b.a.glass + PEG*). C, Test group ceramic tetrapods and collagen matrix (*tetrapods + coll*), each with explosion figure of filling material for size estimation. D, One exemplary specimen after implantation in fixation block with recess areas, prepared for testing with tracking points for relative motion analysis. E, Setup under servo-hydraulic testing machine, shown for one exemplary specimen. Alignment with orientation block such that maximum resultant force during level walking can be applied vertically via 28 mm diameter ceramic head. Orientation of the force vector relative to the setup is indicated with  $\alpha = 102^\circ$  and  $\beta = 63^\circ$  [Color figure can be viewed at [wileyonlinelibrary.com](http://wileyonlinelibrary.com)]

*B.a.glass + PEG* consisted of S53P4 bioactive glass granules based on silicon-oxide, sodium-oxide, calcium-oxide, and phosphorus pentoxide with granule size 1.0 to 2.0 mm (80 wt.%) and a PEG matrix (20 wt.%) (Bonalive Biomaterials Ltd, Turku, Finland). The glass granules can inhibit bacterial growth by an elevation of pH and osmotic pressure and have already been used as bone void filler in infection treatments.<sup>22,23</sup> *Tetrapods + coll* consisted of powder-injection-molded and sintered tricalciumphosphate ( $\beta$ -TCP) tetrapods with an edge-length of 3.3 mm (93 vol%) (IFAM, Bremen, Germany)<sup>9</sup> and a collagen (primarily type I derived from bovine tendon) matrix material (7 vol%) (Collagen Solutions Plc, Glasgow, UK).

All materials were applied using a template to provide reproducible filling of the defects (Figure 2). The materials were compacted manually step-by-step with a hemispherical impactor and an orthopedic hammer. Final compaction was performed with a weight of 456 g which was dropped 10-times<sup>24</sup> from a height of 26 cm on an acetabular cup shaped impactor. 456 g corresponded to the weight of a standard orthopedic hammer and height of 26 cm was chosen for a standardized impulse of 1 Ns. The titanium press-fit cup Plasmakit  $\varnothing$ 48 mm (Aesculap AG Tuttlingen, Germany) with a nominal external diameter of 49.2 mm (NV148T) and a resultant press-fit of 1.2 mm related to the diameter was pressed on the filling material using the Zwick/Roell material testing machine Z005

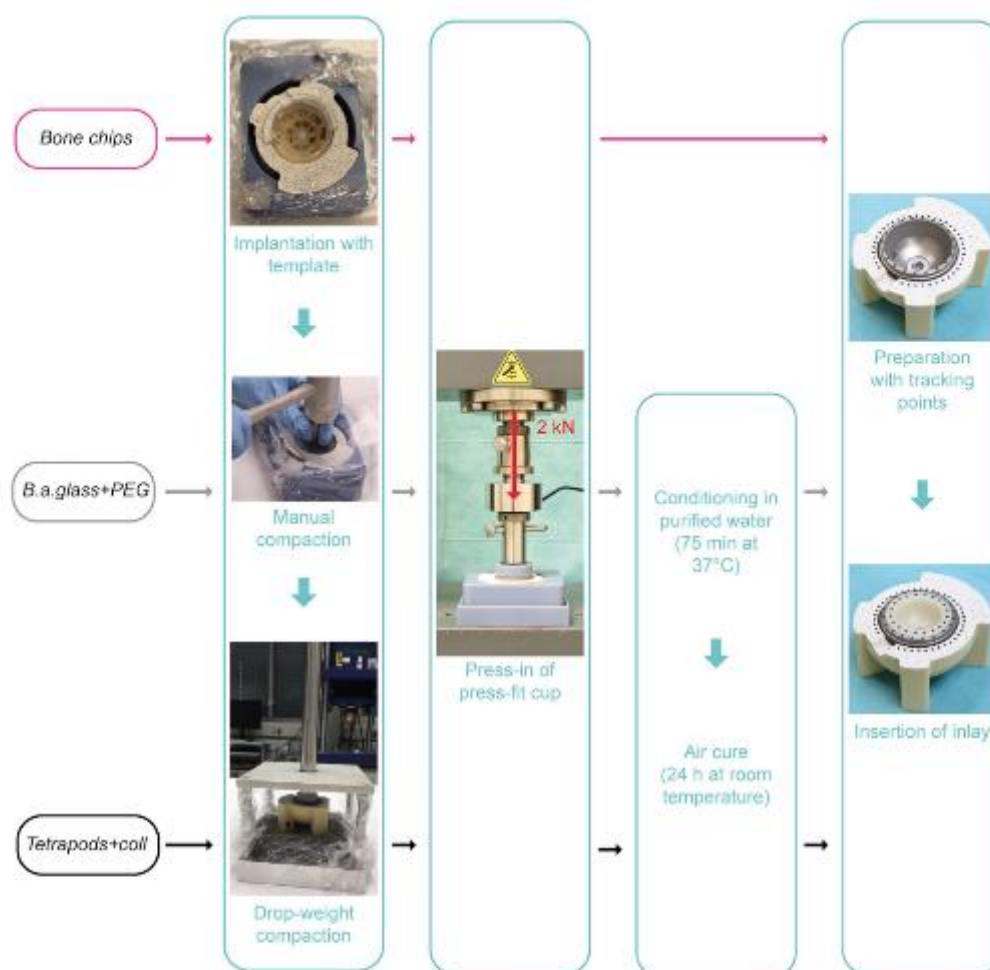


**FIGURE 2** Preparation matrix for the three test groups. In all specimens, the filling material was implanted using a template, which was followed by manual pre-compaction with a hammer and a standardized compaction by dropping a 456 g weight 10-times (Arts et al.<sup>14</sup>) from a height of 26 cm. 456 g corresponded to the weight of a standard orthopedic hammer and a height of 26 cm was used to achieve a standardized impulse of 1 N·s. Using a material testing machine, the cup was pressed on the filling material in the acetabular test model with 2 kN. Test groups *b.a.glass + PEG* and *tetrapods + coll* were then conditioned in purified water at 37°C for 75 minutes and air-cured for 24 hours at room temperature. Specimens of all test groups were prepared with tracking points and the polyethylene inlay was inserted prior to testing [Color figure can be viewed at [wileyonlinelibrary.com](http://wileyonlinelibrary.com)]

(ZwickRoell GmbH & Co. KG, Ulm, Germany), with 2 kN and displacement of 1 mm/min. This aimed at performing the implantation as controlled and reproducible as possible and was oriented towards the implantation procedure described in previous studies assessing primary stability of acetabular cups, in which a static load of 2 to 3 kN was used to insert the cups.<sup>16,25</sup>

Specimens of the test groups *b.a.glass + PEG* and *tetrapods + coll* were then conditioned in purified water at 37°C for 75 min including four (*tetrapods + coll*) and eighteen (*b.a.glass + PEG*) rinsing procedures to simulate matrix dissolution in the body after surgery. Eighteen rinsing procedures for *b.a.glass + PEG* were defined based on a pretest to remove as much of the water-soluble PEG-matrix as possible. For

*tetrapods + coll*, the number of rinsing procedures was reduced to four, as the collagen matrix was not expected to be removed by water anyway.

A central hole at the bottom, that is, at the pole of the cup and several holes drilled in the ground of the acetabular test model allowed the fluid to get around the back of the cup. However, this was partially restricted by the tight press-fit between the cup and the BGS. Hence, the fluid had full access to the BGS in the central area, that is, near the pole of the acetabular cup, but reduced access to the BGS in the remaining areas behind the cup. The specimens were air-cured at room temperature for 24 hours before testing.

In all three test groups, a PE inlay was inserted and tracking points for optical motion measurement were placed on the acetabular test model, cup and inlay (Figures 1D and 2).

### 2.3 | Load protocol and relative motion measurement

The specimens were loaded dynamically with the servo hydraulic testing machine MTS 858 Mini Bionix II (MTS, Minneapolis) in the direction of maximum resultant force during level walking, that is, during contralateral toe-off,<sup>14,26</sup> with a normalized force vector of

$$\begin{pmatrix} -0.86 \\ +0.21 \\ +0.46 \end{pmatrix}$$

in relation to the loading coordinate system (Figure 1 and Figure 3).

Relative motions were measured in 3D with the optical measurement system GOM Pontos (GOM GmbH Braunschweig) with two 5 MP cameras with 50 mm lenses (Figure 3). Twenty tracking points (size 0.4 mm, ID 35231) were placed on the press-fit cup and 38 on the acetabular test model, whereof 33 could be tracked throughout the tests (Figure 3B). Thereby, a series of images was acquired and load information from the testing machine was used to identify the images at maximum and minimum loads, which were then used to assess the relative motions between cup and test model in terms of inducible displacement and migration (Figure 3).

First, a reference image was taken at zero load (t0) and at static pre-load of 300 N (t1) (Figure 3A). Specimens were then loaded dynamically in a sinusoidal wave form, whereby minimum load was 300 N throughout the tests and maximum load was increased stepwise from 600 to 3000 N. Load was increased by 300 N every 1000 cycles, resulting in nine load steps with 1000 cycles each, whereof the first 900 were applied at 1 Hz and the following 100 at 0.5 Hz. Few cycles of the first load step (600 N) and the last load step (3000 N) are exemplarily shown (Figure 3A). In each load step, at 990 cycles, motion during one cycle of dynamic load was captured by a series of 40 images taken by the optical measurement system at 15 Hz. Images were taken at a dynamic load frequency of 0.5 Hz instead of 1 Hz to reduce the potential error in capturing the minimum and maximum load from 29.5 N at 1 Hz to 7.4 N at 0.5 Hz (Figure S1). In each load step, the image at maximum load and minimum load was identified and used to assess relative motion in the software Aramis Professional 2017 (GOM GmbH Braunschweig): Inducible displacement (I600 and I3000 in Figure 3A) as the motion between minimum and maximum load in each load step and migration (M600 and M3000 in Figure 3A) as the motion between pre-load and minimum load in each load step. The same acquisition and measurement principle applies to the other load steps, not shown in Figure 3A. Resultant relative motions, as well as motions in medial-lateral (x), anterior-posterior (y), and cranial-caudal (z) direction were assessed (Figure 3B). The defined coordinate system originates in the center of the acetabular cup plane. The x-axis represents the normal to this plane, pointing laterally (personal communication with Philipp

Damm, Julius Wolff Institute Berlin). The y-axis points anteriorly and is based on the International Society of Biomechanics reference coordinate system.<sup>27</sup> The z-axis results thereof, pointing cranially (Figure 3C).

After dynamic loading and a waiting time of at least 10 min to allow for viscoelastic recovery, an image at zero load (t11) was taken again for each specimen to measure the resulting cup position.

Relative motions presented within this study correspond to the average motions of the 33 tracking points on the acetabular test model relative to the cup. Values of the three test groups with  $N = 6$  each are presented as median [25th percentile; 75th percentile].

### 2.4 | Cup tilt measurement

The angle between acetabular cup plane and fixation block surface was measured using Aramis Professional 2017 (GOM GmbH Braunschweig) prior to the test (t0) and after the test (t11) at zero load. The cup tilt represents the change in the measured angle between t0 and t11.

## 3 | RESULTS

### 3.1 | Cup translations

Relative motions were measured in terms of inducible displacement and migration, whereby the resultant displacement (Figure 4 and Figure 5), as well as its medial-lateral (x), anterior-posterior (y), and cranial-caudal (z) components were analyzed (Figure 6). Values are given as median [25th percentile; 75th percentile].

Resultant inducible displacement and migration increased with increasing load in all three test groups (Figure 4). Inducible displacement at the first load step (600 N) was lowest for bone chips with 15 [14; 16]  $\mu\text{m}$  and highest for b.a.glass + PEG with 19 [18; 19]  $\mu\text{m}$  (Figure 4A). At the last load step (3000 N), lowest inducible displacement was found for b.a.glass + PEG with 91 [89; 93]  $\mu\text{m}$  and highest for bone chips with 113 [110; 114]  $\mu\text{m}$ . Curves of all test groups showed a linear regression with inducible displacement being the dependent variable and the load level being the independent variable (bone chips:  $R^2 = 0.998$ , b.a.glass + PEG:  $R^2 = 0.982$ ; tetrapods + coll:  $R^2 = 0.998$ ).

Migration at the first load step was lowest for bone chips with 19 [19; 21]  $\mu\text{m}$  and highest for b.a.glass + PEG with 48 [37; 50]  $\mu\text{m}$  (Figure 4B). At the last load step (3000 N), lowest migration was found for tetrapods + coll with 491 [487; 497]  $\mu\text{m}$  and highest for b.a.glass + PEG with 868 [845; 936]  $\mu\text{m}$ . Curves of tetrapods + coll showed a linear regression ( $R^2 = 0.996$ ), bone chips trend to a power function ( $R^2 = 0.983$ ), and b.a.glass + PEG trend to a logarithmic function ( $R^2 = 0.981$ ) with migration being the dependent variable and the load level being the independent variable (Figure 4B).

Inducible displacement vectors of the acetabular test model relative to the cup, exemplarily shown for one specimen of each test

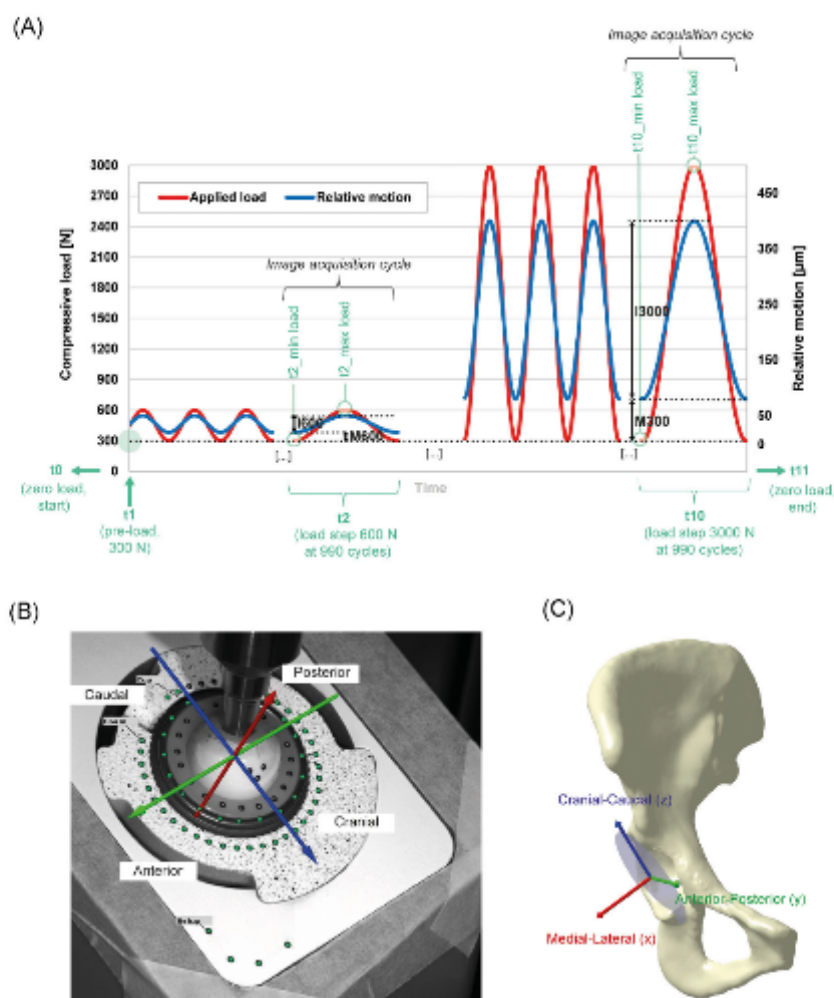
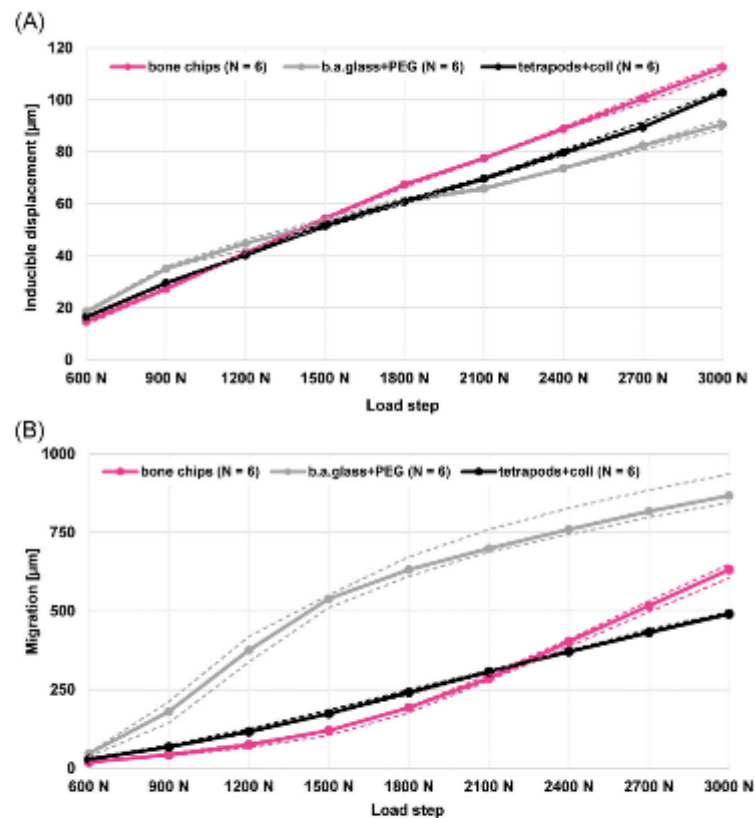


**FIGURE 3** Relative motion measurement. A, Scheme of applied compressive load (red), expected relative motion (blue) and measurement time points (green). Load is applied in a sinusoidal wave form, whereby minimum load is 300 N throughout the test and maximum load is increased from 600 N to 3000 N by 300 N/1000 cycles, resulting in nine load steps. Few cycles of the first load step (600 N) and last load step (3000 N) are shown exemplarily. In each load step, the first 900 cycles are applied with 1 Hz and the last 100 cycles with 0.5 Hz to reduce potential error in capturing the moment of minimum and maximum of the sinusoidal load curve (Figure S1 for more information). At 990 cycles in each dynamic load step (i.e. during dynamic load at 0.5 Hz), a series of 40 images with 15 Hz is taken with the optical measurement system (here shown for time point t2 and t10). Using the load information of the testing machine, the images at minimum load (here t2\_min load and t10\_min load) and maximum load (here t2\_max load and t10\_max load) are determined. Inducible displacements (here 1600 and 13000) are measured between t2\_min load and t2\_max load/between t10\_min load and t10\_max load; migration (here M600 and M3000) between pre-load (t1) and t2\_min load/t10\_min load. The same acquisition/measurement principle applies to the other load steps (900 to 2700 N), which are not displayed here. B, Field of view for relative motion measurement, including tracking points on foam and cup, as well as the defined loading coordinate system. C, Loading and measurement coordinate system ([www.orthoload.com/orthoload-club/](http://www.orthoload.com/orthoload-club/)) shown on right hemipelvis [Color figure can be viewed at [wileyonlinelibrary.com](http://wileyonlinelibrary.com)]

group [Figure 5, left] indicated a closing motion of the test model around the cup with main motion in the medial-lateral axis (Figure 6A). Migration vectors (Figure 5, right) indicated the movement of the cup into the acetabular cavity along the medial-lateral axis, which was predominant in the posterior and caudal aspect of the

model and an additional movement of the cup out of the acetabulum in the cranial-anterior aspect, which was mainly present in b.a.glass + PEG and bone chips (Figure 5, right). In all specimens, main motion was seen along the medial-lateral axis and lowest motion along the anterior-posterior axis (Figure 6A-C).

**FIGURE 4** Relative motion (average values of all 33 visible tracking points) between cup and acetabular test model for all three test groups over all applied load steps. A, Inducible displacement, measured between minimum and maximum load in each load step. B, Migration, measured between the pre-load and minimum load in each load step. Median values of  $N = 6$  are shown as solid lines, 25th and 75th percentiles as dashed lines [Color figure can be viewed at [wileyonlinelibrary.com](http://wileyonlinelibrary.com)]



### 3.2 | Cup tilt

Cup tilt was lowest for *tetrapods+coll* with  $0.97^\circ$  [ $0.75^\circ$ ;  $1.00^\circ$ ] and highest for *b.a.glass+PEG* with  $2.51^\circ$  [ $2.34^\circ$ ;  $2.63^\circ$ ]. Cup tilt for *bone chips* was  $1.40^\circ$  [ $1.23^\circ$ ;  $1.53^\circ$ ] (Figure 7).

## 4 | DISCUSSION

The objectives of this study were to assess the primary stability of a press fit cup in a standardized acetabular defect test model, which was filled with compacted *bone chips*, and to compare it to the primary stability achieved by a filling with two different bone graft substitutes: *B.a.glass+PEG* and *tetrapods+coll*.

This study has some limitations. First, a simplified acetabular test model made of PU foam was used instead of human donor specimens, which represent the most realistic test models. However, the latter are limited in supply and associated with high inter-specimen variability and limited test time. PU foam models were used to increase reproducibility and comparability between the test groups and were designed to mimic the main support structures of the pelvis. Second, primary stability was assessed in one specific type of defect. The defect was chosen based on a previously conducted quantitative

defect analysis<sup>2,28</sup> and in consultation with four senior hip revision surgeons from four European clinical centers as a common and representative defect which is likely to be treated with *bone chips* or BGS. However, there is a wide variation of bone defects and results of the present primary stability tests might be different in a different kind of defect. Third, the three test groups could not be prepared in the exact same way, that is, test group *bone chips* could not be conditioned in water due to hygienic reasons and number of rinsing procedures of *tetrapods+coll* were less than for *b.a.glass+PEG* as the collagen matrix was not expected to dissolve significantly in deionized water<sup>29</sup> with 5.5 to 7.0pH, but by acidic or alkaline processing<sup>30,31</sup> or enzymes.<sup>32</sup> It is not expected that the described difference in soaking and rinsing has a significant influence on the test results, but that the interface characteristics at the cup-foam and cup-defect filling contact areas, that is, the (remaining) humidity is more relevant for the primary stability. Humidity was controlled by a drying period of 24 hours prior to testing for both soaked test groups (*tetrapods+coll*, *b.a.glass+PEG*) and by testing the test group *bone chips*, which was not soaked, directly after implantation. Due to the fact that cancellous *bone chips* from fresh-frozen femoral heads were used, humidity at cup-*bone chips* interface could be expected to be comparable to the other test groups. Fourth, relative motions were measured at the end of each load step and hence information

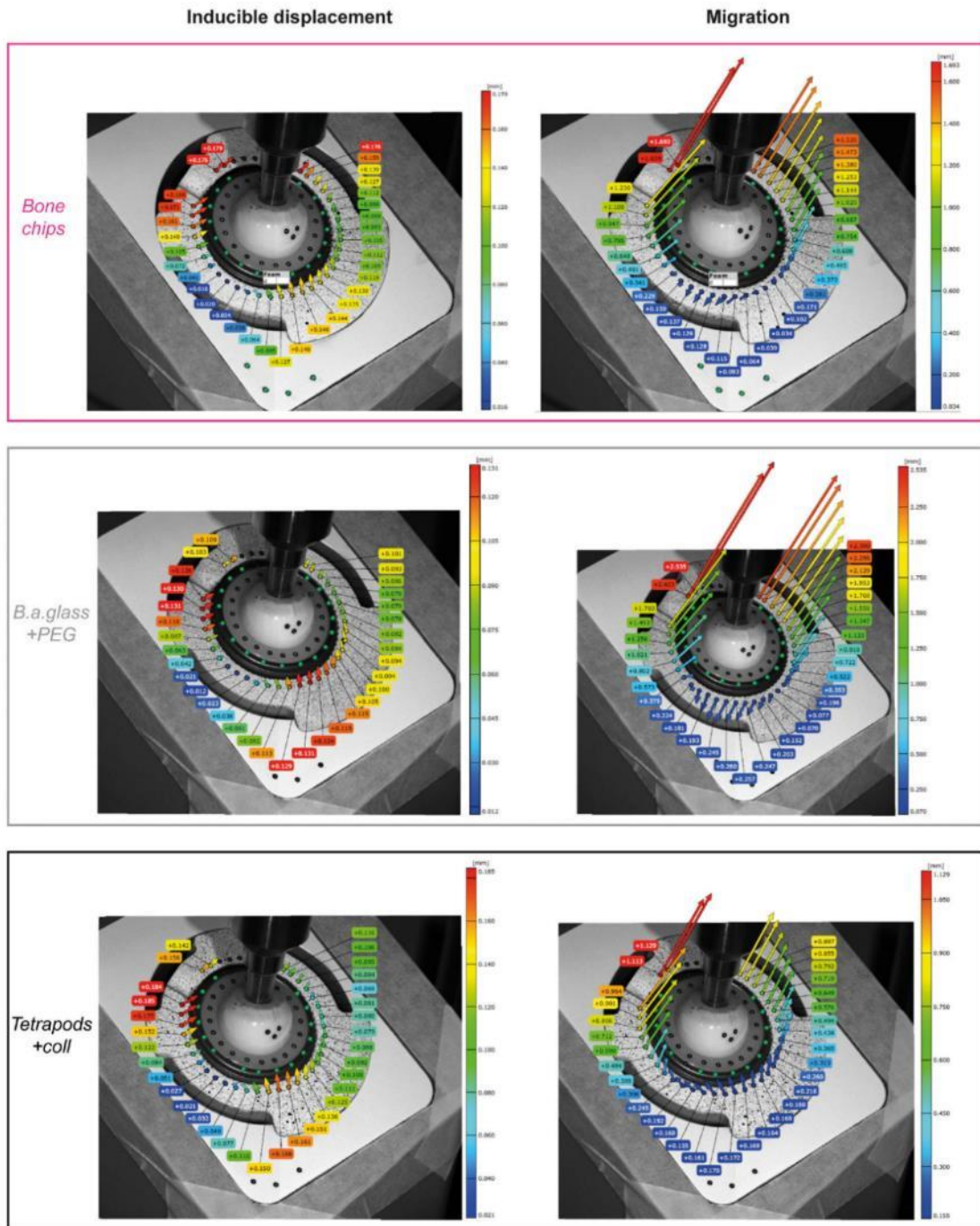


**FIGURE 5** Vectors of relative motion between cup and acetabular test model, that is, inducible displacement (left) and migration (right), shown in an exemplary way for one specimen of each test group at the last load step (3000 N). Relative motion of test model relative to the cup is shown based on the 33 tracking points, arrow direction indicates direction of motion, arrow color and length indicate magnitude of motion at the corresponding tracking point [Color figure can be viewed at [wileyonlinelibrary.com](http://wileyonlinelibrary.com)]

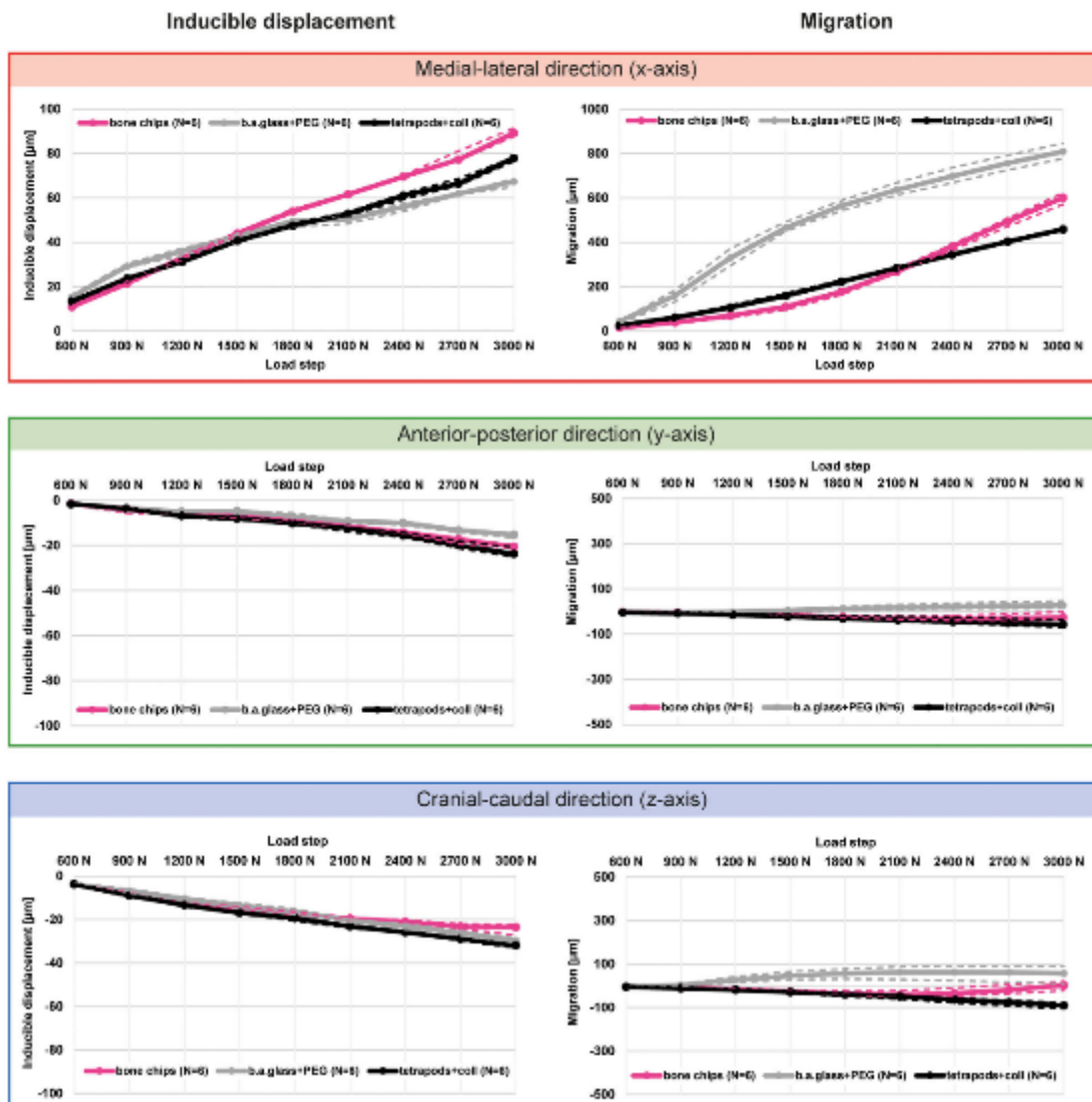


**FIGURE 6** Relative motion components along x-, y-, and z-axis (in medial-lateral, anterior-posterior and cranial-caudal direction) of inducible displacement (left) and migration (right) for all three test groups. Median values of N = 6 are shown as solid lines, 25th and 75th percentiles as dashed lines [Color figure can be viewed at [wileyonlinelibrary.com](http://wileyonlinelibrary.com)]

on their temporal progress cannot be provided. However, this does not jeopardize comparability among the test groups. Fifth, dynamic uniaxial loading was applied, although simulation of a complete motion cycle may induce higher relative motions.<sup>33</sup> However, uniaxial loading was chosen in this study to allow optical relative motion tracking throughout the tests, which is in good accordance with previous primary stability studies<sup>26,34,35</sup> and does not jeopardize comparability among the test groups.

In the present study, relative motion between press fit cup and acetabular test model were successfully assessed in terms of

inducible displacement and migration using an optical measurement system. Motion increased with increasing load (Figure 4), which is in good accordance with previous primary stability studies under dynamic load.<sup>26,35</sup> At the first load step (600 N), inducible displacement and migration were lowest for *bone chips* and highest for *b.a.glass+PEG*. At the last load step (3000 N), inducible displacement was lowest for *b.a.glass+PEG* and highest for *bone chips*, whereas migration was lowest for *tetrapods+coll* and highest for *b.a.glass+PEG*. This is in contrast to a study by Morosato et al.<sup>36</sup> who performed a left-right comparison of *bone chips* and *tetrapods+coll* with a press fit cup

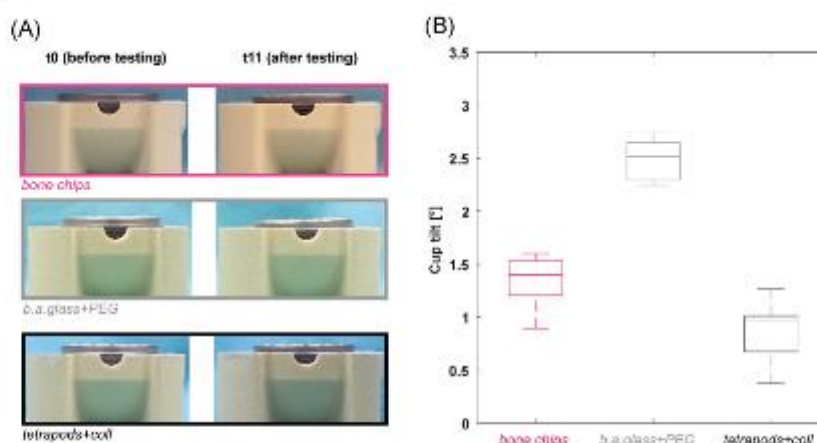


**FIGURE 7** Change of cup position due to dynamic loading. A, Cup positions before (t0) and after testing (t1), view from incisura acetabuli, exemplarily shown for one specimen of each test group. B, Cup tilt, that is, the difference between cup angle at t0 and t1 given as boxplots of  $N = 6$  in each test group [Color figure can be viewed at [wileyonlinelibrary.com](http://wileyonlinelibrary.com)]

in human donor specimens. Under uniaxial dynamic loading in the same direction as applied in the present study, they found that inducible displacements and migrations were slightly higher (but without statistically significant difference) for *tetrapods + coll* than for bone chips throughout all applied load packages from 0.5\*BW to 3.0\*BW, which corresponded to median values of approximately 387 and 2325 N based on the donors' weight. This difference could be related to the very thin remaining medial wall (periosteum) in those human pelvises in contrast to the medial wall thickness of 5.6 mm in the present study. First, it could be that the higher wall thickness allowed for denser compaction of *tetrapods + coll* which then provided more stability in the present study. Second, it could be that in the donor specimens, the relatively pointed and small *tetrapods* could push more against the periosteum, leading to a larger amount of motion, whereas the smoother bone chips might rather interlock to a meshwork that covers the periosteum and hence reduces relative motion. Bone chips size could be an additional contributing factor, as size, size distribution and preparation of bone chips can influence their behavior.<sup>4,8</sup> Another study which applied the same direction of load to assess primary stability of a press-fit cup in combination with cancellous bone chips was carried out by Jacofsky et al. They performed tests in human donor specimens with an artificial cavitary superior posterior defect, which was filled with either a calcium phosphate cement as BCS or cancellous allografts, and found that relative motion in the bone substitute specimens was lower than in the allograft specimens.<sup>13</sup> This is in good accordance with the findings in the present study, where *tetrapods + coll* showed lower relative motion than bone chips towards the higher applied loads (Figure 4). In numerous studies which assessed relative motion of bone chips and different BGS (TCP/hydroxyapatite [HA] and titanium granules) in combination with a cemented PE cup, it was also found that relative motions were lower for BGS granules or bone chips granules mixtures than for bone chips alone.<sup>10-12</sup>

In the present study, median values of inducible displacement at 3000 N were 113  $\mu\text{m}$  for *bone chips* and 103  $\mu\text{m}$  for *tetrapods + coll*, and therefore 25% and 57% lower than reported by Morosato et al.<sup>36</sup> Median values of migration at 3000 N were 632  $\mu\text{m}$  for *bone chips* and 491  $\mu\text{m}$  for *tetrapods + coll*, and therefore 25% and 65% lower than reported by Morosato et al., but in a range comparable to a study assessing migration of a PE cup cemented on bone chips and a combination of bone chips and titanium granules.<sup>10</sup>

In the present study, it was found that relative motion appeared mainly along the medial-lateral axis (Figure 6), which is probably related to mainly medially directed load and the mainly medial defect. However, the observed medial migration in combination with cup movement out of the acetabulum in the cranial anterior region, which is best visible in *b.a.glass + PEG*, can also be seen in clinical situations.<sup>37,38</sup>

The results obtained within this study suggest that the bone graft substitute made of  $\beta$ -TCP *tetrapods* in a collagen matrix shows a behavior under load comparable with bone chips. At loads larger than 2000 N, the behavior of *tetrapods + coll* was even more favorable, that is, relative motions were smaller than for bone chips. This might be related to the fact that in the present study the cups were pressed into the acetabulum with 2 kN and although the bone chips were compacted prior to cup press in, they may have been subjected to additional compaction within the dynamic testing at loads larger than 2 kN. However, mean inducible displacements of all three test groups were in a range in which osseointegration may potentially still be possible.<sup>39,40</sup> Migration of *b.a.glass + PEG* was considerably higher than for *tetrapods + coll* and bone chips, but still below the clinically defined radiographic thresholds critical for implant fixation<sup>41-43</sup> and most likely related to the dissolution of the matrix (PEG), not to the bioactive glass granules.

BGS, such as *tetrapods + coll* could represent an attractive alternative to bone chips, which are expensive and restricted in supply.

time consuming to produce, show an inconsistent quality due to biological variation and a remaining infection risk.<sup>5</sup> The present study, alongside with previous studies, showed the favorable properties of bone graft substitutes, in terms of higher in vitro measured primary stability in comparison with bone chips.<sup>20,11,12</sup> Satisfying clinical short- and mid-term results for BGS consisting of TCP and HA have also already been reported.<sup>44,45</sup>

Nevertheless, it cannot be generally applied that bone graft substitutes are always superior to bone chips, but that the performance depends on the defect characteristics. Considering the results of Morosato et al.,<sup>36</sup> it could be concluded that a prerequisite for a good performance for BGS is a contained defect with enough remaining wall thickness for adequate compaction.

Future studies should assess the effect of collagen matrix dissolution on primary stability using enzymes or acidic/alkaline processing. In addition, primary stability of defect treatments with BGS and bone chips should be assessed in additional/more severe defects to further investigate the prerequisites and potential limitations of the different filling materials. Furthermore, osseointegration should be investigated in mechano-biological or large animal studies.

#### ACKNOWLEDGMENTS

The authors would like to thank the senior hip revision surgeons Prof. Dr. med. Heiko Graichen, Prof. Dr. med. Dipl.-Ing. Volkmar Jansson, Prof. Dr. med. Maximilian Rudert, and Prof. Francesco Traina for their advice and input to the surgical technique and choice of cup size; Dr. Fredrik Ollila (Bonalive Biomaterials Ltd, Turku, Finland) and Chris Wattengel (Collagen Solutions Plc, Glasgow, UK) for providing the BGS test samples; Dr.-Ing. Philipp Damm and Prof. Dr.-Ing. Georg Bergmann (Julius Wolff Institute, Berlin, Germany) and the OrthoLoad club ([www.orthoload.com/orthoload-club/](http://www.orthoload.com/orthoload-club/)) for providing the load data and information about the coordinate system.

#### CONFLICT OF INTERESTS

RS, GH, MB, and TG are employees of Aesculap AG Tuttlingen, a manufacturer of orthopedic implants. FM and LC receive institutional support by Aesculap AG. Aesculap AG provided support in form of salaries for RS, GH, MB, and TG, but did not have any role in design of the study, data analysis, decision to publish or manuscript preparation.

#### AUTHOR CONTRIBUTIONS

All authors worked on research design, or acquisition, analysis or interpretation of data. RS worked on drafting the paper and GH, MB, FM, LC, and TG critically revised it. All authors have read and approved the final submitted manuscript.

#### ORCID

Ronja A. Schierjott  <http://orcid.org/0000-0002-0624-1978>

Luca Cristofolini  <http://orcid.org/0000-0002-7473-6868>

#### REFERENCES

1. Wright C, Paprosky WC Acetabular reconstruction: classification of bone defects and treatment options. Accessed 30 November 2019. <https://musculoskeletalkey.com/acetabular-reconstruction-classification-of-bone-defects-and-treatment-options/>
2. Schierjott RA, Hettich G, Graichen H, et al. Quantitative assessment of acetabular bone defects: a study of 50 computed tomography data sets. *PLoS One*. 2019;14(10):e0222511.
3. Slooff TJ, Buma P, Schreurs BW, Schimmel JW, Huiskes R, Gardeniers J. Acetabular and femoral reconstruction with impacted graft and cement. *Clin Orthop Relat Res*. 1996;323(323):108-115.
4. Jones SA. Impaction grafting made easy. *J Arthroplasty*. 2017;32(9S):S54-S58.
5. Pitto RP, Di Muria GV, Hohmann D. Impaction grafting and acetabular reinforcement in revision hip replacement. *Int Orthop*. 1998;22(3):161-164.
6. Green CM, Buckley SC, Harner AJ, Kerry RM, Harrison TP. Long-term results of acetabular reconstruction using irradiated allograft bone. *Bone Joint J*. 2018;100-B(11):1499-1454.
7. Halliday BR, English HW, Timperley AJ, Gie GA, Ling RSM. Femoral impaction grafting with cement in revision total hip replacement. Evolution of the technique and results. *J Bone Joint Surg*. 2003;85-B(6):809-817.
8. Toms AD, Barker RL, Spencer Jones R, Kuiper JJ I. Impaction bone-grafting in revision joint replacement surgery. Current concepts review. *J Bone Joint Surg*. 2004;86-A(9):2050-2060.
9. Hettich G, Schierjott RA, Eppe M, et al. Calcium phosphate bone graft substitutes with high mechanical load capacity and high degree of interconnecting porosity. *Materials*. 2019;12(21):1-16.
10. Walschot LHB, Aquarius R, Schreurs BW, Buma P, Verdonschot N. Better primary stability with porous titanium particles than with bone particles in cemented impaction grafting. An in vitro study in synthetic acetabula. *J Biomed Mater Res B Appl Biomater*. 2013;101(7):1243-1250.
11. Bolder SBT, Verdonschot N, Schreurs BW, Buma P. The initial stability of cemented acetabular cups can be augmented by mixing morsellized bone grafts with tricalciumphosphate/hydroxyapatite particles in bone impaction grafting. *J Arthroplasty*. 2003;18(8):1056-1063.
12. Bolder SBT, Verdonschot N, Schreurs BW, Buma P. Acetabular defect reconstruction with impacted morsellized bone grafts or TCP/HA particles. A study on the mechanical stability of cemented cups in an artificial acetabulum model. *Biomaterials*. 2002;23(3):659-666.
13. Jacofsky DJ, McCamley JD, Jaczynski AM, Shrader MW, Jacofsky MC. Improving initial acetabular component stability in revision total hip arthroplasty calcium phosphate cement vs reverse reamed cancellous allograft. *J Arthroplasty*. 2012;27(2):305-309.
14. Schierjott RA, Hettich G, Ringkamp A, Baxmann M, Morosato F, Grupp TM. A method to assess primary stability of acetabular components in association with bone defects. *J Orthop Res*. 2020;38(8):1769-1778.
15. Jamieson ML, Russell RD, Incevo SJ, Noble PC. Does an enhanced surface finish improve acetabular fixation in revision total hip arthroplasty? *J Arthroplasty*. 2011;26(4):644-648.
16. Huber WO, Noble PC. Effect of design on the initial stability of press-fit cups in the presence of acetabular rim defects: experimental evaluation of the effect of adding circumferential fins. *Int Orthop*. 2014;38(4):725-731.
17. Crosnier EA, Keogh PS, Miles AW. A novel method to assess primary stability of press-fit acetabular cups. *Proc Inst Mech Eng*. 2014;228(11):1126-1134.
18. Yu R, Hofstatter JG, Sullivan T, Costi K, Howie DW, Solomon LB. Validity and reliability of the Paprosky acetabular defect classification. *Clin Orthop Relat Res*. 2013;471(7):2259-2265.

19. Wassilew GI, Janz V, Perka C, Müller M. Treatment of acetabular defects with the trabecular metal revision system. *Orthopäde*. 2017; 46(2):148-157.
20. Beckmann NA, Jaeger S, Janoszka MB, Klotz MC, Bruckner T, Bitsch RG. Comparison of the primary stability of a porous coated acetabular revision cup with a standard cup. *J Arthroplasty*. 2018; 33(2):580-585.
21. Bolder SBT, Schreurs BW, Verdonschot N, van Unen JMJ, Gardeniers JWM, Sloff TJH. Particle size of bone graft and method of impaction affect initial stability of cemented cups. I human cadaveric and synthetic pelvic specimen studies. *Acta Orthop Scand*. 2003;74(6):652-657.
22. Geurts J, van Vugt T, Thijssen E, Arts JJ. Cost effectiveness study of one-stage treatment of chronic osteomyelitis with bioactive glass S53P4. *Materials*. 2019;12(19):1-11.
23. Bigoni M, Turati M, Zanchi N, et al. Clinical applications of Bioactive glass S53P4 in bone infections: a systematic review. *Eur Rev Med Pharmacol Sci*. 2019;23(2 suppl.):240-251.
24. Arts JJC, Verdonschot N, Buma P, Schreurs BW. Larger bone graft size and washing of bone grafts prior to impaction enhances the initial stability of cemented cups: experiments using a synthetic acetabular model. *Acta Orthop*. 2006;77(2):227-233.
25. Zietz C, Fritsche A, Klues D, Mittelmeier W, Bader R. Influence of acetabular cup design on the primary implant stability. An experimental and numerical analysis. *Orthopäde*. 2009;38(11):1097-1105.
26. Morosato F, Traina F, Cristofolini L. A reliable in vitro approach to assess the stability of acetabular implants using digital image correlation. *Strain*. 2019;55(4):1-12.
27. Wu G, Siegler S, Allard P, et al. ISB recommendation on definitions of joint coordinate system of various joints for the reporting of human joint motion - part I: ankle, hip, and spine. *J Biomech*. 2002;35(4):543-548.
28. Hettich G, Schierjott RA, Ramm H, et al. Method for quantitative assessment of acetabular bone defects. *J Orthop Res*. 2019;37(1): 181-189.
29. Wolf KL, Sobral PJA, Telis VRN. Characterizations of collagen fibers for biodegradable films production. IUFOST, 13th world congress of food sciences technology; September 17, 2006; Nantes (France). Accessed 28 December 2019. <https://iufost.edpsciences.org/>
30. Hey CD, Stainsby G. The enhanced solubility of collagen following alkaline treatment. *Biochim Biophys Acta*. 1965;97:364-366.
31. Bowes JH, Elliott RG, Moss JA. The composition of collagen and acid-soluble collagen of bovine skin. *Biochem J*. 1955;61(1):143-150.
32. Meyer M. Processing of collagen based biomaterials and the resulting materials properties. *Biomed Eng Online*. 2019;18(24):1-74.
33. Crosnier EA, Keogh PS, Miles AW. The effect of dynamic hip motion on the micromotion of press-fit acetabular cups in six degrees of freedom. *Med Eng Phys*. 2016;38(8):717-724.
34. Morosato F, Traina F, Cristofolini L. Effect of different motor tasks on hip cup primary stability and on the strains in the periacetabular bone: an in vitro study. *Clinical Biomech*. 2019;70:137-145.
35. Beckmann NA, Bitsch RG, Gondan M, Schonhoff M, Jaeger S. Comparison of the stability of three fixation techniques between porous metal acetabular components and augments. *Bone Joint Res*. 2018; 7(4):282-288.
36. Morosato F, Traina F, Schierjott RA, Hettich G, Grupp TM, Cristofolini L. Primary stability of revision acetabular reconstructions using an innovative bone graft substitute: a comparative biomechanical study on cadaveric pelvises [manuscript submitted for publication]. *Hip International*. 2020.
37. Goodman S, Saastamoinen H, Shaha N, Gross A. Complications of ilioischial reconstruction rings in revision total hip arthroplasty. *J Arthroplasty*. 2004;19(4):436-446.
38. Sporer SM, Bottros JJ, Hulst JB, Kancherla VK, Moric M, Paprosky WG. Acetabular distraction: an alternative for severe defects with chronic pelvic discontinuity? *Clin Orthop Relat Res*. 2012; 470(11):3156-3163.
39. Pilliar RM, Lee JM, Maniopoulos C. Observations on the effect of movement on bone ingrowth into porous-surfaced implants. *Clin Orthop Relat Res*. 1986;208(208):108-113.
40. Bragdon CR, Burke D, Lowenstein JD, et al. Differences in stiffness of the interface between a cementless porous implant and cancellous bone in vivo in dogs due to varying amounts of implant motion. *J Arthroplasty*. 1996;11(8):945-951.
41. Ng T-P, Chiu K-Y. Acetabular revision without cement. *J Arthroplasty*. 2003;18(4):435-441.
42. Pijls BG, Nieuwenhuijsen MJ, Fiocco M, et al. Early proximal migration of cups is associated with late revision in THA. A systematic review and meta-analysis of 26 RSA studies and 49 survival studies. *Acta Orthop*. 2012;83(6):583-591.
43. Delaunay CP, Kapandji AI. Survivorship of rough-surfaced threaded acetabular cups. 382 consecutive primary Zweymüller cups followed for 0.2-12 years. *Acta Orthop Scand*. 1998;69(4):379-383.
44. Whitehouse MR, Dacombe PJ, Webb JCJ, Blom AW. Impaction grafting of the acetabulum with ceramic bone graft substitute: high survivorship in 43 patients with a mean follow up period of 4 years. *Acta Orthop*. 2013;84(4):371-376.
45. Haenle M, Schütter S, Ellenrieder M, Mittelmeier W, Bader R. Treatment of acetabular defects during revision total hip arthroplasty: preliminary clinical and radiological outcome using bone substitute materials. *Hip Int*. 2013;23(1):44-53.

#### SUPPORTING INFORMATION

Additional supporting information may be found online in the Supporting Information section.

**How to cite this article:** Schierjott RA, Hettich G, Baxmann M, Morosato F, Cristofolini L, Grupp TM. Primary stability of a press-fit cup in combination with impaction grafting in an acetabular defect model. *J Orthop Res*. 2020;1-12. <https://doi.org/10.1002/jor.24810>

## 5 Additional content

### 5.1 Additional content I: Accuracy assessment of the optical measurement system

#### Introduction

Optical measurement systems such as GOM Pontos (GOM GmbH Braunschweig, Germany) can for example be used to measure relative motions between an implant and the surrounding setup / bone or to assess interfragmentary motions [87–90].

In the present dissertation, GOM Pontos was used in combination with optical tracking points to assess relative motion in 3D between a press-fit cup and a simplified acetabular test model made of polyurethane foam.

The theoretical measurement accuracy of GOM Pontos is given by the manufacturer as 20  $\mu\text{m}/\text{m}$  in-plane and 40  $\mu\text{m}/\text{m}$  out-of-plane, i.e. in depth of the cameras (personal communication with GOM GmbH). However, the actual measurement accuracy depends on numerous parameters such as the used charge-coupled device (CCD) sensor, tracking points, calibration, measurement volume, camera focus, light conditions, as well as potential sources of disturbance in the surrounding areas, such as heat sources between the sensor and the measurement object or vibrations caused by other testing machines.

Therefore, the objectives of the here presented additional content were to assess the accuracy of the optical measurement system in terms of (1) image noise, (2) displacement measurement error in X-, Y- and Z-direction, and (3) angle measurement error under laboratory conditions similar to those present during the tests for the second and third publication of this dissertation.

#### Materials and methods

Within this dissertation, the optical measurement system GOM Pontos 5M (GOM GmbH Braunschweig, Germany) with two 5 megapixel (MP) cameras, equipped with CCD sensors and 50 mm lenses, was used in combination with 0.4 mm diameter tracking points (ID 35231).

The system was calibrated with the calibration plate CP20 90 x 72 for a measurement volume of 130 x 110 x 90 mm.

Relative motions were analyzed in the software Aramis Professional 2017 (GOM GmbH Braunschweig, Germany).



Displacement error in X- and Y-direction was assessed using a XY-table which could be moved using outside micrometers with an accuracy of 4  $\mu\text{m}$ . To assess displacement error in Z-direction, a set of Johansen gauges was used (Figure 8).

First, the cameras were positioned such that they faced the frontal surface of the XY-table, i.e. the object to be measured, as recommend by GOM GmbH (Figure 8). The XY-table was prepared with matt tape to avoid any reflection-related inconsistencies and five 0.4 mm diameter tracking points (ID 35231) were placed on its frontal surface (Figure 7) for relative motion measurement.

A metal block was positioned next to the XY-table and was prepared with three tracking points to enable measurement of the table motion relative to a fixed reference (Figure 7). The coordinate system was fixed on the reference block. The X- and Y-axis were defined using the motion direction, i.e. trajectory of the XY-table, and the Z-axis resulted thereof (Figure 7).

To assess the measurement error in X-direction, a reference image was taken at the starting position ( $X = 0 \mu\text{m}$ ). The table was then moved in increments of 500  $\mu\text{m}$  from the starting position  $X = 0 \mu\text{m}$  to  $X = 2500 \mu\text{m}$  and  $X = -2500 \mu\text{m}$  (Figure 8). At each increment, one image was taken. The same principle was applied to assess the measurement error in Y-direction.

To assess the measurement error in Z-direction, one Johansen gauge was prepared with matt tape and five optical tracking points for displacement measurement. A reference image was taken at the starting position ( $Z = 0 \mu\text{m}$ ) (Figure 8). Additional Johansen gauges in thickness increments of 500  $\mu\text{m}$  (minimum: 500  $\mu\text{m}$ , maximum: 5000  $\mu\text{m}$ ) were then placed below the Johansen gauge prepared with tracking points, leading to a displacement in Z-direction from 500  $\mu\text{m}$  to a maximum of 5000  $\mu\text{m}$ . An image was taken at each increment of 500  $\mu\text{m}$ .

Using the Software Aramis Professional, the displacements measured by the optical measurement systems were assessed and compared to the actually applied displacements. Rigid body motion compensation via the metal reference block was applied, resulting in motion measurement of the XY-table / the Johansen gauge relative to the reference block and thereby compensating for potential vibrations / motions induced by the test environment.

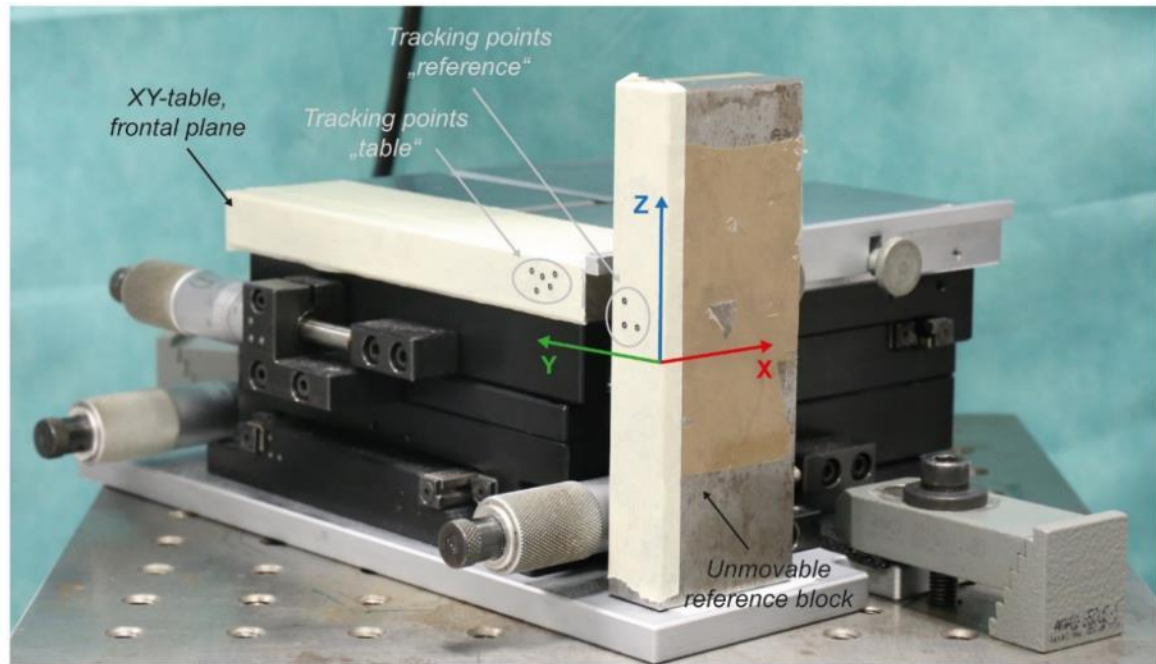


**Figure 7.** Setup to assess displacement measurement error with XY-table, tracking points and reference block for rigid body motion compensation.

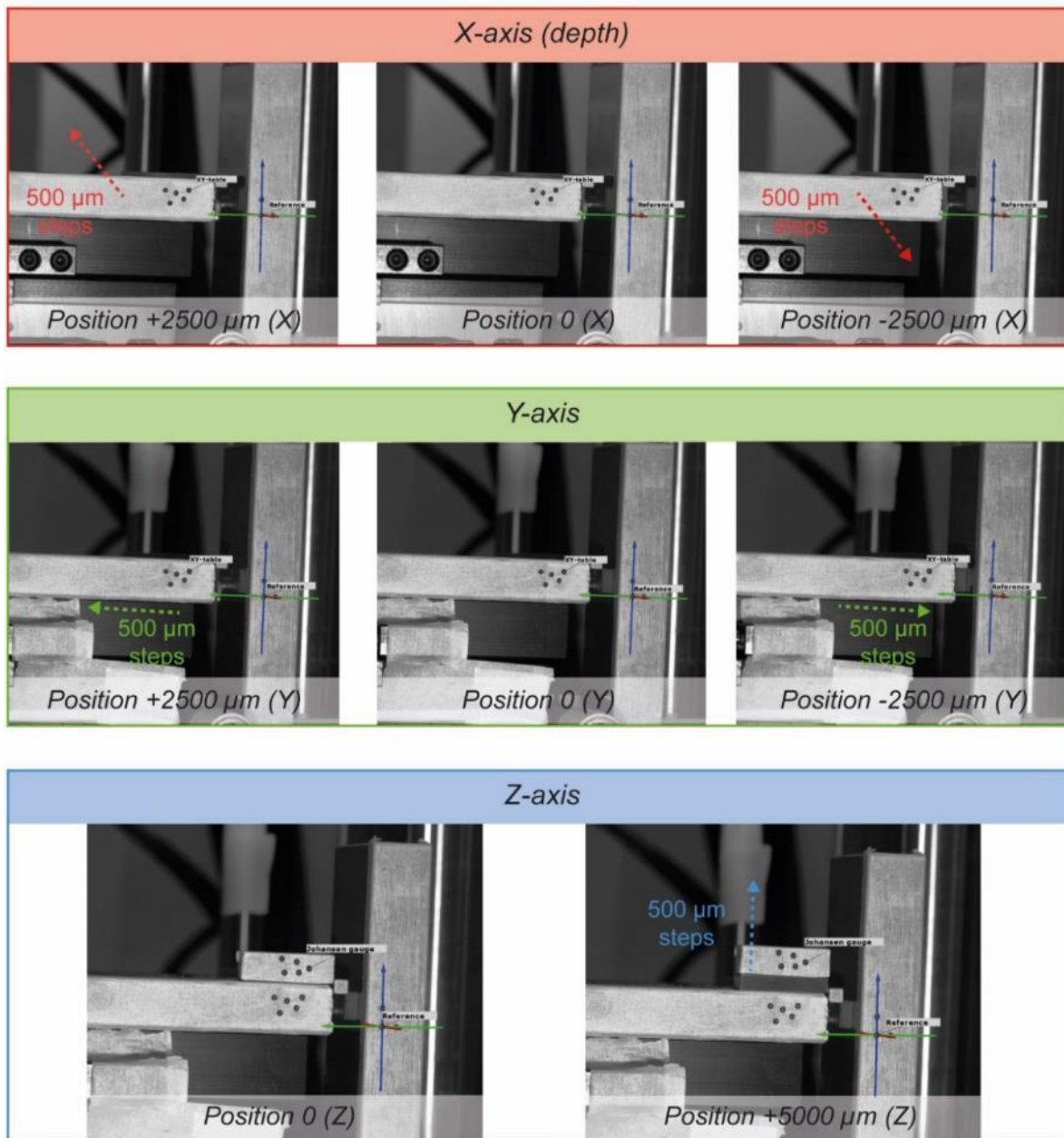


**Figure 8.** Field of view and measurement principle for displacement measurement error in X, Y, and Z with starting positions and maximum displacement positions.

### (3) Angle measurement error

In this context, angle measurement error is defined as the difference between the actually applied angular displacement and the angular displacement determined by the optical measurement system. It was assessed using a precision sinus vice and a set of Johansen gauges (Figure 9).

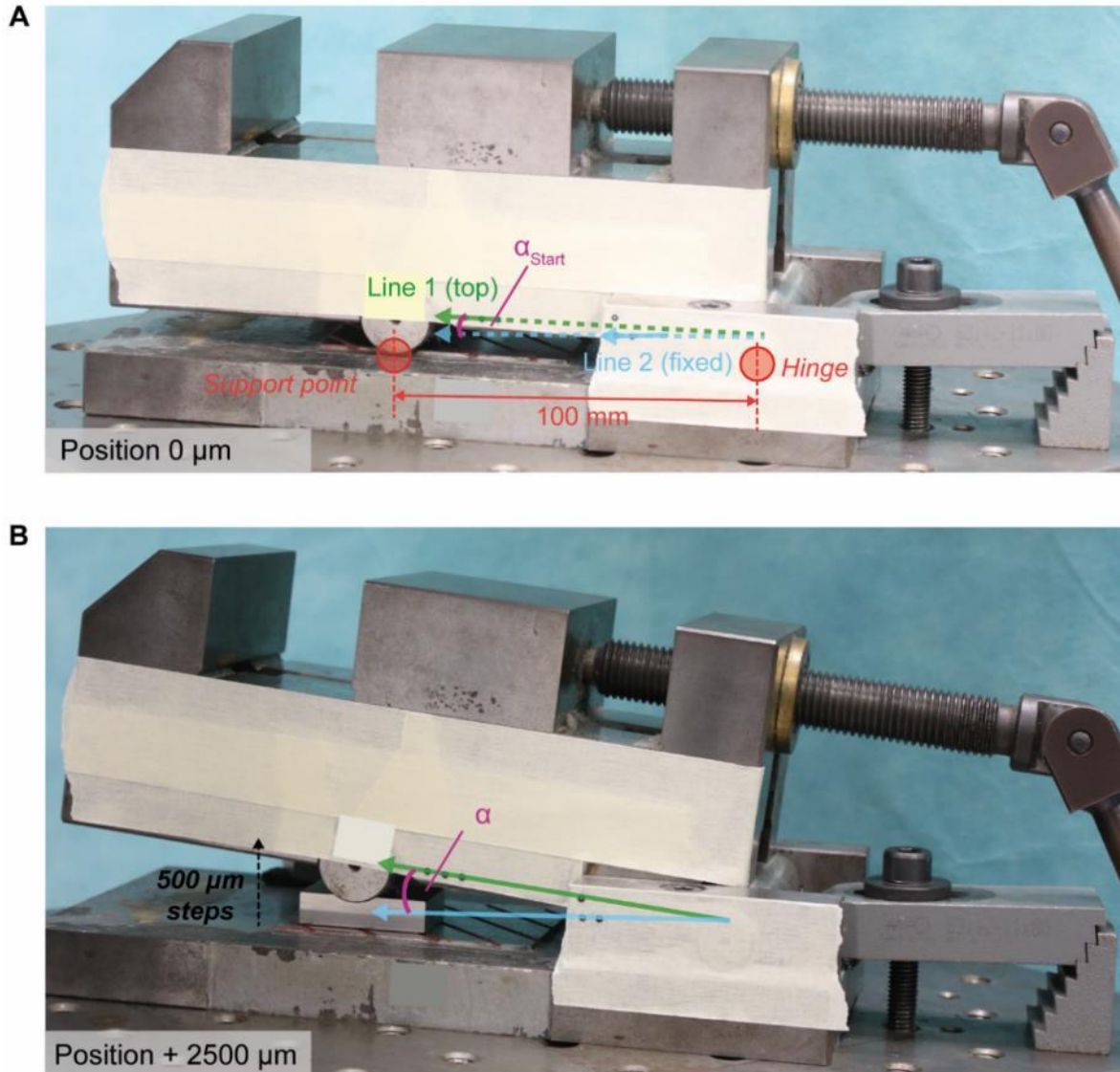
First, the sinus vice was prepared with matt tape. Three tracking points were placed manually on the movable (top) part of the vice and two points on the fixed (lower) part of the vice to form a horizontal line (line 1 and line 2) each (Figure 9).

The two lines were later used to assess the angle measurement error. Due to the uncertainty of the manual positioning of the tracking points, i.e. the difficulty to place the points such they would form an exactly horizontal line, the initial angle between line 1 and 2 was measured as  $\alpha_{start}$ . The angle  $\alpha_{start}$  was considered in the performed angle error measurements, i.e. the measured values were corrected by  $\alpha_{start}$ .

The optical measurement system was oriented such that the cameras faced the sinus vice's frontal surface. Using the software Aramis Professional, first, a reference image at zero angular displacement was taken (Figure 9A). A line was fitted through the tracking points on the top (green, line 1) and through the tracking points at the bottom (blue, line 2) and the initial angle between the lines ( $\alpha_{start}$ ) was assessed to be 2.2°.

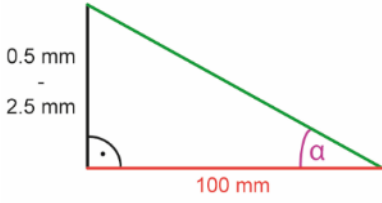
Then, Johansen gauges with thickness increments of 500  $\mu\text{m}$  (minimum: 500  $\mu\text{m}$ , maximum: 2500  $\mu\text{m}$ ) were placed under the sinus vice's support point (Figure 9B). Using the given distance between hinge and support point (100 mm) and the thickness of the Johansen gauges, the theoretical angle between line 1 and line 2 ( $\alpha_{target}$ ) could be calculated with trigonometric functions, i.e. the tangent function (Table 1).

The actual angle between line 1 and line 2 was assessed and the measured value was corrected by the initial angle  $\alpha_{start}$  of 2.2°. Any difference between the thereof resulting angle  $\alpha_{res}$  and the theoretical angle  $\alpha_{target}$  was considered to be an angle measurement error.



**Figure 9.** Setup to assess angle measurement error. (A) Starting position with definition of components / lines for angle measurement. (B) Maximum angular displacement using a Johansen gauge with 2500  $\mu\text{m}$  thickness.

**Table 1.** Calculation of theoretical angles based on thickness of Johansen gauges and the tangent function.

Tangent function	Thickness Johansen gauges = Opposite side length	Theoretical angle $\alpha_{Target}$
$\tan(\alpha) = \frac{\text{Opposite side length}}{100 \text{ mm}}$ 	0.5 mm	0.29°
	1.0 mm	0.57°
	1.5 mm	0.86°
	2.0 mm	1.15°
	2.5 mm	1.43°

## Results

### (1) Image noise

Mean image noise as the relative displacement of cup and acetabular test model at zero load was found to be  $4 \pm 3 \mu\text{m}$ .

### (2) Displacement measurement error in X-, Y- and Z-direction

Mean displacement measurement error was  $-6 \pm 29 \mu\text{m}$  (X-direction),  $-1 \pm 3 \mu\text{m}$  (Y-direction) and  $5 \pm 5 \mu\text{m}$  (Z-direction).

### (3) Angle measurement error

Mean angle measurement error was  $0.06 \pm 0.00^\circ$ .

## Discussion

In the third publication of this dissertation, it was distinguished between relative motion in X-, Y-, and Z-direction.

In relation to the inducible displacement values in X-direction measured within this publication at the first (last) load step, the mean displacement error in X-direction of  $-6 \mu\text{m}$  corresponds to  $77\% \pm 99\%$  ( $16\% \pm 40\%$ ). In relation to the migration values in X-direction measured within this publication at the first (last) load step, the mean displacement error in X-direction of  $-6 \mu\text{m}$  corresponds to  $66\% \pm 107\%$  ( $7\% \pm 39\%$ ).

In relation to the inducible displacement values in Y-direction measured within this publication at the first (last) load step, the mean displacement error in Y-direction of  $-1 \mu\text{m}$  corresponds to  $36\% \pm 30\%$  ( $11\% \pm 18\%$ ). In relation to the migration values in Y-direction

measured within this publication at the first (last) load step, the mean displacement error in Y-direction of  $-1\ \mu\text{m}$  corresponds to  $29\% \pm 29\%$  ( $6\% \pm 14\%$ ).

In relation to the inducible displacement values in Z-direction measured within this publication at the first (last) load step, the mean displacement error in Z-direction of  $5\ \mu\text{m}$  corresponds to  $162\% \pm 148\%$  ( $33\% \pm 69\%$ ). In relation to the migration values in Z-direction measured within this publication at the first (last) load step, the mean displacement error in Z-direction of  $5\ \mu\text{m}$  corresponds to  $147\% \pm 136\%$  ( $22\% \pm 55\%$ ).

In relation to the cup tilt measured in the third publication, the mean angle measurement error of  $0.06^\circ$  corresponds to  $5\% \pm 3\%$ .

Accuracy of the Pontos 5M system (GOM GmbH Braunschweig, Germany) has already been assessed by Doebele et al. who used a tactile measurement system with three digital indicators (span of error  $5\ \mu\text{m}$ , repeatability  $2\ \mu\text{m}$ ) as reference to measure displacements in one plane (left-right, up-down). They found that accuracy of the Pontos 5M system was approximately  $5\ \mu\text{m}$  [87].

In a study by Grupp et al., 2017 who used the GOM Pontos 5M to assess relative motion of a tibial plateau in a cadaver model, accuracy was reported with values of  $5\ \mu\text{m}$  in X and Z (corresponding to Y and Z in the present study, in-plane) and  $10\ \mu\text{m}$  in Y (corresponding to X in the present study, out-of-plane, i.e. in depth of the cameras) [91].

Morosato et al. used a 3D-digital image correlation (DIC) system (Q400, Dantec Dynamics, Denmark) to assess relative motion between a press-fit cup and Sawbone<sup>®</sup> (Malmö, Sweden) hemipelvis [92]. They analyzed the system's measurement accuracy using a dummy specimen, which was subjected to predefined translations and rotations. It was found that the measurement errors were smaller or equal to the errors of the system used to position the specimen ( $2\ \mu\text{m}$  for translations and  $0.1^\circ$  for rotations).

The mean displacement measurement errors of the optical measurement configuration used within this dissertation are hence comparable to the values reported by Grupp et al. and Doebele et al., but partially higher than with the measurement configuration used by Morosato et al. However, angle measurement errors were even lower than the rotation errors in the study by Morosato et al. Furthermore, mean displacement errors in the present study were with  $-6\ \mu\text{m}$  (X),  $-1\ \mu\text{m}$  (Y) and  $5\ \mu\text{m}$  (Z) smaller than or close to the positioning accuracy of  $4\ \mu\text{m}$  provided by the reference object, i.e. the outside micrometers to position the XY-table.

The displacement errors measured within this study also depend on the measurement setup, i.e. the distribution of tracking points within the measurement volume. It is likely that with a more even distribution and larger number of tracking points within the measurement volume / field of view, the measured displacement errors would be reduced.

The fact that the evaluated displacement errors partially correspond to more than 100% of the actually measured relative motion values in Z-direction (1-15  $\mu\text{m}$ ), indicates that at low applied loads, the used optical measurement system is at its resolution limit. In the future, in case of very small expected relative motions, cameras with higher resolution (e.g. 10 MP) and more advanced CCD sensors with improved signal-noise ratio should be used.

## **5.2 Additional content II: Simplification of the representative defect and development of a scaling procedure for the implementation in human donor specimens**

### **Introduction and aims**

As previously described, based on the quantitative analysis of acetabular bone defects, one representative defect was chosen for the pre-clinical testing model.

To implement the defect in a standardized way and to enable defect implementation in human donor specimens using standard acetabular reamers, the defect geometry should be simplified, while still preserving the main characteristics of the defect.

As the size and shape of human donor specimens vary, the defect implementation procedure should also be scalable, i.e. adjustable to individual specimens. Furthermore, some requirements for the defect implementation in the donor specimens already had to be considered during the defect simplification, such as the limited possibilities to adjust the specimen position during defect implementation.

The objectives of the here presented additional content were hence to (1) describe the defect simplification procedure including the underlying requirements and to (2) present the developed scaling procedure including the resulting scaling matrix.

Focus was set on defect increment 1, as this was to be implemented in donor specimens by Morosato et al. in order to compare bone chips and BGS in a left-right comparison [93].

### **Materials and methods**

In cooperation with Morosato et al., who used the herein presented scaling procedure on human donor specimens later on, the requirements for defect implementation in human donor specimens were summarized, such that they could already be considered during the defect simplification procedure:

- Implementation should be made possible using only a XY-table and a vertical drilling machine
- Use of standard hemispherical acetabular reamers
- Minimum number of position adjustments during defect implementation in donor specimens to increase reproducibility and to decrease complexity of the procedure (in this specific case: Tilt of the specimens only along one axis, i.e. the axis connecting the landmarks anterior superior iliac spine (ASIS), and pubic tubercle (PT))

Under consideration of these requirements, the representative defect was simplified. All described procedures were performed based on the 3D-model of bone volume loss, which was obtained with a previously described approach using a SSM (first publication) (Figure 10).

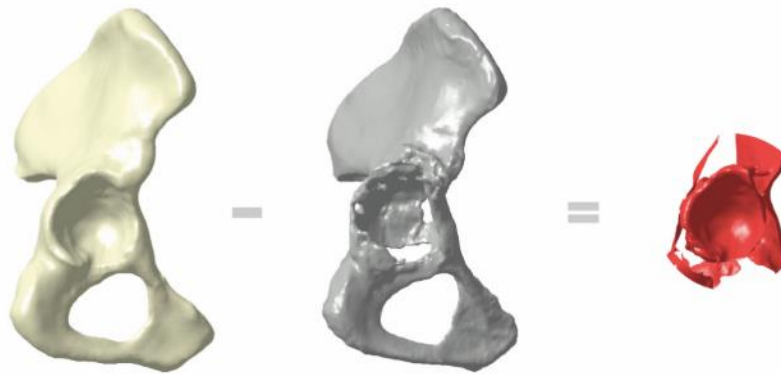


**Figure 10.** Bone volume loss in the representative defect (red) derived by subtraction of 3D-model of defect pelvis (gray) from 3D-model of native pelvis (beige).

First, the shell-like reconstruction inaccuracies and screw holes were removed from the 3D-model of bone volume loss. The distribution of bone volume loss among the four defined defect sectors Cranial roof, Anterior column, Posterior column and Medial wall was assessed (Figure 11).

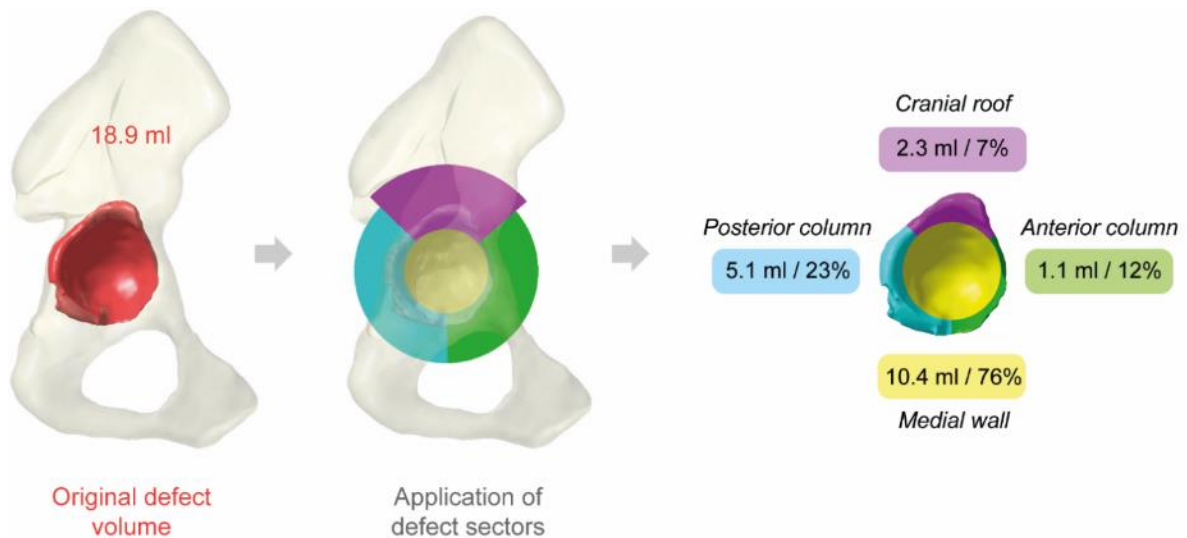


**Figure 11.** Analysis of original bone defect volume after removal of reconstruction inaccuracies and screw holes (red). Total bone volume loss was 18.9 ml, which could be further distinguished in bone volume loss in the defined defect sectors Cranial roof (purple), Anterior column (green), Posterior column (blue) and Medial wall (yellow). Values in % correspond to the bone volume loss in relation to the initial / native bone volume in each defined sector.

In an iterative approach, nine virtual reaming procedures were defined to simplify the defect shape and volume. In order to do so, three CS were defined, which could be used in the virtual 3D-models and in the donor specimens:

- Standard acetabular plane (SAP) coordinate system (SAP-CS)
- Anterior reaming coordinate system (Anterior-CS)
- Posterior reaming coordinate system (Posterior-CS)

The SAP-CS was defined based on the standard acetabular plane with 45° inclination and 20° anteversion [94], which was oriented horizontally.

The CoR of the hemipelvis represented the origin of the CS, the Z-axis was defined by the normal to the SAP pointing medially (left hemipelvis) / laterally (right hemipelvis). The Y-axis was defined as the connection between ASIS and PT pointing cranially and projected on the SAP, and the X-axis resulted thereof. Anterior-CS and Posterior-CS resulted by rotating the SAP-CS around the line connecting ASIS and PT 10° anteriorly and 35° posteriorly, respectively (Figure 12).

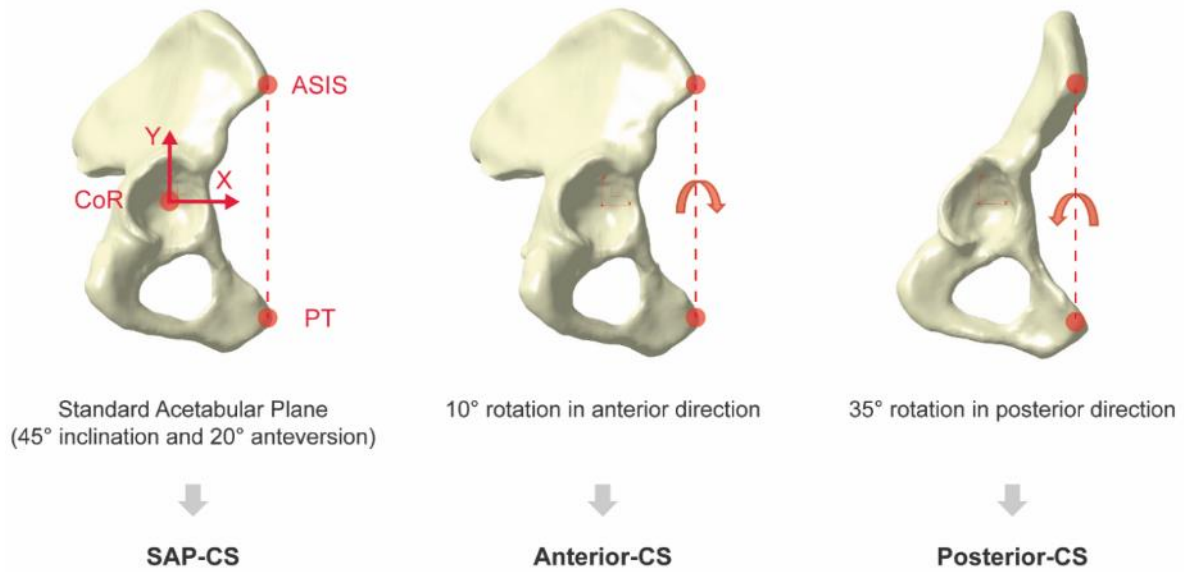


**Figure 12.** Coordinate systems for defect simplification and implementation. SAP-CS based on the standard acetabular plane and the line connecting ASIS and PT, as well as Anterior-CS and Posterior-CS which resulted from tilting the SAP-CS / the specimens around the line connecting ASIS and PT.

The iterative definition of reaming procedures included the variation of reamer sizes, reamer positions in XY (horizontal) plane, reaming depth, as well as the described rotations for Anterior-CS and Posterior-CS. The resulting simplified defect could be implemented with nine reaming procedures (Figure 13) and was comparable to the original defect concerning shape, overall volume loss and distribution of volume loss among the defined sectors (Figure 14).

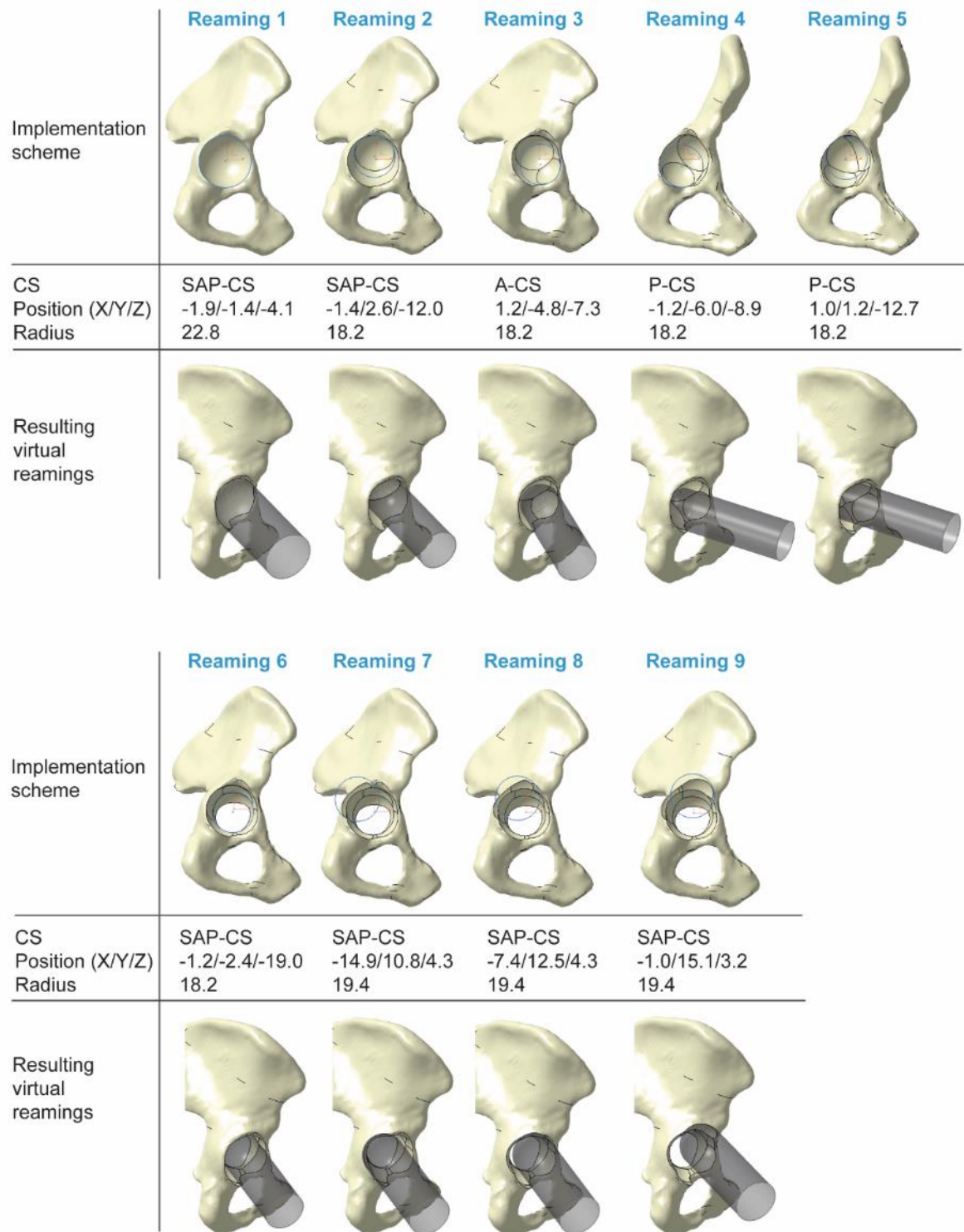


**Figure 13.** Nine reaming procedures for simplified defect implementation with hemispherical reamers. Shown are the implementation schemes with the corresponding coordinate systems (CS), reamer positions and sizes (radius), as well as the resulting virtual reaming procedures (gray). Positions and reamer radii are given in mm. Adapted from Schierjott et al. [86].

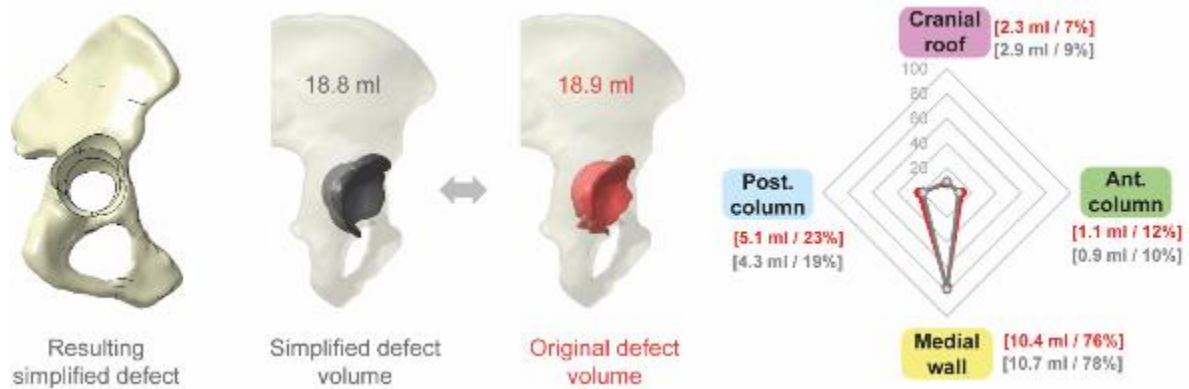


**Figure 14.** Resulting simplified defect and comparison of its corresponding volume (gray) with original defect volume (red) shows high volume conformity and comparable shape, as well as comparable distribution of relative bone loss (% of native bone volume in each sector) among the four defined defect sectors Cranial roof, Anterior column, Posterior column and Medial wall (spider plot). Adapted from Schierjott et al. [86].

From this simplified defect (increment 4), three additional, less severe defect increments were derived by exclusion of specific reaming procedures (see Figure 5).

Bone defect increment 1 was used in the *in vitro* tests performed within the present dissertation, as well as within the human donor specimen tests performed by Morosato et al. Hence, the following scaling procedure was focused on bone defect increment 1, which represented a mainly medial contained defect with rim damage in the inferior-posterior area, which reduced cup-contact area by 1/3 of the circumference (Figure 15).

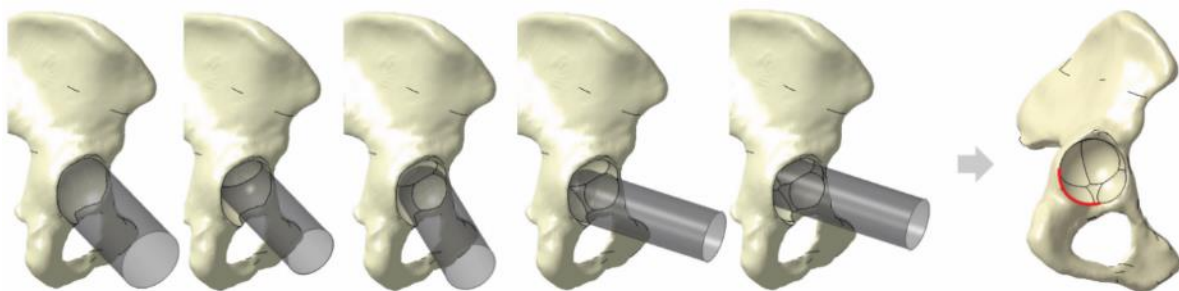


**Figure 15.** Implementation using five reaming procedures and resulting bone defect increment 1 with rim damage of approximately one-third of the circumference (marked in red). Adapted from Schierjott et al. [86].

The basic idea was to define measurements to be taken on the individual donor specimen which could be inserted into a scaling matrix, which would then provide the specific reamer sizes and positions, as well as reaming depths suitable for each individual hemipelvis.

In order to implement this, first, measurements were defined which could be useful for defect scaling and which could be taken on the virtual 3D-models of the hemipelvises, as well as on the actual donor specimens (Figure 16): Native acetabular radius (NR), anterior column

width (AW), posterior column width (PW) and medial wall thickness (MT) with all measurements taken with the SAP aligned horizontally (SAP-CS). In addition, the planned reaming radius for the primary acetabular cup was defined as scaling parameter (RR).

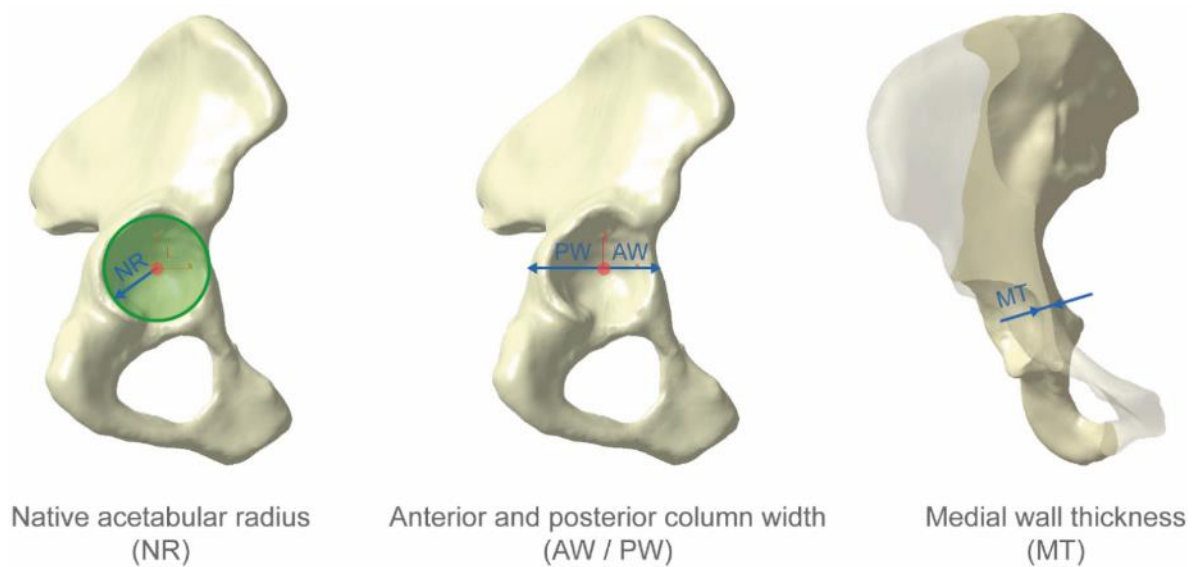


**Figure 16.** Measurements for defect scaling, exemplarily shown on virtual 3D-model of native pelvis.

To define suitable scaling relations and factors, these were first developed on the simplified representative defect and then applied to two additional 3D-models of native hemipelvises. The scaling procedure was adapted in an iterative approach using the information obtained from the two additional models until it was possible to successfully implement the defect in all three specimens.

**Results**

The resulting scaling factors and corresponding parameters for each reaming procedure are presented in Table 2.

Applying this method to the two exemplary native 3D-models, the defect could be reproduced quite well concerning shape and remaining cup contact area (Figure 17).

An excel-template was developed in which the measurements of an individual hemipelvis could be inserted and the information necessary for defect implementation (specific for each individual case) could be extracted (Figure 18).

**Table 2.** Overview of developed scaling procedure. For each reaming step (Reamer 1 to Reamer 5\_POST), the position in X, Y, and Z (reaming depth), as well as the reamer size is scaled using the corresponding scaling factor and parameter.

Reamer 1			Reamer 2		
SAP-coordinate system			SAP-coordinate system		
	Scaling factor	Parameter		Scaling factor	Parameter
X-position	-0.08	RR	X-position	-0.06	RR
Y-position	-0.06	RR	Y-Position	0.11	RR
Z-position	(-)1.3	MT	Z-Position	(-)3.8	MT
Reamer size	0.95	RR	Reamer size	0.76	RR
Reamer 3_ANT			Reamer 4_POST		
Anterior coordinate system			Posterior coordinate system		
	Scaling factor	Parameter		Scaling factor	Parameter
X-Position	0.05	AW	X-Position	-0.04	PW
Y-Position	-0.22	NR	Y-Position	-0.28	NR
Z-Position	(-)0.31	AW	Z-Position	(-)0.28	PW
Reamer size	0.76	RR	Reamer size	0.76	RR
Reamer 5_POST					
Posterior coordinate system					
	Scaling factor	Parameter			
X-Position	0.03	PW			
Y-Position	0.06	NR			
Z-Position	(-)0.41	PW			
Reamer size	0.76	RR			

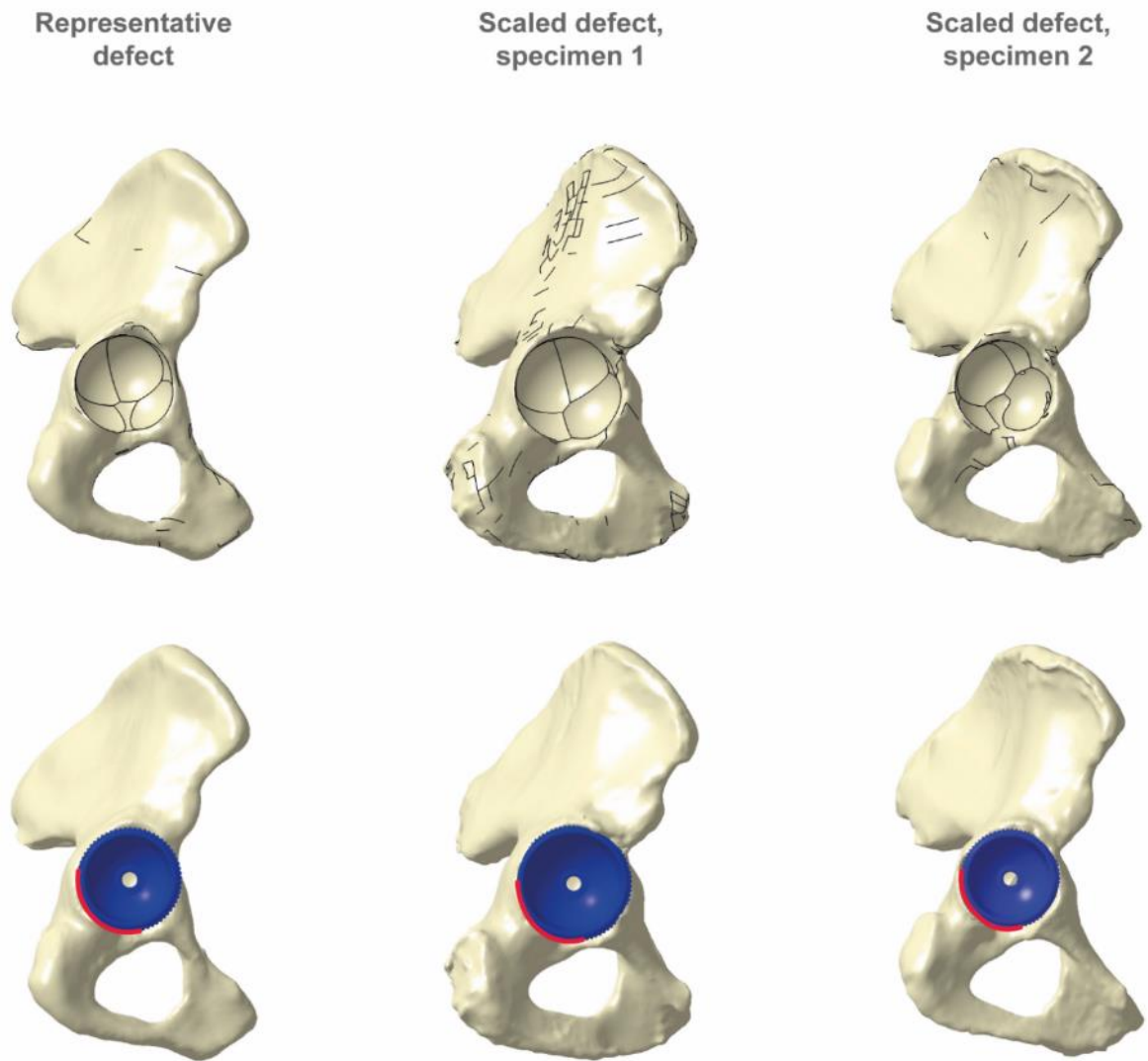


**Figure 17.** Comparison of representative simplified defect (increment 1), including the virtually implanted press-fit cup in comparison with two specimens in which the scaling procedure was applied to implement defect increment 1 (top). At the bottom, the specimens are depicted with virtually implanted press-fit cups, whereby the red area indicates the approximately 1/3 of circumference without implant-bone contact.

RIGHT HEMIPELVIS					
<b>Measurements</b>					
		Value [mm]			
Native acetabular radius	NR	25.0			
Primary Reaming (Radius)	RR	26.0			
Medial wall thickness	MT	1.1			
Anterior column width	AW	30.8			
Posterior column width	PW	32.0			
<b>Resulting Reamer positions and sizes</b>					
	Position [mm]			Reamer diameter (rounded) [mm]	
	X	Y	Z		
Reamer 1	-2.2	-1.6	-1.4	51	
Reamer 2	-1.6	3.0	-4.1	41	
Reamer 3_ANT	1.5	-5.5	-9.6	41	
Reamer 4_POST	-1.3	-7.0	-9.0	41	
Reamer 5_POST	1.0	1.5	-13.1	41	
<b>Scaling factors</b>					
	Position			Reamer size factor	Reamer size (not Rounded)
	X	Y	Z		
Reamer 1	-0.08	-0.06	-1.30	0.95	51.30
Reamer 2	-0.06	0.11	-3.80	0.76	41.04
Reamer 3_ANT	0.05	-0.22	-0.31	0.76	41.04
Reamer 4_POST	-0.04	-0.28	-0.28	0.76	41.04
Reamer 5_POST	0.03	0.06	-0.41	0.76	41.04

**Figure 18.** Screenshot of excel-template to calculate the required reamer sizes, positions (X and Y) and reaming depth (Z) (blue-white box) based on the measurement values inserted above (orange box) and the defined scaling factors (bottom).

## Discussion

To the author's knowledge, this is the first approach to simplify a clinically existing acetabular bone defect and to define a scaling procedure such that it could be implemented in donor specimens of different sizes. In the light of the biological variation in pelvis shape and size, the fact that the scaling procedure was defined using only three virtual 3D specimens certainly represents a limitation. Nevertheless, using the provided excel-template, the defect could be implemented by Morosato et al. in 10 hemipelvises for a left-right comparison (Figure 19) [93]. Future work should include the verification of the scaling procedure on a larger number of virtual specimens, as well as the development of a scaling procedure for the additionally derived bone defect increments.



**Figure 19.** Exemplary application of defect scaling and implementation procedure in human donor hemipelvises, performed within a study of Morosato et al., 2020 with implemented defect (left), which was filled with a synthetic BGS (right). Adapted from Morosato et al. [93].

---

**References**

- [1] Foran JRH. Treatment: Total hip replacement; 2015. Available from: <https://orthoinfo.aaos.org/en/treatment/total-hip-replacement/>. Last accessed 9<sup>th</sup> February 2020.
- [2] Varacallo M, Luo TD, Johanson NA. Total hip arthroplasty (THA) techniques; 2019. Available from: <https://www.ncbi.nlm.nih.gov/books/NBK507864/>. Last accessed 9<sup>th</sup> February 2020.
- [3] Pivec R, Johnson AJ, Mears SC, Mont MA. Hip arthroplasty. *The Lancet* 2012;380(9855):1768–77, doi:10.1016/S0140-6736(12)60607-2.
- [4] Robert Koch-Institut, Statistisches Bundesamt. Die 50 häufigsten Operationen der vollstationären Patientinnen und Patienten in Krankenhäusern (Rang, Anzahl, Anteil in Prozent): Gliederungsmerkmale: Jahre, Deutschland, Geschlecht, Art der Operation; 2018. Available from: [http://www.gbe-bund.de/oowa921-install/servlet/oowa/aw92/dboowasys921.xwdevkit/xwd\\_init?gbe.isgbetol/xs\\_start\\_neu/&p\\_aid=3&p\\_aid=36540186&nummer=666&p\\_sprache=D&p\\_indsp=99999999&p\\_aid=94027092](http://www.gbe-bund.de/oowa921-install/servlet/oowa/aw92/dboowasys921.xwdevkit/xwd_init?gbe.isgbetol/xs_start_neu/&p_aid=3&p_aid=36540186&nummer=666&p_sprache=D&p_indsp=99999999&p_aid=94027092). Last accessed 25<sup>th</sup> February 2020.
- [5] Organisation for Economic Co-operation and Development (OECD). Health at a glance 2019: OECD Indicators. Hip and knee replacement; 2019. Available from: <https://www.oecd-ilibrary.org/sites/2fc83b9a-en/index.html?itemId=/content/component/2fc83b9a-en>. Last accessed 1<sup>st</sup> March 2020.
- [6] Gwynne-Jones DP, Iosua EE, Stout KM. Rationing for total hip and knee arthroplasty using the New Zealand Orthopaedic Association score: Effectiveness and comparison with patient-reported scores. *The Journal of Arthroplasty* 2016;31(5):957–62, doi:10.1016/j.arth.2015.11.022.
- [7] Evans JT, Evans JP, Walker RW, Blom AW, Whitehouse MR, Sayers A. How long does a hip replacement last? A systematic review and meta-analysis of case series and national registry reports with more than 15 years of follow-up. *The Lancet* 2019;393(10172):647–54, doi:10.1016/S0140-6736(18)31665-9.
- [8] Learmonth ID, Young C, Rorabeck C. The operation of the century: total hip replacement. *The Lancet* 2007;370(9597):1508–19, doi:10.1016/S0140-6736(07)60457-7.
- [9] Bayliss LE, Culliford D, Monk AP, Glyn-Jones S, Prieto-Alhambra D, Judge A, Cooper C, Carr AJ, Arden NK, Beard DJ, Price AJ. The effect of patient age at intervention on risk of implant revision after total replacement of the hip or knee: a population-based cohort study. *The Lancet* 2017;389(10077):1424–30, doi:10.1016/S0140-6736(17)30059-4.
- [10] Australian Orthopaedic Association. Australian Orthopaedic Association National Joint Replacement Registry (AOANJRR), Hip Knee & Shoulder Arthroplasty: 2019 Annual Report. Adelaide; 2019.
- [11] Kärrholm J, Rogmark C, Nauclér E, Vinblad J, Mohaddes M, Rolfson O. Swedish Hip Arthroplasty Register: Annual report 2018; 2019.

- [12] The National Joint Registry Editorial Board. 16<sup>th</sup> Annual Report 2019: National Joint Registry for England, Wales, Northern Ireland and the Isle of Man; 2020.
- [13] Grimberg A, Jansson V, Melsheimer O, Steinbrück A. Endoprothesenregister Deutschland - Jahresbericht 2019; 2019.
- [14] Sadoghi P, Liebensteiner M, Agreiter M, Leithner A, Böhler N, Labek G. Revision surgery after total joint arthroplasty: A complication-based analysis using worldwide arthroplasty registers. *The Journal of Arthroplasty* 2013;28(8):1329–32, doi:10.1016/j.arth.2013.01.012.
- [15] Cooper RA, McAllister CM, Borden LS, Thomas WB. Polyethylene debris-induced osteolysis and loosening in uncemented total hip arthroplasty: A cause of late failure. *The Journal of Arthroplasty* 1992;7(3):285–90.
- [16] Hallab NJ, Jacobs JJ. Biologic effects of implant debris. *Bulletin of the NYU Hospital for Joint Diseases* 2009;67(2):182–88.
- [17] Wooley PH, Schwarz EM. Aseptic loosening. *Gene therapy* 2004;11(4):402–07, doi:10.1038/sj.gt.3302202.
- [18] Oparaugo PC, Clarke IC, Malchau H, Herberts P. Correlation of wear debris-induced osteolysis and revision with volumetric wear-rates of polyethylene: A survey of 8 reports in the literature. *Acta orthopaedica Scandinavica* 2001;72(1):22–28, doi:10.1080/000164701753606644.
- [19] Sundfeldt M, Carlsson LV, Johansson CB, Thomsen P, Gretzer C. Aseptic loosening, not only a question of wear: A review of different theories. *Acta orthopaedica* 2006;77(2):177–97, doi:10.1080/17453670610045902.
- [20] Huiskes R. Mechanical failure in total hip arthroplasty with cement. *Current Orthopaedics* 1993;7:239–47.
- [21] Albrektsson T, Brånemark PI, Hansson HA, Lindström J. Osseointegrated titanium implants. Requirements for ensuring a long-lasting, direct bone-to-implant anchorage in man. *Acta orthopaedica Scandinavica* 1981;52(2):155–70, doi:10.3109/17453678108991776.
- [22] Goodman SB, Gómez Barrena E, Takagi M, Konttinen YT. Biocompatibility of total joint replacements: A review. *Journal of biomedical materials research. Part A* 2009;90(2):603–18, doi:10.1002/jbm.a.32063.
- [23] Bragdon CR, Burke D, Lowenstein JD, O'Connor DO, Ramamurti B, Jasty M, Harris WH. Differences in stiffness of the interface between a cementless porous implant and cancellous bone in vivo in dogs due to varying amounts of implant motion. *The Journal of Arthroplasty* 1996;11(8):945–51.
- [24] Pilliar RM, Lee JM, Maniopoulos C. Observations on the effect of movement on bone ingrowth into porous-surfaced implants. *Clinical Orthopaedics and Related Research* 1986(208):108–13.
- [25] Maloney WJ, Jasty M, Burke DW, O'Connor DO, Zalenski EB, Bragdon C, Harris WH. Biomechanical and histologic investigation of cemented total hip arthroplasties: A study of autopsy-retrieved femurs after in vivo cycling. *Clinical Orthopaedics and Related Research* 1989(249):130–40.

- [26] Carter DR, Beaupré GS, Giori NJ, Helms JA. Mechanobiology of skeletal regeneration. *Clinical Orthopaedics and Related Research* 1998(355S):S41-S55.
- [27] Carter DR, Blenman PR, Beaupré GS. Correlations between mechanical stress history and tissue differentiation in initial fracture healing. *J. Orthop. Res.* 1988;6(5):736-48.
- [28] Leucht P, Kim J-B, Wazen R, Currey JA, Nanci A, Brunski JB, Helms JA. Effect of mechanical stimuli on skeletal regeneration around implants. *Bone* 2007;40(4):919-30, doi:10.1016/j.bone.2006.10.027.
- [29] Anderson JM, Rodriguez A, Chang DT. Foreign body reaction to biomaterials. *Semin Immunol* 2008;20(2):86-100.
- [30] Koh TJ, DiPietro LA. Inflammation and wound healing: The role of the macrophage. *Expert reviews in molecular medicine* 2013;13(e23):1-14, doi:10.1017/S1462399411001943.
- [31] Gao X, Fraulob M, Haïat G. Biomechanical behaviours of the bone-implant interface: A review. *Journal of the Royal Society, Interface* 2019;16(156):1-20, doi:10.1098/rsif.2019.0259.
- [32] Paprosky WG, Perona PG, Lawrence JM. Acetabular defect classification and surgical reconstruction in revision arthroplasty: A 6-year follow-up evaluation. *The Journal of Arthroplasty* 1994;9(1):33-44, doi:10.1016/0883-5403(94)90135-X.
- [33] Bettin D, Katthagen BD. Die DGOT-Klassifikation von Knochendefekten bei Hüft-Totalendoprothesen-Revisionsoperationen. *Zeitschrift für Orthopädie und Unfallchirurgie* 1997;135(4):281-84, doi:10.1055/s-2008-1039389.
- [34] Saleh KJ, Holtzman J, Gafni A, Saleh L, Jaroszynski G, Wong P, Woodgate I, Davis A, Gross AE. Development, test reliability and validation of a classification for revision hip arthroplasty. *J. Orthop. Res.* 2001;19(1):50-56, doi:10.1016/S0736-0266(00)00021-8.
- [35] D'Antonio JA, Capello WN, Borden LS, Bargar WL, Bierbaum BF, Boetticher WG, Steinberg ME, Stulberg DS, Wedge JH. Classification and management of acetabular abnormalities in total hip arthroplasty. *Clinical Orthopaedics and Related Research* 1989(243):126-37.
- [36] Wright G, Paprosky WG. Acetabular reconstruction: Classification of bone defects and treatment options; 2016. Available from: <https://musculoskeletalkey.com/acetabular-reconstruction-classification-of-bone-defects-and-treatment-options/>. Last accessed 12<sup>th</sup> December 2019.
- [37] Paprosky WG, Sporer SS, Murphy BP. Addressing severe bone deficiency: What a cage will not do. *The Journal of Arthroplasty* 2007;22(4 Suppl. 1):111-15, doi:10.1016/j.arth.2007.01.018.
- [38] Campbell DG, Garbuz DS, Masri BA, Duncan CP. Reliability of acetabular bone defect classification systems in revision total hip arthroplasty. *The Journal of Arthroplasty* 2001;16(1):83-86, doi:10.1054/arth.2001.19157.
- [39] Hettich G, Schierjott RA, Ramm H, Graichen H, Jansson V, Rudert M, Traina F, Grupp TM. Method for quantitative assessment of acetabular bone defects. *Journal of Orthopaedic Research* 2019;37(1):181-89, doi:10.1002/jor.24165.

- [40] Gelaude F, Clijmans T, Delpont H. Quantitative computerized assessment of the degree of acetabular bone deficiency: Total radial acetabular bone Loss (TrABL). *Advances in orthopedics* 2011;2011:1–12, doi:10.4061/2011/494382.
- [41] Schierjott RA, Hettich G, Graichen H, Jansson V, Rudert M, Traina F, Weber P, Grupp TM. Quantitative assessment of acetabular bone defects: A study of 50 computed tomography data sets. *PloS one* 2019;14(10):1-22, doi:10.1371/journal.pone.0222511.
- [42] Haddad FS, Shergill N, Muirhead-Allwood SK. Acetabular reconstruction with morcellized allograft and ring support: A medium-term review. *The Journal of Arthroplasty* 1999;14(7):788-795.
- [43] Gross AE, Lavoie MV, McDermott P, Marks P. The use of allograft bone in revision of total hip arthroplasty. *Clinical Orthopaedics and Related Research* 1985(197):115–22.
- [44] Sheth NP, Nelson CL, Springer BD, Fehring TK, Paprosky WG. Acetabular bone loss in revision total hip arthroplasty: Evaluation and mangement. *Journal of American Academy of Orthopaedic Surgeons* 2013;21:128–39.
- [45] DePuy Synthes. PINNACLE revision acetabular cup system; 2019. Available from: <https://www.jnjmedicaldevices.com/en-EMEA/product/pinnacle-revision-acetabular-cup-system>. Last accessed 22<sup>nd</sup> February 2020.
- [46] implantcast GmbH. ic-reinforcement cage & ic acetabular ring; 2020. Available from: <https://www.implantcast.de/en/for-medical-professionals/products/standard-tumour-prosthetics/pelvis-and-hip-endoprosthetics/primary-endoprosthetics-femoral-heads-acetabulum/ic-reinforcement-cage-acetabular-ring/>. Last accessed 22<sup>nd</sup> February 2020.
- [47] Kawanabe K, Akiyama H, Goto K, Maeno S, Nakamura T. Load dispersion effects of acetabular reinforcement devices used in revision total hip arthroplasty: A simulation study using finite element analysis. *The Journal of Arthroplasty* 2011;26(7):1061–66, doi:10.1016/j.arth.2011.04.019.
- [48] VirtualExpo. Revision acetabular prosthesis / cemented: Trabecular Metal™; 2020. Available from: <https://www.medicalexpo.com/prod/zimmer/product-74894-526007.html>. Last accessed 22<sup>nd</sup> February 2020.
- [49] Zimmer Biomet. Trabecular Metal™ Restriktor und Augment: Operationstechnik; 2007. Available from: [https://www.zimmersuisse.ch/content/dam/zimmer-web/documents/de-DE/pdf/surgical-techniques/hip/zimmer\\_trabecular\\_metal\\_retractor\\_and\\_augment\\_surgical\\_technique\\_de.pdf](https://www.zimmersuisse.ch/content/dam/zimmer-web/documents/de-DE/pdf/surgical-techniques/hip/zimmer_trabecular_metal_retractor_and_augment_surgical_technique_de.pdf). Last accessed 22<sup>nd</sup> February 2020.
- [50] Zimmer Biomet. Trabecular Metal™ Acetabular Revision System Cup-Cage Construct: Surgical Technique; 2010. Available from: <https://www.zimmerbiomet.com/content/dam/zimmer-biomet/medical-professionals/000-surgical-techniques/hip/zimmer-trabecular-metal-acetabular-revision-system-cup-cage-construct-2-surgical-technique.pdf>. Last accessed 22<sup>nd</sup> February 2020.
- [51] Perka C, Fink B, Millrose M, Sentürk U, Wagner M, Schröder J, Bail HJ, Ascherl R, Pruss A, Thiele K, Götze C. Revisionsendoprothetik. In: Claes, L, Kirschner, P, Perka,

- C, Rudert, M, editors. *AE-Manual der Endoprothetik*. Heidelberg, Dordrecht, London, New York: Springer. 2012. p. 441–587.
- [52] Nwankwo C, Dong NN, Heffernan CD, Ries MD. Do jumbo cups cause hip center elevation in revision THA? A computer simulation. *Clinical Orthopaedics and Related Research* 2014;472(2):572–76, doi:10.1007/s11999-013-3169-2.
- [53] Kim Y-H. Acetabular cup revision. *Hip & pelvis* 2017;29(3):155–58, doi:10.5371/hp.2017.29.3.155.
- [54] Clement RGE, Ray AG, MacDonald DJ, Wade FA, Burnett R, Moran M. Trabecular metal use in paprosky type 2 and 3 acetabular defects: 5-year follow-up. *The Journal of Arthroplasty* 2016;31(4):863–67, doi:10.1016/j.arth.2015.10.033.
- [55] Wachtl SW, Jung M, Jakob RP, Gautier E. The Burch-Schneider antiprotrusio cage in acetabular revision surgery: A mean follow-up of 12 years. *The Journal of Arthroplasty* 2000;15(8):959–63, doi:10.1054/arth.2000.17942.
- [56] Saleh KJ, Jaroszynski G, Woodgate I, Saleh L, Gross AE. Revision total hip arthroplasty with the use of structural acetabular allograft and reconstruction ring: A case series with a 10-year average follow-up. *The Journal of Arthroplasty* 2000;15(8):951–58, doi:10.1054/arth.2000.9055.
- [57] Ilyas I, Alrumaih HA, Kashif S, Rabbani SA, Faqih AH. Revision of type III and type IVB acetabular defects with Burch-Schneider anti-protrusio cages. *The Journal of Arthroplasty* 2015;30(2):259–64, doi:10.1016/j.arth.2014.08.014.
- [58] Regis D, Sandri A, Bonetti I, Bortolami O, Bartolozzi P. A minimum of 10-year follow-up of the Burch-Schneider cage and bulk allografts for the revision of pelvic discontinuity. *The Journal of Arthroplasty* 2012;27(6):1057-63.e1, doi:10.1016/j.arth.2011.11.019.
- [59] Morsi E, Garbuz D, Gross AE. Revision total hip arthroplasty with shelf bulk allografts: A long-term follow-up study. *The Journal of Arthroplasty* 1996;11(1):86–90.
- [60] Waddell Bs, Gonzalez Della Valle A. Reconstruction of non-contained acetabular defects with impaction grafting, a reinforcement mesh and a cemented polyethylene acetabular component. *The bone & joint journal* 2017;99-B(1 Suppl. A):25–30.
- [61] Jones SA. Impaction grafting made easy. *The Journal of Arthroplasty* 2017;32(9S):S54-S58, doi:10.1016/j.arth.2017.02.045.
- [62] Hansen E, Shearer D, Ries MD. Does a cemented cage improve revision THA for severe acetabular defects? *Clinical Orthopaedics and Related Research* 2011;469(2):494–502, doi:10.1007/s11999-010-1546-7.
- [63] Mäkinen TJ, Kuzyk P, Safir OA, Backstein D, Gross AE. Role of cages in revision arthroplasty of the acetabulum. *The Journal of Bone and Joint Surgery. American Volume* 2016;98(3):233–42, doi:10.2106/JBJS.O.00143.
- [64] Slooff TJ, Buma P, Schreurs BW, Schimmel JW, Huiskes R, Gardeniers J. Acetabular and femoral reconstruction with impacted graft and cement. *Clinical Orthopaedics and Related Research* 1996(323):108–15, doi:10.1097/00003086-199603000-00013.

- [65] Verdonschot N, Buma P, Gardeniers J, Schreurs BW. Basics of the impaction bone-grafting technique in the acetabulum. In: Thümler, P, Forst, R, Zeiler, G, editors. *Modulare Revisionsendoprothetik des Hüftgelenks*. Heidelberg: Springer Medizin. 2005. p. 51–58.
- [66] García-Rey E, Madero R, García-Cimbreló E. THA revisions using impaction allografting with mesh is durable for medial but not lateral acetabular defects. *Clinical Orthopaedics and Related Research* 2015;473(12):3882–91, doi:10.1007/s11999-015-4483-7.
- [67] Galia CR, Pagnussato F, Ribeiro TA, Moreira LF. Biology of bone graft and the use of bovine bone for revision of total hip arthroplasty with acetabular reconstruction. In: Kummoona, R, editor. *Bone grafting: Recent advances with special references to cranio-maxillofacial surgery*: IntechOpen. 2018. p. 57–71.
- [68] Pitto RP, Di Muria GV, Hohmann D. Impaction grafting and acetabular reinforcement in revision hip replacement. *International orthopaedics* 1998;22:161–64.
- [69] Slooff TJJH, Buma P, Schimmel JW, Gardeniers J, Huiskes R. Impaction grafting and cement in acetabular revision arthroplasty. In: Czitrom, AA., Winkler, H, editors. *Orthopaedic Allograft Surgery*. Vienna: Springer Vienna. 1996. p. 125–133.
- [70] Koob S, Scheidt S, Randau TM, Gathen M, Wimmer MD, Wirtz DC, Gravius S. Biologisches Downsizing: Azetabuläre Knochendefekte in der Hüftrevisionsendoprothetik. *Der Orthopäde* 2017;46(2):158–67, doi:10.1007/s00132-016-3379-x.
- [71] Toms AD, Barker RL, Spencer Jones R, Kuiper JH. Impaction bone-grafting in revision joint replacement surgery. Current concepts review. *The Journal of Bone and Joint Surgery* 2004;86-A(9):2050–60.
- [72] van Haaren EH. Clinical, mechanical and biological aspects of impaction bone grafting in orthopaedic revision implantology. Dissertation. Vrije Universiteit Amsterdam, Amsterdam; 2011. Available from: <https://research.vu.nl/ws/portalfiles/portal/42214263/complete+dissertation.pdf>.
- [73] Heinemann S, Gelinsky M, Worch H, Hanke T. Resorbierbare Knochenersatzmaterialien: Eine Übersicht kommerziell verfügbarer Werkstoffe und neuer Forschungsansätze auf dem Gebiet der Komposite. *Der Orthopäde* 2011;40(9):761–73, doi:10.1007/s00132-011-1748-z.
- [74] Haenle M, Schlüter S, Ellenrieder M, Mittelmeier W, Bader R. Treatment of acetabular defects during revision total hip arthroplasty - preliminary clinical and radiological outcome using bone substitute materials. *HIP international* 2013;23(1):46–53, doi:10.5301/HIP.2013.10713.
- [75] Whitehouse MR, Dacombe PJ, Webb JCJ, Blom AW. Impaction grafting of the acetabulum with ceramic bone graft substitute: High survivorship in 43 patients with a mean follow-up period of 4 years. *Acta orthopaedica* 2013;84(4):371–76, doi:10.3109/17453674.2013.824801.
- [76] Walschot LHB, Aquarius R, Verdonschot N, Buma P, Schreurs BW. Porous titanium particles for acetabular reconstruction in total hip replacement show extensive bony armoring after 15 weeks. A loaded in vivo study in 10 goats. *Acta orthopaedica* 2014;85(6):600–08, doi:10.3109/17453674.2014.960660.

- [77] van Gestel NAP, Gabriels F, Geurts JAP, Hulsen DJW, Wyers CE, van de Bergh JP, Ito K, Hofmann S, Arts JJ, van Rietbergen B. The Implantation of bioactive glass granules can contribute the load-bearing capacity of bones weakened by large cortical defects. *Materials (Basel, Switzerland)* 2019;12(21):1–13, doi:10.3390/ma12213481.
- [78] Oonishi H, Kim SC, Doiguchi Y, Takao Y, Fujita H, Itoh S, Dookawa H, Oomamiuda K. Revision THA by using hydroxyapatite in acetabular massive bone defect. In: Thümler, P, Forst, R, Zeiler, G, editors. *Modulare Revisionsendoprothetik des Hüftgelenks*. Heidelberg: Springer Medizin. 2005. p. 32–41.
- [79] Kang Y, Ren L, Yang Y. Engineering vascularized bone grafts by integrating a biomimetic periosteum and  $\beta$ -TCP scaffold. *ACS applied materials & interfaces* 2014;6(12):9622–33, doi:10.1021/am502056q.
- [80] Jacofsky DJ, McCamley JD, Jaczynski AM, Shrader MW, Jacofsky MC. Improving initial acetabular component stability in revision total hip arthroplasty: Calcium phosphate cement vs reverse reamed cancellous allograft. *The Journal of Arthroplasty* 2012;27(2):305–09, doi:10.1016/j.arth.2011.05.009.
- [81] Hettich G, Schierjott RA, Epple M, Gbureck U, Heinemann S, Mozaffari-Jovein H, Grupp TM. Calcium phosphate bone graft substitutes with high mechanical load capacity and high degree of interconnecting porosity. *Materials (Basel, Switzerland)* 2019;12(21):1–16, doi:10.3390/ma12213471.
- [82] Bolder SBT, Verdonschot N, Schreurs BW, Buma P. Acetabular defect reconstruction with impacted morsellized bone grafts or TCP/HA particles. A study on the mechanical stability of cemented cups in an artificial acetabulum model. *Biomaterials* 2002;23(3):659–66, doi:10.1016/S0142-9612(01)00153-3.
- [83] Walschot LHB, Aquarius R, Schreurs BW, Buma P, Verdonschot N. Better primary stability with porous titanium particles than with bone particles in cemented impaction grafting: An in vitro study in synthetic acetabula. *Journal of biomedical materials research. Part B, Applied biomaterials* 2013;101(7):1243–50, doi:10.1002/jbm.b.32936.
- [84] Arts JJC, Schreurs BW, Buma P, Verdonschot N. Cemented cup stability during lever-out testing after acetabular bone impaction grafting with bone graft substitutes mixes containing morsellized cancellous bone and tricalcium phosphate-hydroxyapatite granules. *Proceedings of the Institution of Mechanical Engineers. Part H, Journal of Engineering in Medicine* 2005;219(4):257–63, doi:10.1243/095441105X34266.
- [85] Gelaude F, Demol J, Clijmans T, Delpont H. CT-based quantification of bone loss for refined classification of acetabular deficiencies: Comparison of 30 Paprosky type IIIA-B cases. *Orthopaedic Proceedings* 2013;95-B(SUPP\_1).
- [86] Schierjott RA, Hettich G, Ringkamp A, Baxmann M, Morosato F, Grupp TM. A method to assess primary stability of acetabular components in association with bone defects. *Journal of Orthopaedic Research* 2020;38(8):1769–78, doi:10.1002/jor.24591.
- [87] Doebele S, Siebenlist S, Vester H, Wolf P, Hagn U, Schreiber U, Stöckle U, Lucke M. New method for detection of complex 3D fracture motion - Verification of an optical motion analysis system for biomechanical studies. *BMC musculoskeletal disorders* 2012;13(33):1–9, doi:10.1186/1471-2474-13-33.

- 
- [88] Lázaro González Á, Martínez Reina J, Cano Luis P, Jiménez Baquero J, Sueiro Fernández J, Giráldez Sánchez MÁ. Is cannulated-screw fixation an alternative to plate osteosynthesis in open book fractures? A biomechanical analysis. *Injury* 2016(47S3):S72-S77.
- [89] Nadorf J, Kinkel S, Gantz S, Jakubowitz E, Kretzer JP. Tibial revision knee arthroplasty with metaphyseal sleeves: The effect of stems on implant fixation and bone flexibility. *PloS one* 2017;12(5):e0177285, doi:10.1371/journal.pone.0177285.
- [90] Small SR, Rogge RD, Malinzak RA, Reyes EM, Cook PL, Farley KA, Ritter MA. Micromotion at the tibial plateau in primary and revision total knee arthroplasty: fixed versus rotating platform designs. *Bone & joint research* 2016;5(4):122–29, doi:10.1302/2046-3758.54.2000481.
- [91] Grupp TM, Saleh KJ, Holderied M, Pfaff AM, Schilling C, Schroeder C, Mihalko WM. Primary stability of tibial plateaus under dynamic compression-shear loading in human tibiae - Influence of keel length, cementation area and tibial stem. *Journal of Biomechanics* 2017;59:9–22, doi:10.1016/j.jbiomech.2017.04.031.
- [92] Morosato F, Traina F, Cristofolini L. A reliable in vitro approach to assess the stability of acetabular implants using digital image correlation. *Strain* 2019;55(4):1–12, doi:10.1111/str.12318.
- [93] Morosato F, Traina F, Schierjott RA, Hettich G, Grupp TM, Cristofolini L. Primary stability of revision acetabular reconstructions using an innovative bone graft substitute: A comparative biomechanical study on cadaveric pelvises (Manuscript submitted for publication). *HIP International* 2020.
- [94] Morosato F, Traina F, Cristofolini L. Standardization of hemipelvis alignment for in vitro biomechanical testing. *Journal of Orthopaedic Research* 2018;36(6):1645–52, doi:10.1002/jor.23825.

### Acknowledgements

First, I would like to express my sincerest gratitude to my supervisor Prof. Dr. med. habil. Dr.-Ing. Thomas M. Grupp who inspired me with his enthusiasm for biomechanics to perform this doctoral thesis. I would like to thank him for giving me this great opportunity, for his valuable advice and feedback on my work, as well as for all his guidance and support throughout the years.

I would also like to thank our project partners Prof. Dr. med. Dipl.-Ing. Volkmar Jansson, Prof. Dr. med. Maximilian Rudert, Prof. Dr. med. Heiko Graichen, Prof. Francesco Traina, PD Dr. med. Patrick Weber, Prof. Luca Cristofolini, Federico Morosato PhD, Heiko Ramm and Dr.-Ing. Philipp Damm for all their valuable input and feedback, for all our conversations which taught me so much, and for enabling my dissertation to be so closely related to clinical issues.

Special thanks also to Dr. Fredrik Ollila and Chris Wattengel for providing the bone graft substitute test samples.

Furthermore, I would like to thank my colleagues for the amazing working atmosphere and for all their support along the way. My special thanks to Dr. Georg Hettich and Dr. Marc Baxmann for the close cooperation and fruitful discussions, all their support and valuable input to my work; to the colleagues from the Biomechanical Research Laboratory for enabling the in vitro tests and for providing advice on testing machines and measurement equipment; to Jessica Stübler for doing a great job segmenting a large part of the CT data sets; to Alexandra Ringkamp for doing a great job performing part of the in vitro tests within her Bachelor thesis; to the colleagues from the hip development department for their support and the fruitful discussions; to the colleagues from the prototype workshop team for their support and timely fabrication of the test setup components.

Last but not least, I would like to thank my family and friends for all their support, for being so sympathetic about how much time I spent on my dissertation, for cheering me up whenever I needed it and for celebrating every successful step forward together. My heartfelt thanks to my parents for all their love, their great support and encouragement I have always received and for supporting me in every way they could during this challenging period; to my partner Markus who has been by my side throughout this PhD and before, who always believes in me and who always supported my goals and encouraged me to pursue this path .